

Dissertation zur Erlangung des Doktorgrades
der Fakultät für Chemie und Pharmazie
der Ludwig-Maximilians-Universität München

**Functional analysis of RNA transport mediated
by Pur-alpha in *Drosophila melanogaster***



Verena Nicole Aumiller

aus

Dachau

2011

Erklärung

Diese Dissertation wurde im Sinne von § 13 Abs. 3 bzw. 4 der Promotionsordnung vom 29. Januar 1998 (in der Fassung der vierten Änderungssatzung vom 26. November 2004) von Herrn Prof. Dr. Klaus Förstemann betreut.

Ehrenwörtliche Versicherung

Diese Dissertation wurde selbständig, ohne unerlaubte Hilfe erarbeitet.

München, 15.04.2011

Verena Nicole Aumiller

Dissertation eingereicht am 15.04.2011

1. Gutacher: Prof. Dr. Klaus Förstemann

2. Gutachter: Prof. Dr. Dietmar Martin

Mündliche Prüfung am 26.05.2011

1. SUMMARY	4
2. INTRODUCTION	5
2.1 mRNA transport	5
2.2 <i>Drosophila</i> oogenesis	6
2.2.1 Process of oogenesis	7
2.2.2 Signaling by <i>Drosophila</i> follicle cells during oogenesis	8
2.3 Messenger ribonucleoprotein complexes.....	10
2.4 Pur-alpha	10
2.4.1 Structure of <i>Drosophila</i> Pur-alpha	11
2.4.2 DNA bound functions of Pur-alpha	13
2.4.3 Pur-alpha in cell cycle control and tumor suppression.....	13
2.4.4 RNA bound functions of Pur-alpha.....	14
2.4.5 Pur-alpha knockout mouse	15
2.5 Triplet-repeat associated diseases.....	15
2.6 Fragile-X associated tremor and ataxia syndrome (FXTAS)	15
2.7 Aims of this thesis	17
3. MATERIALS AND METHODS	18
3.1 Materials	18
3.1.1 Laboratory equipment	18
3.1.2 Laboratory chemicals	19
3.1.3 Enzymes.....	20
3.1.4 Other materials	21
3.1.5 Bacterial cells.....	22
3.1.6 <i>Drosophila melanogaster</i> cells	23
3.1.7 Fly stocks	23
3.1.8 Flyfood.....	24
3.1.9 Plasmids.....	24
3.1.10 Oligonucleotides.....	25
3.1.10.1 RNA-Interference	25
3.1.10.2 Molecular Cloning	26
3.1.10.3 Fly stock mapping.....	26
3.1.10.4 Quantitative PCR	27
3.1.10.5 MicroRNA profiling.....	30
3.1.10.6 Northern Blotting	32
3.1.10.7 Electrophoretic mobility shift assays (EMSA).....	32

3.1.11	Antibodies	32
3.1.11.1	Primary antibodies	32
3.1.11.2	Secondary antibodies	33
3.1.12	Commonly used buffers and stock solutions	34
3.2	Methods	37
3.2.1	Methods for molecular cloning.....	37
3.2.2	Methods with <i>Drosophila</i> Schneider 2 cells.....	38
3.2.2.1	RNA-Interference (RNAi).....	38
3.2.2.2	Transfection of plasmid DNA.....	39
3.2.2.3	Analysis of Schneider cells by fluorescence microscopy.....	40
3.2.3	Methods with flies.....	40
3.2.3.1	Maintenance and handling.....	40
3.2.3.2	Egg laying experiments.....	41
3.2.3.3	Rescue experiments.....	41
3.2.3.4	Analysis of ovaries by fluorescence microscopy.....	41
3.2.4	Protein analysis	42
3.2.4.1	Protein extraction.....	42
3.2.4.2	Co-immunoprecipitation.....	42
3.2.4.3	Western-Blotting	42
3.2.4.4	Mass spectrometry	43
3.2.4.5	Electrophoretic mobility shift assay (EMSA)	43
3.2.5	RNA analysis	44
3.2.5.1	RNA isolation	44
3.2.5.2	Northern Blotting	44
3.2.5.3	Quantitative RT-PCR	44
3.2.5.4	microArray	45
4.	RESULTS.....	46
4.1	Pur-alpha has no impact on small RNA biogenesis pathways.....	46
4.2	Localization of Pur-alpha	49
4.2.1	<i>Drosophila</i> Schneider 2 cells.....	49
4.2.1.1	Pur-alpha bodies are no P-Bodies	49
4.2.1.2	Pur-alpha is associated with FMRP, Ago1 and Ago2 in Schneider cells	52
4.2.2	Localisation of Pur-alpha during <i>Drosophila</i> oogenesis	56
4.2.2.1	Pur-alpha is enriched in the polar cells of the follicular epithelium	57

4.2.2.2 RNA-binding and dimerization are required for correct transport of GFP-Pur-alpha during oogenesis	59
4.3 Defects in oogenesis in Pur-alpha hypomorphic alleles	61
4.3.1 Decreased egg laying in Pur-alpha hypomorphic alleles.....	62
4.3.2 Malformation of follicular epithelium in Pur-alpha hypomorphic alleles.....	63
4.3.3 Knock-down of Pur-alpha in follicle cells	69
4.3.4 Morphological analysis of main ovary components in <i>pur-alpha</i> ^{KG05743} flies	71
4.3.4.1 Oocyte and polar cell determination	71
4.3.4.2 Adherens junctions and ring canals	73
4.4 Pur-alpha associated proteins.....	75
4.5 Pur-alpha associated RNAs.....	78
4.5.1 Pur-alpha associated messengerRNAs	78
4.5.1.1 microArray and GO-Analysis.....	78
4.5.1.2 Analysis of Pur-alpha associated mRNAs with qRT-PCR	80
4.5.1.3 Pur-alpha binds to sequences similar to the opa sequence	81
4.5.1.4 Recombinant Pur-alpha binds to (CAG) ₄ and (CAG) ₃ CAA RNA in vitro.....	82
4.5.2 Pur-alpha associated microRNAs	84
4.5.2.1 Pur-alpha associated microRNAs from FLAG-Pur-alpha transfected Schneider cells	84
4.5.2.2 Pur-alpha associated microRNAs from GFP-Pur-alpha transgenic ovary-extracts..	85
4.5.2.3 GO-term analysis of top three enriched or depleted microRNA predicted targets.	87
5. DISCUSSION.....	89
5.1 Pur-alpha's structure to function relation	89
5.2 Identified Pur-alpha associated proteins	90
5.3 Pur-alpha mutant flies display a new early follicle cell phenotype.....	92
5.4 Cell fates appear unchanged in <i>pur-alpha</i> mutant ovaries.....	94
5.5 Pur-alpha's RNA cargoes	95
5.6 Implication of Pur-alpha for metastasis and neurodegeneration.....	98
5.7 Conclusion	99
6. APPENDIX	100
6.1 Abbreviations	100
6.2 Acknowledgements.....	104
6.3 Curriculum Vitae.....	105
7. References.....	106

1. SUMMARY

Pur-alpha is a highly conserved, yet poorly understood, DNA- and RNA-binding protein. When bound to DNA, it activates transcription and functions as tumor suppressor, while cytoplasmic Pur-alpha was found in transported mRNP-particles that also contained e.g. Staufen and FMRP. In the neurodegenerative disease fragile-X associated tremor and ataxia syndrome (FXTAS) Pur-alpha is sequestered from its normal function by binding to (CGG)_n repeats in the mutated *Fmr1* mRNA, thereby contributing to the pathogenesis of the disease.

This thesis presents a functional analysis of *Drosophila melanogaster* Pur-alpha using the well-studied RNA transport processes during oogenesis. The analysis of truncated and/or mutated GFP-fusion Pur-alpha protein variants revealed that *Drosophila* Pur-alpha is predominantly cytoplasmic at steady-state but accumulates in the nucleus when RNA binding or protein dimerization is impaired. Pur-alpha is enriched in the oocyte during early oogenesis and co-purifies with the known RNA transport components Me31B, Cup, Trailor Hitch and Exuperantia. The two polar cells at each tip of an egg chamber have particularly high Pur-alpha levels. Flies carrying hypomorphic alleles of *pur-alpha* show a temperature-sensitive deficiency in egg production due to a follicle cell migration defect, consistent with the observed expression in polar cells, which are the main organizers of the follicular epithelium. In this newly described early oogenesis phenotype the follicle cells fail to ensheathe the germline cyst after budding from the germarium and form a lump on one side of the egg chamber. Messenger RNAs, as well as predicted targets of miRNAs associated with Pur-alpha, are enriched for gene ontology terms of cell-cell junctions. Furthermore, the mRNAs coding for the planar cell polarity factor *diego* (*dgo*), *disheveled* (*dsh*), argonaute-2 (*ago2*), *larp* and *notch* appear to be associated with Pur-alpha, suggesting molecular links to the cell migration defect in ovaries of the *pur-alpha* mutant flies. Many of the mRNAs bound by Pur-alpha share an *opa* like sequence motif consistent of r(CAG)_n and r(CAA)_n repeats, which can be found in many other developmentally regulated transcription units. *In vitro* studies could confirm this binding, suggesting a role of Pur-alpha in other triplet repeat expansion associated neurodegenerative diseases.

2. INTRODUCTION

2.1 mRNA transport

It is a well known fact that every single cell of a whole organism is equipped with the same genetic material, and that differentiation of precursor cells or stem cells into specialized cell types and tissues which are essential for the existence of the organism is dependent on exact regulation of gene and protein expression. This regulation is achieved on different levels. On the one hand transcription of genes is extensively regulated by different transcription factors and epigenetic mechanisms; on the other hand the product of transcription, the mRNA underlies many different regulations. Especially mRNA export from the nucleus, mRNA decay, mRNA halflife, mRNA stability, splicing and mRNA accessibility for translation can be regulated powerfully by different mechanisms. Furthermore, each transcriptional and posttranscriptional regulation stage can be modulated at different steps, e.g. gene transcription: transcriptional initiation and elongation can be regulated independently. These various regulatory mechanisms constitute a huge field which was and still is extensively worked on during the last years of research in molecular biology.

An important and in the past underestimated mechanism (LECUYER *et al.* 2007) for spatial and temporal regulation of protein expression is mRNA transport (reviewed in (MARTIN and EPHRUSSI 2009)). Proteins are synthesized at specific cellular compartments after their mRNAs were transported actively by molecular motors from the nucleus to the required site of translation. During this transport the mRNAs are silenced for translation which can be achieved by posttranscriptional regulation through microRNAs (KIEBLER and BASSELL 2006) or binding of translational repressors to the transported mRNA (NAKAMURA *et al.* 2001). The translational repression is released at the target site of the mRNA and its translation can take place. This allows cells with complex architecture, like neurons, to make independent decisions about the protein content at particular cellular regions, for example at dendrites (KINDLER *et al.* 2005). Spatial translation of mRNAs is also important for energetic reasons. This way, protein synthesis only occurs at sites where the protein is needed.

Furthermore, through localized translation protein gradients can be established which are very important during development e.g. in *Drosophila* oogenesis or in neuronal cells (WANG *et al.* 2010).

The most intensively studied mRNA localization events are depicted in Figure 2-1 (taken from (MARTIN and EPHRUSSI 2009)). Famous examples are the localization of *ash1* mRNA in budding yeast

(Figure 2-1A), localization of the maternal determinants *bicoid*, *oskar* and *nanos* in the *Drosophila* embryo (Figure 2-1B) and *VG1* mRNA in *Xenopus* oocytes (Figure 2-1C). Moreover, there are localized mRNAs in Fibroblasts and neuronal cells (Figure 2-1D-E).

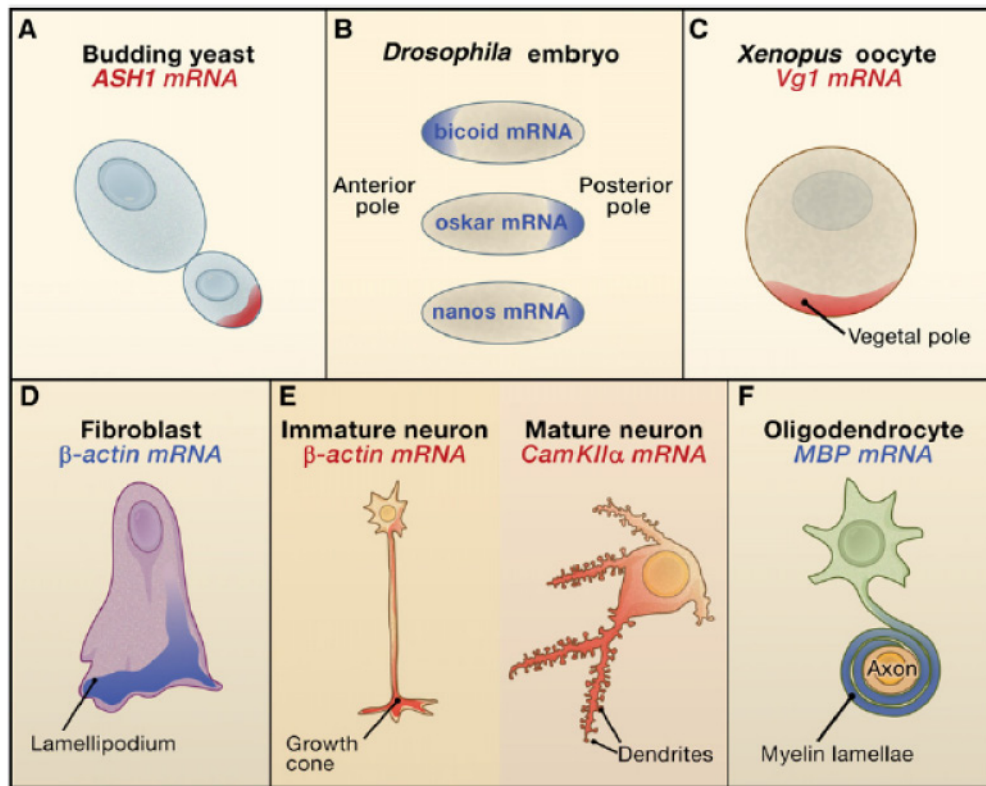


Figure 2-1: Classic examples of localized mRNAs

(A) In budding yeast, the *ASH1* mRNA localizes to the bud tip. (B) In *Drosophila* embryos, *bicoid* mRNA localizes to the anterior pole; *oskar* and *nanos* mRNAs to the posterior pole. (C) In *Xenopus* oocytes (stage IV), *Vg1* mRNA localizes to the vegetal pole. (D) In chicken and mammalian fibroblasts, β -actin mRNA localizes to lamellipodia. (E) In developing, immature mammalian neurons, β -actin mRNA is present in distal growth cones and in mature, fully polarized pyramidal neurons, *CamKII α* mRNA is present in distal dendrites. (F) In mammalian oligodendrocytes, *myelin basic protein (MBP)* mRNA localizes to myelinating processes that ensheathe neuronal axons. (Picture and text taken from Martin & Ephrussi, 2009)

2.2 *Drosophila* oogenesis

Drosophila oogenesis is another important biological process where mRNA localization plays a major role. In detail, the localization of three RNAs namely *oskar*, *bicoid* and *gurken* leads to embryonic axis formation and ensures correct embryogenesis during *Drosophila* development. The translational regulation of the maternal determinants is coupled to their localization.

2.2.1 Process of oogenesis

Every female fly has two ovaries, each composed of 14 - 16 ovarioles. Ovarioles are strings of six to seven egg chambers which are at sequentially different developmental stages (KING 1970). The egg chambers are separated by five to eight stalk cells. At the anterior tip of each ovariole a so called germarium is located. Germ line and somatic stem cells are present in the germarium and egg chambers bud from this structure. The egg chambers mature along the ovarioles until they are laid as mature eggs after 14 developmental stages. Top panel of figure 2-2 shows a schematic picture of a *Drosophila* ovariole (taken from (ROTH and LYNCH 2009)).

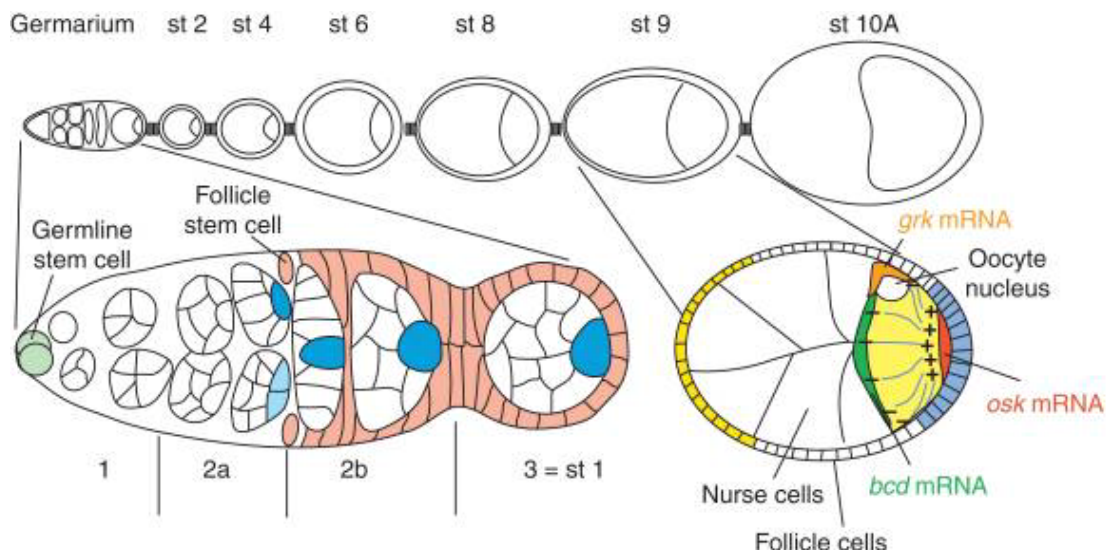


Figure 2-2: Schematic picture from a *Drosophila* ovariole

germarium at the anterior tip and budding egg chambers at different developmental stages (stage 2 to stage 10A) (top picture); germarium (left, bottom picture), stage 9 egg chamber (right, bottom picture) (figure taken from (ROTH and LYNCH 2009))

As shown in Figure 2-2 in the lower left picture the development of a *Drosophila* egg starts with an asymmetric cell division of the germ line stem cells at the anterior end of the germarium (reviewed in (BASTOCK and ST JOHNSTON 2008)). The mother cell closer to the stem cell niche stays a germ line stem cell and the produced daughter cell starts to differentiate. After four mitotic divisions with incomplete cytokinesis the daughter cell becomes a germline cyst consisting of 16 cells which are interconnected by ring canals. One of the 16 cells will become the oocyte and the 15 others assume the nurse cell fate in order to supply the oocyte with nutrients, proteins and RNA during the course of development. The two cells with four ring canals develop into pro-oocytes in the germline cyst (light blue color, figure 2-2, bottom left picture). Following during this

process, cell-fate markers and meiotic chromosome pairing markers become restricted to one of the pro-oocytes which then becomes the oocyte (dark blue color, figure 2-2, bottom left picture). The germline cyst is enveloped by somatic follicle cells (pink color, figure 2-2, bottom left picture) which derive from follicle stem cells in region 2b of the germarium; and finally a stage 1 egg chamber with the oocyte located at the posterior buds from the germarium. During the different stages of oogenesis the oocyte matures and gets bigger until the nurse cell are squeezed out and the mature egg is released at stage 14.

The polarity of the egg chamber and the oocyte which later defines the body axes of the embryo is achieved by complex cell-cell signaling events between somatic and germ line cells. The major signaling pathways which are active during these developmental steps are the JAK/STAT and Notch signaling pathways. In the end all those signaling events lead to the formation of the anterior-posterior-body axis which is defined by *oskar* mRNA-localization at the posterior pole of the oocyte and by anterior localization of *bicoid* mRNA. The dorso-ventral body axis is defined by the position of the nucleus and *gurken* mRNA (scheme of a stage 9 egg chamber: figure 2-2, bottom right picture).

2.2.2 Signaling by *Drosophila* follicle cells during oogenesis

The follicular epithelium plays a crucial role during all signaling events (reviewed in (Wu *et al.* 2008)). The first patterning event is the differentiation of a pair of polar cells out of the follicle cells at the anterior of the stage 1 egg chamber (red nuclei in Figure 2-3). This differentiation is achieved by a Notch signal which is sent from the germ line cyst itself (RUOHOLA *et al.* 1991) (Figure 2-3 A, arrow 1). The polar cells become the main organizers of the follicular epithelium (GRAMMONT and IRVINE 2002) during oogenesis. They express the JAK/STAT-ligand Unpaired (Figure 2-3 A, arrow 2) which induces the cells anterior to the polar cells to become stalk cells (light blue nuclei in Figure 3B) (ASSA-KUNIK *et al.* 2007; XI *et al.* 2003). Stalk formation itself induces the follicle cells anterior to the stalk cells which belong to the younger cyst in the ovariole to overexpress E-cadherin (GODT and TEPASS 1998) (Figure 2-3 A, arrow 3). E-cadherin now initiates the positioning of the oocyte of the younger germ line cyst at the posterior site. This important step is referred to the first symmetry-breaking event during development. This germline cyst now buds from the germarium and starts a new cycle by inducing its anterior follicle cells to become polar cells (TORRES *et al.* 2003). By stage 5 a further Unpaired signal from the polar cells drives the surrounding follicle cells to become terminal follicle cells (black nuclei in figure 2-3). Then a signaling cascade between the oocyte, *gurken* mRNA and Grk protein which are both localized at

the posterior side at that time point and the posterior follicle cells induces repolarisation of the oocyte. This results in a reorganization of oocyte microtubules which then direct *bicoid* and *oskar* mRNA to their final destinations, where they at the end determine the anterior-posterior axis of the oocyte. This is followed by a movement of the nucleus and *gurken* mRNA to the anterior corner of the oocyte, where a Grk protein signal defines the other main body axis, dorso-ventral (Figure 2-3A, stage 7 egg chamber).

A further important patterning event induced by the follicular epithelium especially by the polar cells is border cell formation. Polar cells recruit four to six adjacent follicle cells which become border cells (green nuclei, Figure 2-3B). At stage 9 of oogenesis these cells start to delaminate from the remaining epithelium, surround the polar cells and start migrating along with the polar cells posteriorly through the nurse cells until they reach the anterior tip of the oocyte.

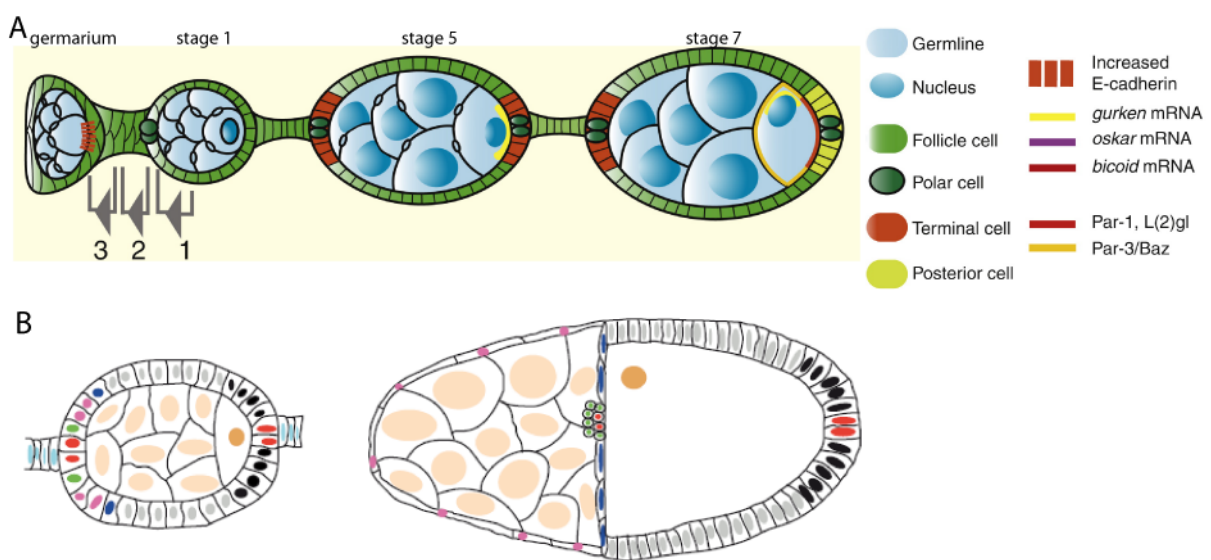


Figure 2-3: Signaling by *Drosophila* follicle cells

A: Polarization of the egg chamber

The posterior egg chamber (right) induces polar follicle cell differentiation (dark green) by secreting Delta (arrow 1). These induce stalk cell differentiation by secreting Unpaired (arrow 2). This induces E-Cadherin upregulation (orange lines, arrow 3), which positions the oocyte of the neighbouring cyst. By stage 5 a second Unpaired signal from the polar follicle cells has induced their neighbours to become terminal follicle cells (dark orange). *gurken* RNA (yellow) and protein are present at the oocyte posterior. By stage 7 the posterior Gurken has induced the nearest terminal cells to become posterior follicle cells (light green). These induce oocyte repolarisation. The oocyte nucleus (dark blue) moves to an anterior lateral position (figure and text taken from (BASTOCK and ST JOHNSTON 2008)).

B: Schematic picture of stage 6 (left) and 10 (right) follicles

Nuclei of follicle cells are color coded: oocyte (brown), nurse cells (light brown), central follicle cells (gray), polar cells (red), stalk cells (light blue), outer border cells (green), stretched cells (pink), centripetal cells (dark blue) and posterior terminal cells (black) (figure taken from (GRAMMONT and IRVINE 2002)).

2.3 Messenger ribonucleoprotein complexes

To achieve transport of RNAs to distinct target sites of translation, the cell assembles mRNAs already during or shortly after their synthesis within messenger ribonucleoprotein (mRNP) complexes. mRNPs are not only mRNA transport granules, they rather serve as key modulators of post-transcriptional gene expression in cells (ANDERSON and KEDERSHA 2009). Among the proteins in the granules are e.g. RNA binding proteins, translation factors and proteins for mRNA modification and decay. The mRNAs which will be transported to their final translation site contain *cis*-acting elements or “zipcodes” which are recognized by *trans*-acting factors (JAMBHEKAR and DERISI 2007). These factors mediate the connection of the mRNPs which contain locally needed RNAs, to the cellular transport machinery e.g. to molecular motors like kinesin. Kanai and colleagues characterized a RNA transport granule from an adult mouse brain by purification of the complex via kinesin (KIF5) (KANAI *et al.* 2004). Among the 42 proteins identified they found the two transported mRNAs *Arc* and *CaMKIIalpha*. Using RNA-interference, the following factors were found to be essential for the localization of the *CaMKII-alpha* mRNA: Pur-alpha, hnRNP-U, polypyrimidine tract binding protein-associated splicing factor (PSR) and Staufen. Further, they identified fragile-X mental retardation protein (FMRP), and its two related proteins (FXR-1 and FXR-2), Pur-beta, DDX1/3, SYNCRIPI, TLS, NonO, HSPC117, ALY, CGI-99 and EF-1 alpha as components of the transport granule. The proteins Pur-alpha and Staufen were identified as factors which were associated with kinesin linked RNA-transport in additional studies (ELVIRA *et al.* 2006; OHASHI *et al.* 2002).

2.4 Pur-alpha

Pur-alpha is one of the main components in RNA transport granules as it was found in three independent studies (ELVIRA *et al.* 2006; KANAI *et al.* 2004; OHASHI *et al.* 2002). It is a highly conserved protein from bacteria to metazoans with only a two amino acid difference between human and mouse Pur-alpha (GALLIA *et al.* 2000; MA *et al.* 1994). It belongs to the PUR-protein family which consists also of Pur-beta and Pur-gamma (reviewed in (JOHNSON 2003)). The name of the protein family derives from the binding capacity of the proteins, which bind to purine rich nucleic acids. Pur-alpha binds to (GGN)_n repeats, so called PUR sequence elements (BERGEMANN and JOHNSON 1992). Common structural features of the PUR-protein family are a flexible glycine rich N-terminus and a glutamate/glutamine rich C-terminus. The C-terminus also contains a

psycho motif (GALLIA *et al.* 2000; MA *et al.* 1994). The central regions are the most conserved parts of the proteins. Functionally, Pur-alpha has various cellular responsibilities. It is a ubiquitous protein expressed in many tissues and present as well in the nucleus of cells as in the cytoplasm.

2.4.1 Structure of *Drosophila* Pur-alpha

Graebisch and colleagues were able to solve the crystal structure of *Drosophila melanogaster* Pur-alpha (GRAEBSCH *et al.* 2009). The central region of Pur-alpha can be separated into three repeats (PUR-repeats) (Figure 2-4A) and the crystal structure of repeat I and II was solved with a resolution of 2.1 angstroms (Figure 2-4B). Every PUR-repeat consists of a four-stranded anti-parallel β -sheet followed by an α -helix at the C-terminus; the repeats are inter-connected by a linker region and together make up a PUR-domain. Analysis of all three repeats with SAXS and size-exclusion-chromatography revealed that a dimerization of two PUR I+II+III proteins occurs via repeat III which is folding into a PUR-domain together with repeat III of the second protein (Figure 2-4C).

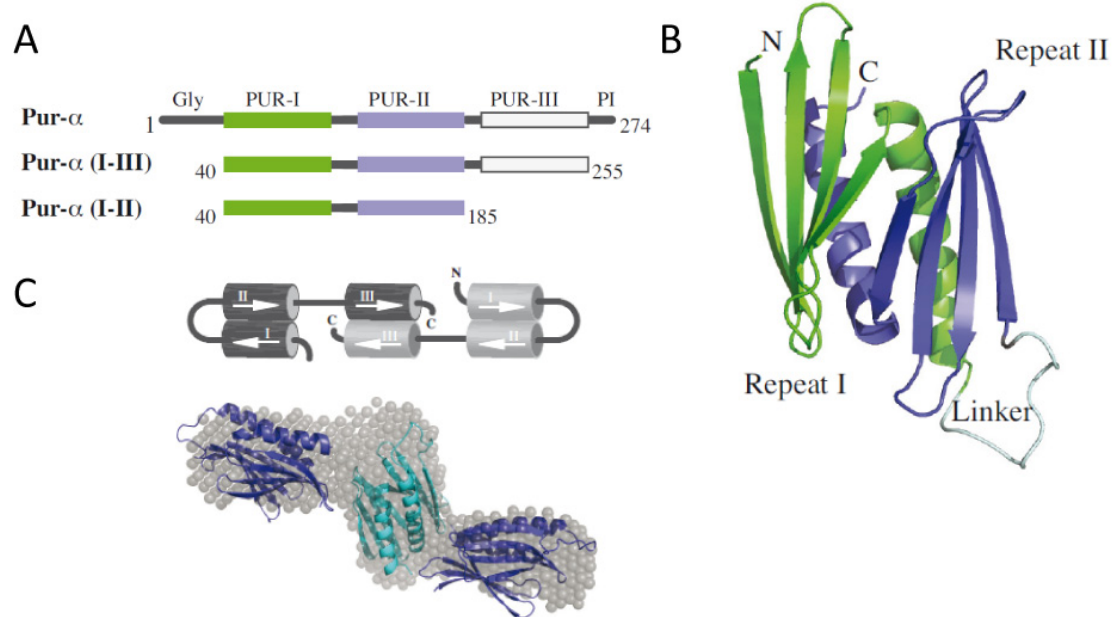


Figure 2-4: Structural models of *Drosophila* Pur-alpha

A: domain structure of the for structural studies used protein truncations

B: crystal structure of PUR-repeat I (green) + II (blue)

C: top: scheme of dimerization of two Pur-alpha proteins (light grey and dark grey);

bottom: SAXS model of PUR-domains (blue: repeat I+II, cyan: repeat III+III)

figures taken from (GRAEBSCH *et al.* 2009)

Functional analyses in this study (GRAEBSCH *et al.* 2009) revealed that full-length Pur-alpha protein binds to a CGG 12mer of single stranded (ss) RNA (Figure 2-5A), which represents the consensus sequence of the so called PUR-elements. Binding of one PUR-domain (Pur-alpha I+II) to the 12mer CGG ssRNA was less efficient but still reasonable (Figure 2-5B, left panel). If two point mutations R80A and R158A were introduced into the protein, the binding to the RNA was completely abolished (Figure 2-5B, right panel). The introduction of two other point mutations R65A and R142A resulted in slightly reduced binding capacity compared to the unchanged Pur-alpha I+II (Figure 2-5C, left panel). As an unspecific control for the experiments PolyA RNA was used (Figure 2-5C, right panel).

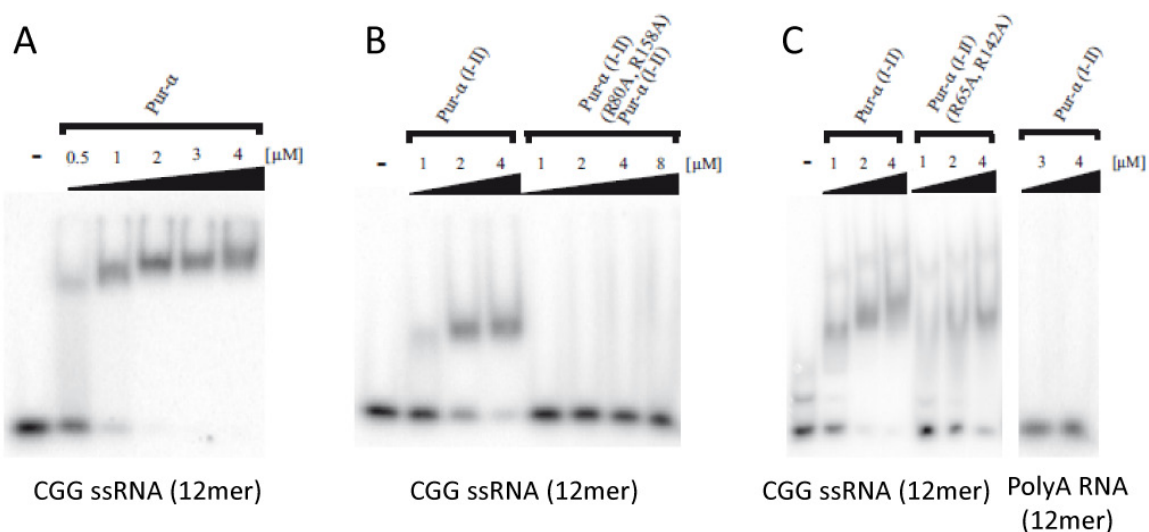


Figure 2-5: RNA binding of different Pur-alpha variants

- A: EMSA with full length Pur-alpha and CGG ssRNA (12mer);
- B: EMSA with Pur-alpha repeat I+II and to CGG ssRNA (12mer); Pur-alpha repeat I+II (R80A R158A) fails to bind to CGG ssRNA (12mer)
- C: EMSA with Pur-alpha repeat I+II (R80A R142A) and CGG ssRNA (12mer); PolyA RNA: control; figures modified after Graebsch et al., 2009

2.4.2 DNA bound functions of Pur-alpha

In humans Pur-alpha was discovered by its binding to a DNA sequence upstream of the *c-myc* gene (BERGEMANN and JOHNSON 1992). There it binds to the purine-rich element (PUR) next to the center of chromosomal replication. The function of Pur-alpha in this case is not fully understood but it is proposed that Pur-alpha stimulates unwinding of the DNA, because it has helix-destabilizing activity (DARBINIAN *et al.* 2001a). Furthermore, in eukaryotes, the PUR elements are conserved in origins of replication (ITOH *et al.* 1998), which argues for a role of Pur-alpha in replication initiation. Pur-alpha might be also involved in replication-dependent repair of DNA lesions, as Pur-alpha deficient cells showed an increased sensitivity for hydroxyurea (a DNA replication inhibitor) (WANG *et al.* 2007) and the anti-tumor drug cisplatin (KAMINSKI *et al.* 2008). In mouse brain extracts Pur-alpha was discovered through its binding capacity to DNA sequences in the promoter region of the *myelin basic protein* gene (HAAS *et al.* 1995). Pur-alpha works as a transcriptional activator for this gene (TRETIKOVA *et al.* 1999), but Pur-alpha can also function as transcriptional repressor. At least 19 genes are known whose transcription might be regulated by Pur-alpha (WHITE *et al.* 2009). Among these target genes are tumor necrosis factor α (TNF- α) (DARBINIAN *et al.* 2001c), Bax (KIM *et al.* 2008), Somatostatin (SADAKATA *et al.* 2000) and transforming growth factor- α (TGF- α) (THATIKUNTA *et al.* 1997). Other negatively regulated genes are genes like α -actin (KNAPP *et al.* 2006), α -myosin (GUPTA *et al.* 2003) and amyloid- β protein precursor (DARBINIAN *et al.* 2008). The transcriptional activation capacity of Pur-alpha can also be hijacked by viruses like e.g. JC polyomavirus (CHEN and KHALILI 1995) and HIV-1 (KRACHMAROV *et al.* 1996). Pur-alpha has negative effects on the transcription of its own gene by auto-regulation of the *pur-alpha* promoter (MURALIDHARAN *et al.* 2001). Additionally, Pur-alpha can control gene expression on translational level, as it was shown that it binds to the mRNA transcript of *vascular smooth muscle α -actin* gene to suppress its translation (KELM *et al.* 1999).

2.4.3 Pur-alpha in cell cycle control and tumor suppression

Many of the genes which are regulated by Pur-alpha are involved in cell proliferation and apoptosis like TNF- α , TGF- β , Bax and Somatostatin (see 2.4.2), one may thus consider Pur-alpha to have a function in cell cycle control. This is underlined by the interaction of Pur-alpha with cellular regulatory proteins like retinoblastoma tumor suppression protein (JOHNSON *et al.* 1995), E2F-1 (DARBINIAN *et al.* 1999), Y-box binding protein (SAFAK *et al.* 1999), CyclinT1/Cdk9(DARBINIAN *et al.* 2001c), Sp1 (TRETIKOVA *et al.* 1999) and CyclinA/Cdk2 (LIU *et al.* 2005). During the cell cycle Pur-

alpha level is oscillating with a peak at mitosis (ITOH *et al.* 1998). Furthermore, a tumor suppressive function of Pur-alpha was observed in several studies. In many transformed and tumor cells, e.g. glioblastoma cells, an overexpression of Pur-alpha suppresses growth (DARBINIAN *et al.* 2001b). Loss of Pur-alpha in prostate cancer leads to faster tumor progression (INOUE *et al.* 2008; WANG *et al.* 2008). This leads to the assumption that Pur-alpha is an essential factor to suppress tumor formation and an important cell cycle regulator which can prevent cell cycle dysfunctions.

2.4.4 RNA bound functions of Pur-alpha

The role of Pur-alpha as a RNA binding protein is linked to the transport of mRNAs in neurons. Pur-alpha binds to BC1 RNA (KOBAYASHI *et al.* 2000). This RNA is a 152-nt long non coding (nc) RNA and controls activity dependent neuronal plasticity by targeting silenced mRNA in RNA transport granules to their final destinations (LIN *et al.* 2008; WANG *et al.* 2005). Both, Pur-alpha and its family member Pur-beta crosslink BC1 mRNA to microtubules (OHASHI *et al.* 2000). The mRNPs in dendrites are equipped with a kinesin motor and are suggested to transport polyribosomes along actin filaments and microtubules. Besides Pur-alpha, mammalian (m)-Staufen, Myosin Va and FMRP are protein components of the transport granules (OHASHI *et al.* 2002). A further study could also identify Pur-alpha in transport complexes in mouse brain together with m-Staufen and FMRP on BC-1 RNA, MAP2- and MAP1B-mRNA (JOHNSON *et al.* 2006).

Pur-alpha also binds to the HIV-1 TAR element, which is a RNA element localized in HIV-1-transcripts (CHEPENIK *et al.* 1998; KRACHMAROV *et al.* 1996). The transcriptional activating ability of Pur-alpha is hijacked by the virus to stimulate its own transcription. A recent study revealed that the HIV-TAR RNA element is processed by Dicer and consequently is a viral microRNA precursor (KLASE *et al.* 2007). Pur-alpha also binds to 7SL-RNA in mouse brain which is involved in developmental stage regulation of the *myelin basic protein* gene (TRETIKOVA *et al.* 1998). 7SL-RNA, BC-1 RNA and the HIV-TAR RNA are all noncoding RNAs which have an intrinsic stem loop structure. This might indicate a common sequence motif for the RNA binding of Pur-alpha.

2.4.5 Pur-alpha knockout mouse

The analysis of homozygous Pur-alpha lacking (PURA-/-) mice revealed a crucial role for Pur-alpha in post natal brain development. The animals appear normal at birth, at two weeks of age the knockout (k.o.) mice develop neurological problems and die at an age of four weeks suffering from tremor and seizures (KHALILI *et al.* 2003). A detailed analysis of the brains showed that there were fewer cells in hippocampus, cerebellum and cortex and also cells that lack proliferation. Furthermore, significantly reduced numbers of synapses were observed (KHALILI *et al.* 2003). A combination of the important functions of Pur-alpha in RNA transport in neurons and the functions in regulation of gene expression might be the reason for this severe phenotype. The presence of the Pur-alpha ortholog Pur-beta might diminish the severity of the phenotype by adopting some of Pur-alpha's functions.

2.5 Triplet-repeat associated diseases

Proper mRNP transport is extremely crucial for maintenance of cellular functions especially in cells with polar structures like neurons. Triplet repeat expansions in non-coding regions of RNAs cause a number of human diseases like myotonic dystrophy, Huntington's disease, spinocerebellar ataxia type 8 and fragile-X associated tremor and ataxia syndrome (FXTAS) (LI and BONINI 2010; ORR and ZOGHBI 2007). One supposed molecular mechanism for the development of these diseases is the sequestration of RNA binding proteins to the overrepresented repeats. Thus, the proteins cannot fulfill their normal cellular functions anymore. In case of a RNA-transport protein, binding to the repeats instead of binding to "zipcode"-sequences may impair transport of mRNAs to their destinations.

2.6 Fragile-X associated tremor and ataxia syndrome (FXTAS)

One of these triplet repeat associated diseases is the fragile-X associated tremor and ataxia syndrome (FXTAS). FXTAS is caused by (CGG)_n-repeats in the 5'-untranslated region (UTR) of the *fragile X mental retardation1 (FMR1)* gene. Normal *FMR1* alleles contain up to 55 CGG-repeats, between 55 and 200 repeats a permutation is persisting, which is causing FXTAS. This permutation occurs in 1 of 1000 males with an onset of the disease in the 5th decade (O'DONNELL and WARREN

2002). The patients suffer from progressive action tremor with ataxia and general brain atrophy leading to cognitive decline and dementia (BERRY-KRAVIS *et al.* 2007). The full mutation of the *FMR1* gene with over 200 CGG repeats causes the Fragile-X syndrome. The hallmarks of the FXTAS pathology are nuclear inclusions in neurons and astrocytes containing *FMR1* mRNA and up to 20 proteins including Pur-alpha (GRECO *et al.* 2006; GRECO *et al.* 2002).

Pur-alpha is supposed to play a major role in the pathogenesis of FXTAS. Jin and colleagues used a *Drosophila* model for FXTAS to show that the expression of r(CGG)₉₀ repeats is sufficient to cause a severe neurodegeneration (JIN *et al.* 2007). They propose that r(CGG)_n-binding proteins like *Drosophila* Pur-alpha are sequestered from the normal functions through their binding to the permutation RNA. The binding of Pur-alpha to r(CGG)_n RNA is direct and specific. Furthermore, overexpression of Pur-alpha can rescue the rough eye-phenotype in their fly FXTAS-model which was caused by the r(CGG)_n mediated neurodegeneration. Thus, they proposed a model in which the loss of functional Pur-alpha protein impairs mRNA-transport in neurons and leads to neuronal cell death.

2.7 Aims of this thesis

Taken all facts together, Pur-alpha is a highly conserved multifunctional protein with widespread roles in replication, transcription, cell cycle control and mRNA transport in neurons. It is therefore relevant for both, neurological diseases and cancer. All these functions are mediated by Pur-alpha as a on the one hand DNA- and RNA-binding protein and on the other hand by interaction with its multiple protein binding partners. Although much is already known about Pur-alpha, some important clues to reveal Pur-alpha's whole implications in cellular functions are still missing.

I therefore wanted to establish functional analysis of Pur-alpha in *Drosophila melanogaster*. The advantage of experiments in this model organism is that in the *Drosophila* genome only one Pur-alpha gene exists, while in mammals there are potentially redundant paralogs like Pur-beta and Pur-gamma. Furthermore, *Drosophila* oogenesis is a well studied and easily accessible model system for the analysis of RNA transport, thus facilitating the analysis of Pur-alpha's role as an RNA transport factor.

As Pur-alpha can bind to hairpin-structures in non coding RNAs like BC-1 RNA (KOBAYASHI *et al.* 2000) and 7SL-RNA (TRETIKOVA *et al.* 1998), and to the viral microRNA precursor HIV-TAR RNA (CHEPENIK *et al.* 1998) I also analyzed a possible function of Pur-alpha in the biogenesis of small RNAs. A possible hint for the implication in these processes is the homology to the discovery of TAR-RNA binding protein (TRBP), which was also found by binding to the HIV-TAR RNA, and is now known as the cofactor of human Dicer (HAASE *et al.* 2005).

The discovery of new Pur-alpha bound proteins and RNAs might shed light on the pathogenesis of FXTAS. The sequestration of Pur-alpha to the overrepresented (CGG)_n-repeats seems to be sufficient for the development of the disease (JIN *et al.* 2007). It is therefore essential to identify the physiological binding partners of Pur-alpha, both proteins and mRNAs, as their de-regulation may be in part responsible for the pathology of the disease.

3. MATERIALS AND METHODS

3.1 Materials

3.1.1 Laboratory equipment:

ABI PRISM 7000 qPCR cycler	Applied Biosystems; Foster City, USA
Agarose gel running chamber	Carl Roth GmbH; Karlsruhe, Germany
FACSCalibur flow cytometer	Becton, Dickinson; Franklin Lakes, USA
Flow buddy CO2-distributer	Genesee Scientific; San Diego, USA
Fly anesthetic pad and pistol	Genesee Scientific; San Diego, USA
INTAS UV Imaging System	INTAS; Göttingen, Germany
LAS 3000 mini Western Imager	Fujifilm; Tokyo, Japan
Leica MZ7 stereomicroscope	Leica Microsystems; Wetzlar, Germany
Leica TCS SP2 confocal microscope	Leica Microsystems; Wetzlar, Germany
PAGE-electrophoresis	BioRad; Hercules, USA
Poly-lysine coated microscope slides	Carl Roth GmbH; Karlsruhe, Germany
Power supply	BioRad; Hercules, USA
Semi-dry blotter BioRad	BioRad; Hercules, USA
SpectroLinker XL1500 UV Crosslinker	Spectronics Corporation; Westbury, USA
SterilGARD cell culture workbench	The Baker Company; Sanford, USA
Table top centrifuge (5417R and 5415R)	Eppendorf AG; Hamburg, Germany
Tank-blotting chamber	BioRad; Hercules, USA
Thermocycler Sensoquest	Sensoquest; Göttingen, Germany
Typhoon 9400 Variable Mode Imager	GE Healthcare; Freiburg, Germany

3.1.2 Laboratory chemicals:

Acrylamide 40%	Carl Roth GmbH; Karlsruhe, Germany
Agarose Biozym	Biozym Scientific GmbH; Oldendorf, Germany
Ampicillin	Carl Roth GmbH; Karlsruhe, Germany
Ammonium peroxodisulfate (APS)	Roth GmbH; Karlsruhe, Germany
Bacto Agar	Becton, Dickinson; Franklin Lakes, USA
Bradford Assay	BioRad; Hercules, USA
Bovine serum albumin (BSA)	New England Biolabs; Ipswich, USA
Chloroform	Merck Biosciences GmbH; Schwalbach, Germany
Complete® without EDTA (Protease-inhibitor)	Roche Diagnostics; Mannheim, Germany
Coomassie G250	Carl Roth GmbH; Karlsruhe, Germany
Desoxyribonucleotides (dA/C/G/TTP)	Sigma Aldrich; Taufkirchen, Germany
Dimethyl sulfoxide (DMSO)	Carl Roth GmbH; Karlsruhe, Germany
Dithiothreitol (DTT)	Carl Roth GmbH; Karlsruhe, Germany
Ethanol (p.a.)	Merck Biosciences GmbH; Schwalbach, Germany
FACS Flow/Clean/Rinse	Becton, Dickinson; Franklin Lakes, USA
Fetal bovine serum (FBS)	Thermo Fisher Scientific; Waltham, USA
Formaldehyde	Sigma Aldrich; Taufkirchen, Germany
Formamide	Sigma Aldrich; Taufkirchen, Germany
Fugene® HD transfection reagent	Roche Diagnostics GmbH; Mannheim, Germany
H2O HPLC quality	VWR; Ismaning, Germany
Hepes	Carl Roth GmbH; Karlsruhe, Germany

Isopropanol (p.a.)	Merck Biosciences GmbH; Schwalbach, Germany
Kanamycin	Carl Roth GmbH; Karlsruhe, Germany
Methanol (p.a.)	Merck Biosciences GmbH; Schwalbach, Germany
Normal goat serum (NGS)	Dianova
Powdered milk	Rapilait Migros; Zürich, Switzerland
Roti®Aqua Phenol/C/I	Carl Roth GmbH; Karlsruhe, Germany
Roti-liquid barrier marker	Carl Roth GmbH; Karlsruhe, Germany
Saponin	Fluka BioCemika; Ulm, Germany
Sodium dodecyl sulphate (SDS)	Merck Biosciences GmbH; Schwalbach, Germany
Sequagel Sequencing System	National Diagnostics; Atlanta, USA
Syber Safe/Gold	Invitrogen; Karlsruhe, Germany
TEMED	Carl Roth GmbH; Karlsruhe, Germany
Triton X-100	Sigma Aldrich; Taufkirchen, Germany
Trizol	Invitrogen; Karlsruhe, Germany
Tween 20	Carl Roth GmbH; Karlsruhe, Germany
[γ 32P] ATP (SRP 501) 10 mCi/ml; 6000 Ci/mmol; 250 µCi	Hartmann Analytic; Braunschweig, Germany

All other standard laboratory chemicals were purchased from the Gene Center in house supply.

3.1.3 Enzymes:

DNase I, RNase free	Fermentas; St. Leon-Rot, Germany
Polynucleotidekinase (PNK) with Buffer	Fermentas; St. Leon-Rot, Germany

Proteinase K	Fermentas; St. Leon-Rot, Germany
T4-DNA Ligase	New England Biolabs; Ipswich, USA
Pfu DNA Polymerase	Fermentas; St. Leon-Rot, Germany
Phusion Hot Start DNA Polymerase	Finnzymes
Superscript II, Reverse Transcriptase	Invitrogen; Karlsruhe, Germany
T7-polymerase	laboratory stock
Taq DNA Polymerase	laboratory stock
Restriction enzymes <i>BamHI, BgIII, NotI, SpeI</i> <i>HinP1I, Mspl, XbaI</i>	New England Biolabs; Ipswich, USA

3.1.4 Other materials:

DyNAmo Flash SYBR Green qPCR Kit	Finnzymes
miScript SYBR Green PCR Kit	Qiagen; Hilden, Germany
QIAGEN Gel extraction Kit	Qiagen; Hilden, Germany
QIAGEN PCR Purification Kit	Qiagen; Hilden, Germany
QIAGEN Plasmid Midi Kit	Qiagen; Hilden, Germany
QIAGEN Plasmid Mini Kit	Qiagen; Hilden, Germany
Sephadex spin column (G25)	Roche Diagnostics GmbH; Mannheim, Germany
Spin column (empty, for IP)	MoBiTec; Göttingen, Germany
SuperSignal West Dura Extended Duration	Thermo Fisher Scientific; Waltham, USA
Whatman 595 ½ Folded Filters	Whatman GmbH; Dassel, Germany

Blotting paper	Machery-Nagel; Düren, Germany
α -Flag affinity agarose A2220	Sigma Aldrich; Taufkirchen, Germany

3.1.5 Bacterial cells:

<i>E.coli</i> XL2-blue CaCl_2 -competent cells	Laboratory stock
---	------------------

All *E. coli* strains were cultivated in LB-medium or in SOC-medium following transformation. Antibiotic containing agar plates were purchased from in-house supply.

SOB-medium

0.5% (w/v) yeast extract
 2% (w/v) Tryptone
 10 mM NaCl
 2.5 mM KCl
 10 mM MgCl₂
 10 mM MgSO₄
 pH 7

SOC-medium

SOB-medium
 20 mM Glucose

LB-medium 1% (w/v) Tryptone

0.5% (w/v) yeast extract
 1% (w/v) NaCl
 pH 7.2

Antibiotics added to medium after autoclaving:

100 µg/ml ampicillin (100 mg/ml stock)
 10 µg/ml kanamycin (10 mg/ml stock)
 25 µg/ml chloramphenicol (34 mg/ml stock)

3.1.6 *Drosophila melanogaster* cells:

63N1	endo-siRNA reporter	Hartig et al., 2009
67-1D	siRNA reporter; two perfect binding sites for miR-277 in <i>gfp</i> 3'-UTR	Förstemann et al., 2007
ban-mi	miRNA reporter; four bulged binding sites for bantam in <i>gfp</i> 3'-UTR	Laboratory stock
S2 B2	parental cell line	Invitrogen; Karlsruhe, Germany

Cell culture medium and additives for *Drosophila* Schneider cells was purchased from Bio & Sell (Nürnberg, Germany) and supplemented with 10% heat-inactivated Fetal Bovine Serum (FBS; Thermo Fisher; Waltham, USA).

3.1.7 Fly stocks:

KG05743	P-element insertion, Dmel\ P{SUPor-P}Pur- $\alpha^{KG05743}$	BL14276	Bloomington Stock center
KG05177	P-element insertion, Dmel\ P{SUPor-P}Pur- $\alpha^{KG05177}$	BL13876	Bloomington Stock center
VDRC101363	<i>pur-alpha</i> RNAi	VDRC101363	VDRC stock center, Vienna
tj-GAL4	traffic-jam GAL4 driver		Kyoto
Actin-GAL4	Actin5C-Gal4 driver	BL3954	Bloomington Stock center

Tubulin-GAL4	Tubulin GAL4 driver	BL5138	Bloomington Stock center
UAS-GFP	UAS-GFP	BL1521	Bloomington Stock center
OrR	wilde type stock		Bloomington Stock center
w¹¹¹⁸	recessive <i>white</i> mutation	BL6326	Bloomington Stock center

3.1.8 Flyfood

Standard fly food was obtained from in-house supply.

5.8% corn meal

5.5% molasses

2.4% yeast extract

Grape-juice plates for egg counting

750 ml grape juice

24 g agar

10 g sucrose

20 ml ethanol

10ml acetic acid

H₂O (ad 1000 ml)

3.1.9 Plasmids:

pKF63	constitutive myc-GFP expression under ubiquitin-promotor control	(FORSTEMANN <i>et al.</i> 2005)
pUAST	conditional expression under GAL4-control	(BRAND and PERRIMON 1993)

pAc5.1B-EGFP-DmDCP1	constitutive GFP-Dcp1 expression, main P-body component	(EULALIO <i>et al.</i> 2007)
pAc5.1B-lambdaN-HA-DmGW182	constitutive GFP-GW182 expression, main P-body component	(BEHM-ANSMANT <i>et al.</i> 2006)
pAc5.1B-EGFP-DmStaufen	Constitutive GFP-Staufen expression, main P-body component	(EULALIO <i>et al.</i> 2007)
pUC18	transfection control vector	(YANISCH-PERRON <i>et al.</i> 1985)
pBluescript	subcloning vector	(ALTING-MEES <i>et al.</i> 1992)

3.1.10 Oligonucleotides:

3.1.10.1 RNA-Interference:

pur-alpha 5'UTR	puralpha5pr_s	CGTAATACGACTCACTATAAGGCAGGGAAATGTTGTACACCGGAC
	puralpha5pr_as	CGTAATACGACTCACTATAAGGCCTCCACTTCCAAATCGGACATTA
pur-alpha 3'UTR	puralpha3pr_s	CGTAATACGACTCACTATAAGGACAACATACCGTGATTACTAAGT
	puralpha3pr_as	CGTAATACGACTCACTATAAGGATATTGGCTAAATGCTACAAAAT
pur-alpha coding	puralpha_cod_s	CGTAATACGACTCACTATAAGGTGTTGCAAATATGGAGGGTTC
	puralpha_cod_as	CGTAATACGACTCACTATAAGGCTCCAAACTCTTAACAAATCTG
GFP	T7prom_GFP_ORF_fw	CGTAATACGACTCACTATAAGGATGGTGAGCAAGGGCGAGGAGCTG
	T7prom_GFP_ORF_rev	CGTAATACGACTCACTATAAGGTTACTTGTACAGCTCGTCCATG
T7-Promotor	T7-Promotor	CGTAATACGACTCACTATAAGG

3.1.10.2 Molecular Cloning:

Ubiquitin-promotor	ubi_prom_sense	GGTTTCTCAACAAAGTTGGCGTCG
SV40-Poly A	SV40polyA_rev	GTGAATTCTACATTGATGAGTTGGAC
GFP in pBluescript	BamHI-GFP-sense	GAGGATCCATGGTGAGCAAGGGCGAGG
	Spel-GFP-as	AGACTAGTCTTGTACAGCTCGCCATGCCG
Pur- α in pBluescript-GFP	Xba-pura-sense	AGTCTAGAACATGCCATTGGAAAGTGGAGA
	notl_pura_as	GAGCGGCCGCTATTAAAGACTATTGAAGATGTAGGTAAGTTA
FLAG-Pur- α in pKF63	Bam_flag_pura_s	ACGGATCCTAAATCGAACAAAAAGCTTACAAATGGATTATAAA GATGATGATGATAAAGGCTCCGATTGGAAAGTGGAGATG
	as pur alpha not	ATGCAGGCCATTATTAAAGACTATTGAAGATGTAGGTAAG
Pur- α -point mutations	puraxba40s	AATCTAGAGTCGAACAGGAATTGGCT
	puraxba115s	AATCTAGACCGGAAGATGGTAAACTT
	Puranot105as	TTATGCGGCCGCTAAGAACCGTAGTAATC
	Puranot185as	TGATGCGGCCGCTAATCATTAGCTCCAAC
	Puranot255as	TTATGCGGCCGCTATTTTCATTTCTCGCA

3.1.10.3 Fly stock mapping:

plac	plac 1	GCTGCACCCAAGGGCTCTGCTCCCACAAT
	plac 4	CGTGAATGTGCGTTAGGTCTGTTATTGTT
pry	pry 1	TTAACCCCTAGCATGTCCGTGGGTTGAAT
	pry 4	TCAACAATCATATCGCTGTCTCACTCA
KG05177	KG05177 sense	CGTGTGTTGATCACTTAAAGCCGTC
	KG05177 antisense	CTGCCCTTACAAATGACATCGAC
KG05743	KG05743 sense	TCTGCCGGATTCTACACGTACATAG
	KG05743 antisense	CCAAACTGCTTATAACGTTCTGTACA

3.1.10.4 Quantitative PCR:

<i>bazooka</i>	baz_forw	GGTCACATGTTCCGCTTG
	baz_rev	TTCTCTCCAGAGCAGCCAAT
	baz_fwd2	TACGAGACGGTTAACAGCA
	baz_rev2	GTCACAAACGGACCTCGACT
<i>torsolike</i>	tsl_s	AAAGATGGCGAGAAGGAA
	tsl_as	CTCGTGGTACCAAGCTCTCCT
	tsl_fwd2	CTGCTGAAACTGCACGGTAA
	tsl_rev2	TGACTCTCGGGCATGTTAAG
<i>absent, small, or homeotic discs 1</i>	ash1_forw	CCGATTGTTGACGACAGTG
	ash1_rev	TTTCCTGCCCTCATCATC
<i>pimet</i>	pimet_forw	ACAATTGAACTCCGAGA
	pimet_rev	GATCAGACCATTCCGATTCC
<i>Decapping protein 2</i>	dcp2_forw	AAATCCTGGACAAACAGCAG
	dcp2_as	CTGTGCATGTACTGGGCATC
<i>ftz transcription factor 1</i>	ftz-f1_s	TGATCGACTTCAAGCACCTG
	ftz-f1_as	CTCGAGGCACCTCTGGAATC
<i>Lim-Kinase</i>	Limk1_s	AATGTGACCACAACGACCAA
	Limk1_as	GACTTGGCAGTGGCTTCAGT
	limK_fwd2	TCACCGATCAGAAGCAGAAA
	limK_rev2	TAGCAGCGCGTATTGAAATG
<i>scarecrow</i>	scro_s	ACCCTTAGCGTGACCGATA
	scro_as	CGTACGGATTGCCATAGTT
<i>Cyclic-AMP resp. element BP A</i>	crebA_s	AACCGTTCCATCTCTGTGG
	crebA_as	CGTTTCTCCTTCCGTCAG
<i>lysosomal enzyme receptor protein</i>	lerp_s	CTTCACACACGAGTCGCCTA
	lerp_as	TTCAAAATTCTGCTGCGTTG

<i>ariadne</i>	ari-1_s	TCGACATACTTGCCAGTGC
	ari-1_as	AGAGCACCGCTTTACAAT
<i>short stop</i>	shot_s	CTGAGCGACAACGAGGGTAG
	shot_as	TGTGATCGTCCGTGCTATCT
<i>dusky body</i>	dyb_s	AGCAACTGGAGGGACTGATG
	dyb_as	GGATGTTGCTGCATCTGCT
<i>CG15745</i>	CG15745_s	AGGATCGCGATGAGGATGAT
	CG15745_as	CGCCTACCTTCTTGGATCG
<i>diego</i>	dgo_s	CCCTTCGCCAACGTATAGTA
	dgo_as	GTGGAATCCTTCCCACGTAA
	dgo_fwd2	TTTACGTGGGAAGGATTCCA
	dgo_rev2	TTGGATGGAAGATTGGGATG
<i>CG4570</i>	CG4570_s	AAGCTGCATTGAGTGTG
	CG4570_as	GGAGGTGTAGTGCGGATTGT
<i>notch</i>	N_fwd	TCAGCAGGCCTTCTACCACT
	N_rev	ATGGCCACCGGATATGTAAA
<i>Abl tyrosine kinase</i>	Abl_fwd	CACAATTGTCGCGTGTGATCTT
	Abl_rev	ACCTGTTAAGCGCATTGGAG
<i>mushroom bodies tiny</i>	mbt_fwd	CCGGAAGTGGATATCTGGTC
	mbt_rev	ATCCGGTCGAGGAAGGACT
<i>Focal Adhesion Kinase</i>	Fak56D_fwd	GATTTGCTTCAAAACACAGGAA
	Fak 56D_rev	GTTCGTTGTCGACCTGGTT
<i>innexin 2</i>	inx2_fwd	TGAGCATCATGTCGGGAATA
	inx2_rev	AGATGAGCGGATCGATGTT
<i>dishevelled</i>	dsh_fwd	GGCTATCAGCCGATCCAGTA
	dsh_rev	GCCGGATGATTGTTAGAGC
<i>delta</i>	DI_fwd	TCGCAAAGCAACTCAACAC

	DI_rev	AAGCTGCAGCCATTAGTTGG
<i>Integrin linked kinase</i>	Ilk_fwd	CTATCAACCGGCTTGGATGT
	Ilk_rev	GGATCCTCGTCATGCAGAT
<i>scab</i>	scb_fwd	TGTCATCCTGACCGACTTGA
	scb_rev	TATCGCAGAGAGAACGAGCA
<i>gapdh</i>	gapdh_s	AATTTTCGCCCGAGTTTC
	gapdh_as	TGGACTCCACGATGTATTG
<i>actin</i>	actin_s	AAGTTGCTGCTCTGGTTGTCG
	actin_as	GCCACACGCAGCTCATTGTA
<i>pur-alpha</i>	for_pura1	CGCTTCTCTAGGTCCACCAAAC
	rev_pura1	CCACCTTCATGTGTCGCTCTTC
<i>rp49</i>	rp49 A2	ATCGGTTACGGATCGAACAA
	rp49 B2	ACAATCTCCTTGCGCTTCTT
<i>argonaute-2</i>	ago2 qPCR s	TCAATGCCGATGATCGAATA
	ago2 qPCR as	GACGCAATGGTGACCTTCTT
<i>piwi</i>	Piwi1 s	TGG AAC ATG GAA CTG GAC AA
	Piwi1 as	GGT CTC TGA AGT GCC TTT GC
<i>argonaute-3</i>	Ago3_1 s	ACA AGC TTA TGC GCG AGA TT
	Ago3_1 as	ACG CCC ACT TAT CTT GTT G
<i>aubergine</i>	Aub1 s	GAT GCT ATT CGC GAC AGT GA
	Aub1 as	AAT GGC GTC GAT TGA AAG TC
<i>argonaute-1</i>	AGO1qPCRs	TGG GAC GAC AAT CAC TTT GA
	AGO1qPCRs	ATG ATA TCT GGC ACG GAA GG
<i>bicoid</i>	BCDqPCRs	ATG AGC ACC GGA ATA AGA GC
	BCDqPCRs	CGT GCA TTG ATA TTG GTT CG
<i>oskar</i>	OSKqPCRs	AAG AGA CGC CAC GAA ATG AC
	OSKqPCRs	TCC ATT CGG GCG AGA TAT AG

<i>gurken</i>	GRKqPCRs	TGC GTT AAC GAC TAC GAT GG
	GRKqPCRas	GTA GAG CGA CGA CAG CAT GA

3.1.10.5 MicroRNA profiling:

scrambled_bantam	AGTGCTAGTATTACAGCTATAT	dme-miR-1003	TCTCACATTACATATTACAG
dme-bantam	TGAGATCATTGAAAGCTGATT	dme-miR-1012	TTAGTCAGGATTTCCCCATAG
dme-let-7	TGAGGTAGTAGGTTGTAGT	dme-miR-1017	GAAAGCTCTACCCAAACTCATCC
dme-miR-1	TGGAATGTAAAGAAGTATGGAG	scrambled_dme-miR-184	AGTAGCGAGATGACATGCGGAC
dme-miR-1	TGGAATGTAAAGAAGTATGGAG	dme-miR-11	CATCACAGTCTGAGTTCTTGC
dme-miR-10	ACCTGTAGATCCGAATTGT	dme-miR-12	TGAGTATTACATCAGGTACTGGT
dme-miR-10*	AAATTGGTTCTAGTGTGGTT	dme-miR-124	TAAGGCACGCCGTGAATGCCAAG
dme-miR-1002	TTAAGTAGTGGATAACAAAGGGCGA	dme-miR-125	TCCCTGAGACCCCTAACTTGTGA
dme-miR-133	TTGGTCCCCTCAACCAGCTGT	dme-miR-252	CTAAGTACTAGTGCCGCAGGAG
dme-miR-13a	TATCACAGCCATTGATGAGT	dme-miR-263a	TTTAATGGCACTGGAAGAATTCAC
dme-miR-13b	TATCACAGCCATTGACGAGT	dme-miR-274	TTTGTGACCGACACTAACGGGT
dme-miR-14	TCAGTCTTTCTCTCTCCTA	dme-miR-275	TCAGGTACCTGAAGTAGCGCGCG
dme-miR-184	TGGACGGAGAACTGATAAGGGC	dme-miR-276*	CAGCGAGGTATAGAGTTCCTACG
dme-miR-184*	CCTTATCATTCTCGCCCCG	dme-miR-276a	TAGGAACCTCATACCGTGCTCT
dme-miR-193	TACTGGCCTACTAAGTCCCAAC	dme-miR-276b	TAGGAACCTTAATACCGTGCTCT
dme-miR-219	TGATTGTCCAACGCAATTCTG	dme-miR-277	TAAATGCACTATCTGGTACGACA
dme-miR-278	TCGGTGGACTTCGTCCGTT	dme-miR-286	TGACTAGACCGAACACTCGTGCT
dme-miR-279	TGACTAGATCCACACTCATTAA	dme-miR-289	TAAATTTAAGTGGAGCCTGCG
dme-miR-281	TGTCATGGAATTGCTCTTTGT	dme-miR-2a	TATCACAGCCAGCTTGATGAGC
dme-miR-282	AATCTAGCCTCTACTAGGCTTG	dme-miR-2b	TATCACAGCCAGCTTGAGGAGC
dme-miR-284	TGAAGTCAGCAACTTGATTCCAG	dme-miR-2c	TATCACAGCCAGCTTGATGGGC

dme-miR-285	TAGCACCATTGAAATCAGTGC	dme-miR-3	TCACTGGGCAAAGTGTCTCA
dme-miR-305	ATTGTACTTCATCAGGTGCTCTG	dme-miR-318	TCACTGGGCTTGTTATCTCA
dme-miR-306	TCAGGTACTTAGTGAECTCTCAA	dme-miR-31a	TGGCAAGATGTCGGCATAGCTGA
dme-miR-306*	GGGGTCACTCTGTGCCGTGC	dme-miR-34	TGGCAGTGTGGTTAGCTGGTTGTG
dme-miR-308	AATCACAGGATTATACTGTGAG	dme-miR-375	TTTGTTCGTTGGCTTAAGTTA
dme-miR-309	GCACTGGTAAAGTTGTCCA	dme-miR-4	ATAAAGCTAGACAACCATATTGA
dme-miR-310	TATTGCACACTTCCCAGCCTT	dme-miR-5	AAAGGAACGATCGTTGTGATATG
dme-miR-311	TATTGCACATTCACCGGCCTGA	dme-miR-7	TGGAAGACTAGTGATTTGTTGT
dme-miR-312	TATTGCACTTGAGACGGCCTGA	dme-miR-79	TAAAGCTAGATTACCAAAGCAT
dme-miR-316	TGTCTTTCCGCTTACTGGCG	dme-miR-8	TAATACTGTCAGGTAAAGATGTC
dme-miR-317	TGAACACAGCTGGTGGTATCCAGT	dme-miR-927	TTTAGAATT CCTACGCTTACC
dme-miR-92a	CATTGCACTTGTCCGGCCTAT	dme-miR-981	TTCGTTGTCGACGAAACCTGCA
dme-miR-92b	AATTGCACTAGTCCGGCCTGC	dme-miR-984	TGAGGTAAATACGGTTGGAATT
dme-miR-932	TCAATTCCGTAGTGCATTGCAG	dme-miR-986	TCTCGAATAGCGTTGTGACTGA
dme-miR-956	TTTCGAGACCACTTAATCCATT	dme-miR-987	TAAAGTAAATAGTCTGGATTGATG
dme-miR-958	TGAGATTCTCTATTCTACTTT	dme-miR-988	CCCCTGTTGCAAACCTCACGC
dme-miR-965	TAAGCGTATAGCTTTCCCCTT	dme-miR-989	TGTGATGTGACGTAGTGGAAC
dme-miR-970	TCATAAGACACACGCGGCTAT	dme-miR-992	AGTACACGTTCTGGTACTAAG
dme-miR-977	TGAGATATTACGTTGTCTAA	dme-miR-993	GAAGCTCGTCTACAGGTATCT
dme-miR-980	TAGCTGCCTGTGAAGGGCTTA	dme-miR-994	CTAAGGAAATAGTAGCCGTGAT
dme-miR-995	TAGCACCACATGATTGGCTT	dme-miR-999	TGTTAACTGTAAGACTGTGTCT
dme-miR-996	TGACTAGATTCATGCTCGTCT	dme-miR-9a	TCTTTGGTTATCTAGCTGTATGA
dme_mdg1	AACAGAAACGCCAGCAACAGC	dme-miR-9b	TCTTTGGTGATTTAGCTGTATG
dme-miR-998	TAGCACCATGAGATTAGCTC	dme-miR-9c	TCTTTGGTATTCTAGCTGTAGA
dme-CG4068_B	TTGACTCCAACAAGTTCGCTC	as_dme_2S-rRNA	CAACCCTCAACCATATGTAGT
dme-tRNA-CR32359	CGTGGGTTCGAACCCCCACTTC	dme-miR-998	TAGCACCATGAGATTAGCTC

dme_RP49_A2	ATCGGTTACGGATCGAACAA	dme-miR-999	TGTTAACTGTAAGACTGTGTCT
dme_RP49_B2	ACAATCTCCTGCGCTTCTT	dme_snRNA_U6	CAAAATCGTAAGCGTTCCAC

3.1.10.6 Northern Blotting

2S-rRNA	2S-rRNA RNA as probe	TACAACCCTAACCATATGTAGTCCAAGCA
bantam	2' O-Me-bantam as probe	AATCAGCTTCAAAATGATCTCA
miR-277	2' O-Me-miR-277 as probe	TGTCGTACCAGATA GTGCATTAA
miR-34	2' O-Me-miR-34 as probe	CACACCCAGCTAACCA CACTGCCA
miR-317	2' O-Me-miR-317 as probe	ACTTGTGTCGACCACCATA GGTCA

3.1.10.7 Electrophoretic mobility shift assays (EMSA)

r(CGG) ₄	Flourescein-conjugated	CGG CGG CGG CGG
r(CAG) ₄	Flourescein -conjugated	CAG CAG CAG CAG
r(CAG) ₃ (CAA)	Flourescein -conjugated	CAG CAG CAG CAA
r(CAA) ₄	Flourescein -conjugated	CAA CAA CAA CAA

3.1.11 Antibodies:

3.1.11.1 Primary antibodies:

α -notch	C458.2H and C17.9C6	1:200 Immunofluorescence 1:1000 Western Blotting	DSHB
α -FasIII	7G10 anti-FasciclinIII	1:200 Immunofluorescence	DSHB

α-eya	eya10H6	1:200 Immunofluorescence	DSHB
α-armadillo	N2_7A1Armadillo	1:200 Immunofluorescence	DSHB
α-hts	hts_RC	1:200 Immunofluorescence	DSHB
α-orb	orb6H4 and 4H8	1:200 Immunofluorescence	DSHB
α-Me31B	α-Me31B	1:1000 Western Blotting	Kind gift of A. Nakamura, RIKEN Center, Kobe, Japan
α-Cup	α-Cup	1:1000 Western Blotting	Kind gift of A. Nakamura
α-Tral	α-Tral	1:1000 Western Blotting	Kind gift of A. Nakamura
α- β-tubulin	β-tub E7	1:2000 Western Blotting	DSHB
α-Flag	α-Flag M2	1:2000 Western Blotting	Sigma, F1804
α-GFP	B-2; sc-9996	1:2000 Western Blotting	Santa Cruz Biotechnology
α-FMRP	5A11 and 5B6	1:1000 Western Blotting	DSHB
α-Ago1	1b8	1:1000 Western Blotting	(OKAMURA <i>et al.</i> 2004)
α-Ago2	rb α-Ago2	1:500 Western Blotting	lab generated peptide antibody, Davids
α-Pur-alpha	7H8 and 1E10	1:1000 Western Blotting 1:3 Immunofluorescence (supernatant)	gift of Elisabeth Kremmer, Helmholtz-Zentrum München, Germany

3.1.11.2 Secondary antibodies:

Goat α-mouse IgG (H+L) HRP-coupled	1:10 000	Pierce (Thermo Scientific)
Goat α-rabbit IgG (H+L) HRP-coupled	1:50 000	Pierce (Thermo Scientific)

Cy3-coupled α-rat IgG (H+L)	1:200	Molecular Probes, Invitrogen, Carlsbad / CA, USA
Cy3-coupled α-mouse IgG (H+L)	1:200	Molecular Probes, Invitrogen, Carlsbad / CA, USA
Alexa-Fluor 488-coupled α-mouse IgG (H+L)	1:200	Molecular Probes, Invitrogen, Carlsbad / CA, USA

3.1.12 Commonly used buffers and stock solutions:

Buffer A for fly DNA extraction	100 mM	Tris/HCl, pH 7.5
	100 mM	EDTA
	100 mM	NaCl
	0.5%	SDS
Church buffer	1% (w/v)	bovine serum albumine (BSA)
	1 mM	EDTA
	0.5 M	phosphate buffer
	7% (w/v)	SDS
		pH 7.2
Colloidal Coomassie staining solution	50 g/l	aluminum sulfate
	2% (v/v)	H ₃ PO ₄ (conc.)
	10% (v/v)	ethanol
	0.5% (v/v)	Coomassie G250 stock
DNA loading buffer (6x)	0.25% (w/v)	bromophenol blue
	0.25% (w/v)	xylene cyanol
	30% (w/v)	glycerol

Formamide loading dye (2x)	80% (w/v)	formamide
	10 mM	EDTA, pH 8
	1 mg/ml	xylene cyanol
	1 mg/ml	bromophenol blue
Laemmli SDS loading buffer (2x)	100 mM	Tris/HCl, pH 6.8
	4% (w/v)	SDS
	20% (v/v)	glycerol
	0.2% (w/v)	bromophenol blue
	200 mM	DTT (freshly added)
 Lysis buffer for protein extraction		
	100 mM	KAc
	30 mM	HEPES
	2 mM	MgCl ₂
	1 mM	DTT
	1% (v/v)	Triton X-100
	2x	Complete® without EDTA (=protease inhibitor cocktail)
 PBS-T/TBS-T	PBS/TBS supplemented with 0.05% Tween-20	
 SDS-running buffer (5x)		
	125 mM	Tris/HCl, pH 7.5
	1.25 M	glycine
	5%	SDS
 SSC (20x)		
	3 M	NaCl
	0.3 M	sodium citrate
 TAE (50x)		
	2 M	Tris-base
	5.71%	acetic acid (0,9 M)
	100 mM	EDTA

TBE (10x)	0.9 M	Tris base
	0.9 M	boric acid
	0.5 M	EDTA (pH 8)

TBS (10x)	50 mM	Tris
	150 mM	NaCl
	pH 7.4	

Western blotting stock (10x)	250 mM	Tris/HCl, pH 7.5
	1.92 M	glycine

Western blotting buffer (1x)	10%	Western blotting stock (10x)
	20%	methanol

3.2 Methods

3.2.1 Methods for molecular cloning

The Pur-alpha sequence was PCR amplified from fly cDNA and N-terminal GFP-fusions of the described Pur-alpha-protein variants were cloned *Bam*HI / *Not*I into the backbone of pKF63, resulting in constitutive expression under control of the ubiquitin promotor (FORSTEMANN *et al.* 2007). The point mutations R80A, R158A and R226A were generated with overlap extension PCR as described in (GRAEBSCH *et al.* 2009).

Standard PCR reaction mix and conditions:

Standard reaction mixture:

Template DNA	1 µl
forward primer (10µM)	0,5 µl
reverse primer (10µM)	0,5 µl
10x Taq-buffer with (NH ₄) ₂ SO ₄	5 µl
25 mM MgCl ₂	4 µl
Taq-polymerase	0,3 µl
Pfu-Polymerase	0,2 µl
H ₂ O	add 50 µl (38,5 µl)

For overlap extension PCR 5 µl DMSO was additionally added.

Standard thermocycler protocol:

	5 minutes	95°C initial denaturation
35 cycles:	1 minute	95°C denaturation
	30 seconds	55°C annealing
	1 minute per kb product size	72°C extension
	5 minutes	72°C final extension
	storage at	4°C

After amplification the PCR-products were analyzed by separation on an agarose gel (0,5-2% according to expected product size), excised and purified with Qiagen Gel Extraction Kit followed by digestion with appropriate required restriction enzymes according to the manufacturer's instructions. All further vector preparation, ligation, bacterial transformation and cloning steps were performed according to common laboratory practice described in (Sambrook and Russell, 2001, "Molecular Cloning", CSHL Press).

The correctness of the sequences of the obtained plasmids was verified by sequencing (Eurofins MWG, Ebersberg, Germany) and for further analysis of the sequences ApE was used (a free online sequence analysis tool, A plasmid Editor; <http://biologylabs.utah.edu/jorgensen/wayned/ape/>). The sequences of the oligonucleotides used for molecular cloning are listed in 3.1.10.2.

3.2.2 Methods with *Drosophila* Schneider 2 cells

Maintenance:

Cells were cultured in Schneider's Medium (Bio&Sell, Nürnberg, Germany) containing 10% heat inactivated fetal bovine serum (Thermo Fisher Scientific, Waltham, USA) in appropriate cell culture dishes (Sarstedt, Nümbrecht, Germany). Cells were split once to twice a week into fresh medium for up to 25 passages.

3.2.2.1 RNA-Interference (RNAi)

DsRNA for RNAi was generated using *in vitro* transcription (IVT) with T7-polymerase. Therefore, templates of the genes of interest were used in which T7-promotor sites were introduced by PCR and afterwards further amplified by PCR using T7-promotor primer (used oligonucleotides see 3.1.10.1).

The resulting PCR products were precipitated with ethanol and applied for over-night *in-vitro* transcription at 37°C.

IVT-Mix:

10 µl T7-template DNA
10 µl 10x T7-buffer
0.5 µl 1 M DTT
5 µl 100 mM ATP
5 µl 100 mM CTP
5 µl 100 mM UTP
8 µl 100 mM GTP
2 µl T7-polymerase
ad 100 µl H₂O (54,5 µl)

1 µl of DNasel was added per reaction and incubated for 30 minutes at 37 °C. The precipitate of magnesium pyrophosphate which formed during the reaction was pelleted and the dsRNA was precipitated from the supernatant with 1x volume of isopropanol and washed twice with 70% ethanol. The pellet was air-dried and re-dissolved in 100 µl of RNase free H₂O. The sample was heated to 95°C for 5 minutes and slowly cooled down to room temperature. Concentration of dsRNA was estimated from an agarose gel in comparison to a DNA Ladder Mix (Fermentas; St. Leon-Rot, Germany).

To induce a knock down of a gene of interest cells were seeded at 0,5*10⁶ cells/ml and 1 µg of the corresponding dsRNA was added to the medium. After incubation with the dsRNA for 5 days the resulting GFP fluorescence of the reporter cell lines was determined in a Becton Dickinson FACSCalibur flow cytometer. For this analysis 100 µl of cells were added to 200 µl of FACS flow. For each sample 10 000 cells were measured. Analysis of fluorescence intensity was carried out with CellQuest software (Becton Dickinson; Franklin Lakes, USA). All measurements were performed in triplicates to calculate mean and standard deviations. GFP-negative reporter cells were excluded from the analysis and the mean fluorescence value for each sample was determined.

3.2.2.2 Transfection of plasmid DNA

Transfection was carried out as described in (SHAH and FORSTEMANN 2008).

50-300 ng DNA of the relevant plasmid was transfected per 24-well cell-culture dish using 4 µl Fugene Transfection reagent (Roche Diagnostics; Mannheim , Germany) and cells were harvested after 48 hours after transfection to perform further experiments.

3.2.2.3 Analysis of Schneider cells by fluorescence microscopy

Transfected cells were harvested and once washed with Schneider's Medium without FBS. Then 100 µl of cell suspension was allowed to settle down within a Roti-Liquid Barrier marker (Carl Roth GmbH; Karlsruhe, Germany) painted circle on a Poly-lysine coated microscope slide (Carl Roth GmbH; Karlsruhe, Germany) for 30 minutes in a humid chamber. Cells were fixed for 15 minutes with 4% formaldehyde and washed three times for 5 minutes in PBS + 0,2% Triton X-100 (PBT), then blocked for 1 hour with PBT containing 5% normal goat serum (NGS) in the humid chamber. Primary antibodies were added in blocking solution and incubated overnight at 4°C. Cells on the slides were washed three times with PBT, secondary antibodies were diluted in PBT and incubated 2-6 hours at room temperature, followed by three 5 minute washing steps with PBT. DNA was stained with DAPI (final concentration 0,5µg/ml) for 5 minutes at RT. Cells were washed with PBT, mounted with DABCO glycerol mounting medium (Ono et al., 2001) and examined with a Leica TCS SP2 confocal microscope (Leica Microsystems, Wetzlar, Germany).

The used primary and secondary antibodies and the applied dilutions can be found in 3.1.11 and 3.1.12.

3.2.3 Methods with flies

3.2.3.1 Maintenance and handling

The fly stocks were maintained on standard agar food at 25°C or 30°C (restrictive temperature). The alleles *pur-alpha*^{KG05177} and *pur-alpha*^{KG05743} were obtained from the Bloomington Stock Center. The plasmids GFP-Pur-alpha full-length, GFP-Pur-alpha repeat I+II, GFP-Pur-alpha repeat I+II R80A R158A, GFP-Pur-alpha full-length R80A R158A, GFP-Pur-alpha full-length R80A R158A R226A and GFP-Pur-alpha R65A R142A were generated as described in 3.2.1 and injected into *w¹¹¹⁸* embryos (Rainbow Transgenic Flies, Newbury Park / Ca, USA), transgenic lines were established after two generations of back-crossing to *w¹¹¹⁸*.

3.2.3.2 Egg laying experiments

Virgin females (OregonR, *pur-alpha*^{KG05177}, *pur-alpha*^{KG05743}, trans-heterozygous animals or rescue lines) were collected over 24 hours and then mated 96 hours at 30°C with wild type (OregonR) males. 15 female flies were kept on grape juice agar (750 ml grape juice, 24 g agar, 10 g sucrose, 20 ml ethanol, 10ml acetic acid, H₂O ad 1000 ml) for 16 hours at 30°C. Subsequently, the deposited eggs were counted under a stereomicroscope.

3.2.3.3 Rescue experiments

For the rescue experiments flies were crossed as depicted in the crossing scheme in the results part of this study (Figure 4-18).

3.2.3.4 Analysis of ovaries by fluorescence microscopy

Ovaries were dissected in FACS-Flow (Becton Dickinson, Franklin Lakes / NJ, USA), fixed for 15 minutes with 4% formaldehyde and washed three times for 10 minutes in PBS + 0,2% Triton X-100 (PBT) then blocked for 1-4 hours with PBT containing 5% normal goat serum (NGS). Primary antibodies were added in blocking solution and incubated overnight at 4°C. Ovaries were washed three times with PBT, secondary antibodies were diluted in PBT and incubated 2-24 hours at 4°C, followed by three 10 minute washing steps with PBT. DNA was stained with DAPI (final concentration 0,5µg/ml) for 5 minutes at RT. Ovaries were washed with PBT three times, mounted with DABCO glycerol mounting medium (ONO *et al.* 2001) and examined with a Leica TCS SP2 confocal microscope (Leica Microsystems, Wetzlar, Germany) .

The used primary and secondary antibodies and the applied dilutions can be found in 3.1.11 and 3.1.12.

3.2.4 Protein analysis

3.2.4.1 Protein extraction

Ovaries were dissected, washed once in PBS (Invitrogen) and the cells lysed with a microcentrifuge tube fitting pestle in lysis buffer (100mM KoAc ph7,4, 30 mM HEPES ph 7,4, 2 mM MgCl₂, 1 mM DTT, 1% Triton X-100, 2x Preotease-Inhibitoren (Roche Diagnostics GmbH; Mannheim, Germany) (HARTIG *et al.* 2009) and frozen in liquid nitrogen. Samples were thawed on ice and cell debris was pelleted in a refrigerated microcentrifuge (Eppendorf; Hamburg, Germany) at 16 400 rpm. To reduce the lipid content, ovary extracts were passed through a Sephadex G-10 spin-column placed in a microcentrifuge tube.

Cells were harvested (2,500 x g, 10 min) and washed with PBS. The pellet was resuspended in lysis buffer and frozen in liquid nitrogen. Samples were thawed on ice and centrifuged at 4°C in a micro-centrifuge at 16,400 rpm (Eppendorf; Hamburg, Germany).

Protein concentrations were determined by Bradford assay (BioRad; Hercules, USA).

3.2.4.2 Co-immunoprecipitation

For immunoprecipitation 0,5-2 µg total protein were incubated with 30 µl of pre-washed GFP-trap A beads (Chromotek, Martinsried, Germany) or FLAG-M2 Agarose (Sigma) for 60 minutes at 4°C, then the unbound fraction and beads were separated by spin colums (MoBiTec; Göttingen, Germany). The beads were washed five times with 600 µl lysis buffer containing 1% Triton as described (HARTIG *et al.* 2009). The bound proteins were eluted by heating the samples to 95 °C with 20 µl 1x Laemmli buffer diluted with lysis buffer.

3.2.4.3 Western-Blotting

Western-Blotting was performed as previously described in (FORSTEMANN *et al.* 2007). Briefly, proteins were separated using 8-15 % polyacrylamide gels for 90 minutes at 150 V in a BioRad electrophoresis tank. Proteins were transferred to a polyvinylidenefluoride (PVDF; Milipore; Billerica, USA) membrane by tank blotting (300 mA for 60 minutes). Afterwards the membrane was blocked in 5% milk for at least 30 minutes at room temperature. Incubation with primary antibodies was carried out over night at 4°C in a 50 ml Falcon tube using 2,5 ml antibody dilution in 1x PBS/TBS-solution with 0,05% Tween. The used antibodies and dilutions employed are listed

in 3.1.11. For rabbit antibodies PBS-T (0.05% Tween) was used during all following washing steps, for mouse antibodies TBS-T (0.05% Tween) was employed. After primary antibody binding the membrane was washed three times 10 minutes in buffer and incubated with appropriate secondary antibody for 4 h at room temperature. After the washing steps, Enhanced Chemiluminescence (ECL) substrate (Thermo Fisher Scientific; Waltham, USA) was applied and the resulting signal was measured in an LAS3000 mini Western Imager System (Fujifilm; Tokyo, Japan). If necessary, Western blots were stripped with 10 ml of Restore Stripping Solution (Thermo Fisher Scientific; Waltham, USA) for 15 minutes at 37°C and 15 minutes at room temperature, washed with buffer and blocked with 5% milk for second primary antibody incubation.

3.2.4.4 Mass spectrometry

The bound fractions after co-immunoprecipitation were analyzed either by Western blotting (3.2.4.3) or separated on a 4-20% polyacrylamide gradient gel (Pierce Thermo Fisher, Rockford / IL, USA) and slices corresponding to a size range of ~30kDa-size were cut out (Chapter 4.4, Figure 4-27). Protein identification was performed by LC-MS/MS (ZfP München).

3.2.4.5 Electrophoretic mobility shift assay (EMSA)

Recombinant protein Pur-alpha I+II and Pur-alpha I+II+III (a kind gift from Janine Weber, Niessing Group, Helmholtz-Zentrum, München) was diluted in binding buffer (20 mM Tris ph 7,4, 100 mM KAc, 3,5 mM MgCl₂, 0,1% BSA, 0,01% Tween) in serial dilutions (0, 250, 500, 750, 1000, 1500, 2000, 3000, 5000, 7500 nM) and incubated for 30 minutes with 100 nM Fluorescein-conjugated RNA-Oligo (see 3.1.10.7) protected from light at room temperature. Reaction mixtures were loaded onto 4% 0,5x TBE polyacrylamide gels in 1x native loading dye (2x loading dye: 10% Glycerin, 2 µg/ml BSA, 2 mM DTT, 0,2 µg/ml Salmon Sperm DNA (SSD)) and analyzed after electrophoresis (180 V, 20 minutes) with Typhoon 9400 Variable Mode Imager (GE Healthcare; Freiburg, Germany) (excitation 488 nm, emission 520 nm). The bound to total ratio was determined using ImageJ (<http://rsbweb.nih.gov/ij/>). Binding curves were fitted using OriginPro 8.1G with the Dose Response (Logistic) fitting function.

$$y = A_2 + (A_1 - A_2) / (1 + (x/x_0)^p)$$

A₁ initial value (left horizontal asymptote)

A₂ final value (right horizontal asymptote)

x₀ center (point of inflection)

p power (similar to dx, but can be loosely described as the parameter that affects the slope of the area about the inflection point)

3.2.5 RNA analysis

3.2.5.1 RNA isolation

RNA was extracted using TRizol (Invitrogen; Carlsbad / CA, USA) from cells, whole ovary extracts or the GFPtrap beads after immunoprecipitation according to the manufacturer's instructions and quantified using spectrophotometry.

3.2.5.2 Northern Blotting

1-5 µg of RNA were separated on a 20% Sequagel Acrylamid-Urea Gel (National Diagnostics; Atlanta/USA) at 200 V for 1-2 hours. RNA transfer was performed on a Nylon membrane (Roche Diagnostics; Mannheim, Germany) by semi dry blotting for 30 minutes at 20 V. Crosslinking of the RNA to the membrane was achieved by radiation with UV-light. Membranes were pre-hybridised in Church buffer (1% (w/v) bovine serum albumine, 1 mM EDTA, 0.5 M phosphate buffer , 7% (w/v) SDS, pH 7.2) for at least 2 hours in an oven under constant rotation. The probes were labeled with [γ -³²P] ATP using PNK (Fermentas). Hybridization with labeled antis-probes was performed overnight in 5 ml Church buffer. Membranes were washed three times for 20 minutes with 2x SSC 0.1% SDS and exposed on Phosphoimager Screens (FujiFilm; Tokio, Japan). Stripping of the membrane was achieved by dipping it into boiling 1% SDS solution and incubating it for 5 minutes in the solution. After a second pre-hybridization the membrane was reused for hybridization with further probes.

3.2.5.3 Quantitative RT-PCR

The messenger RNA content of the co-immunoprecipitates was analyzed with qRT-PCR on an ABI Prism 7000 sequence detection system (Applied Biosystems Life Technologies, Carlsbad / CA, USA). Reverse transcription was performed with Superscript II reverse transcriptase (Invitrogen, Carlsbad / CA, USA) primed with oligo(dT) (New England Biolabs; Ipswich, USA).

The microRNA content of bound and input fractions was analyzed using the miScript system (Qiagen, Hilden, Germany). The obtained bound mRNA after CoIP and 10% of the corresponding input RNA was reverse transcribed according to the miScript protocol.

Reaction mix for reverse transcription:

10 µl RNA
4 µl miScript RT buffer (5x)
5 µl H₂O
1 µl miScript enzyme mix

All samples were incubated at 37°C for 60 min and then inactivated at 95°C for 5 min. 30 µl of water was added to the samples.

The qPCR reaction mix for a 96 well plate was:

500 µl 2x Sybr-Green Mastermix (Dynamo Flash, Finnzymes)
20 µl cDNA
20 µl ROX
360 µl H₂O

9 µl of the mastermix solution was aliquoted in each well of a 96 well plate using an 8-canal pipette. 1 µl of premixed 10 µM sense and antisense oligonucleotide (sequences in 3.1.10.4) was added and the samples cycled on an ABI Prism 7000 sequence detection system using the following PCR-program:

	3 minutes	95°C	initial denaturation
40 cycles:	1 minute	95°C	denaturation
	30 seconds	55°C	annealing
	30 seconds	72°C	extension

The primer sequences for mRNA and miRNA amplification can be found in chapter 3.1.10.4 and 3.1.10.5. Expression was quantified with the $2^{-(\Delta\Delta Ct)}$ method (LIVAK and SCHMITTGEN 2001) and the percentage of recovery after CoIP was determined by comparing input with bound.

3.2.5.4 microArray

Total RNA was prepared from ovary extracts as well as GFP co-immunoprecipitates of GFP-Pur-alpha (full-length) or myc-GFP expressing flies. The RNA was spectrophotometrically quantified and 100 ng were analyzed with Affymetrix Drosophila genome 2.0 arrays (Affymetrix, Santa Clara / CA, USA). One array hybridization was performed for each input and immunoprecipitated RNA sample (four arrays total). Normalization and data analysis was performed with R! / Bioconductor (Björn Schwalb and Achim Tresch, Gene Center; Munich, Germany).

4. RESULTS

4.1 Pur-alpha has no impact on small RNA biogenesis pathways

The binding of Pur-alpha to the HIV-TAR RNA as well as its co-localization and genetic interaction with Ago1 and FMRP, motivated us to search for a role of Pur-alpha in the microRNA biogenesis pathway using cell culture experiments. At first, experiments were carried out to see if a knock down of the Pur-alpha mRNA is possible in *Drosophila* Schneider 2 cells. To achieve the knock down three different double stranded (ds) RNA constructs, which were homologous to the Pur-alpha sequence either in the 3'UTR, the 5'UTR or the coding region of the gene, were used. Using a RNAi trigger outside of the open reading frame (ORF) of *pur-alpha* would alleviate further experiments, e.g. rescue experiments in which a mutated or different ORF construct is analyzed after knock down of the endogenous Pur-alpha protein. Knock down with the unspecific vector RNA served as a control. Figure 4-1 shows *pur-alpha* mRNA expression after 5 day dsRNA treatment normalized to the control. All three constructs were able to knock down *pur-alpha* mRNA. The 5'UTR fragment showed the strongest effect, a 20-fold decrease of *pur-alpha* mRNA level to 5%.

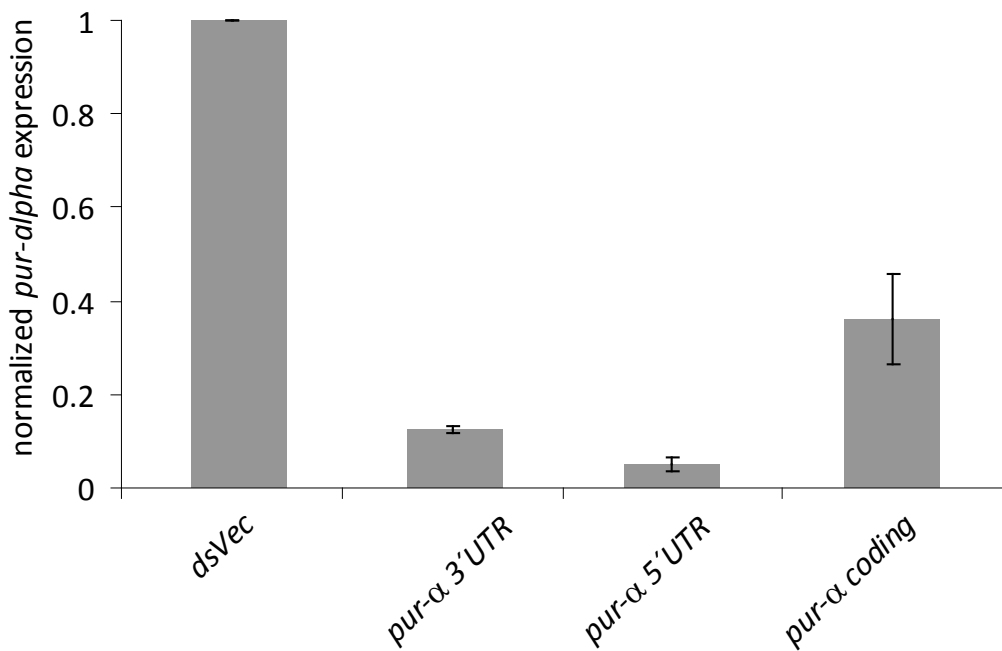


Figure 4-1: Pur-alpha expression in *Drosophila* Schneider cells after RNAi treatment

0,5*10⁶ *Drosophila* Schneider cells were treated with 1 µg of dsRNA as indicated above for 5 days, *pur-alpha* expression was analyzed with qRT-PCR, bar chart displays to the control *dsVec* normalized *pur-alpha* expression.

To assess the question whether Pur-alpha plays a critical role in small RNA biogenesis or their function, reporter cell lines expressing GFP under smallRNA control were used. Thereby an increased or decreased GFP-reporter fluorescence after pur-alpha knock down would reflect the functionality of the different pathways and reveal a potential influence of Pur-alpha.

In Figure 4-2 the mean GFP-fluorescence of Schneider cells after a five day treatment with corresponding dsRNA normalized to the control knock down with *vector* dsRNA measured by flow cytometry is depicted. Figure 4-2A shows the response of a siRNA reporter (67-1D) with two perfect matching sites for miR-277 in the 3'UTR of *gfp*. Knock down of Argonaute-2 (Ago2) results in an increased GFP-fluorescence, which can be explained by the fact that Ago2 is a major component of the RISC (RNA induced silencing complex) which mediates siRNA function. Knock down of GFP itself leads to 55% decrease in fluorescence (Figure 4-2A). No significant decreased or increased fluorescence could be observed, when any of the three dsRNAs against *pur-alpha* mRNA was used. Thus, Pur-alpha seems to be not participating in siRNA mediated gene regulation.

Similar results were observed for the cell line 63N-1 (Figure 4-2B), which served as suitable reporter for the endo-si RNA pathway (Hartig et al., 2009). Control knock-downs with either *dsGFP* or *dsAgo2*, the corresponding effector protein, yielded the expected fluorescence levels whereas dsRNA treatment with *pur-alpha* complementary sequence showed no effects. The analysis of microRNA reporter systems also showed no influence of the knock down of pur-alpha on reporter fluorescence (data not shown).

Altogether, Pur-alpha has no direct effect on small RNA function.

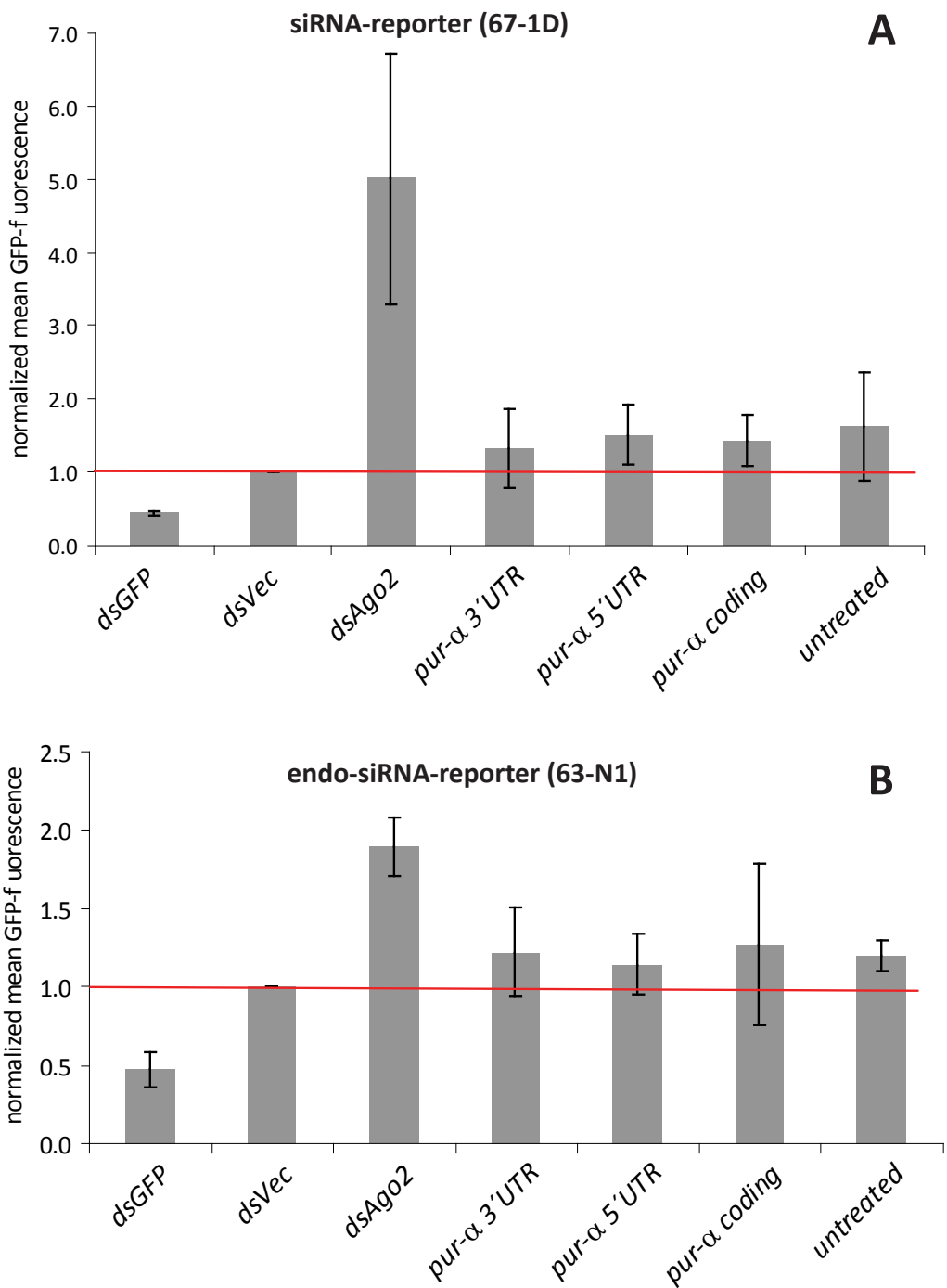


Figure 4- 2: GFP-fluorescence of reporter cell-lines after dsRNA treatment

Reporter cell-lines were treated with 1 μ g of the appropriate dsRNA as depicted at the x-axis for five days, the resulting GFP-fluorescence was analyzed by FACS, the bar-charts display the normalized mean GFP-fluorescence; the red line at 1 indicates no change

A: siRNA reporter 67-1D with two perfect match microRNA-277 sites

B: endo-siRNA reporter 63N-1

4.2 Localization of Pur-alpha

4.2.1 *Drosophila* Schneider 2 cells

4.2.1.1 Pur-alpha bodies are no P-bodies

P-bodies are cytoplasmic foci of mRNA storage and decay. To find out whether Pur-alpha is localized in P-bodies and might have an internal function in mRNA turnover, immunostainings of *Drosophila* Schneider cells were prepared and analyzed using confocal microscopy.

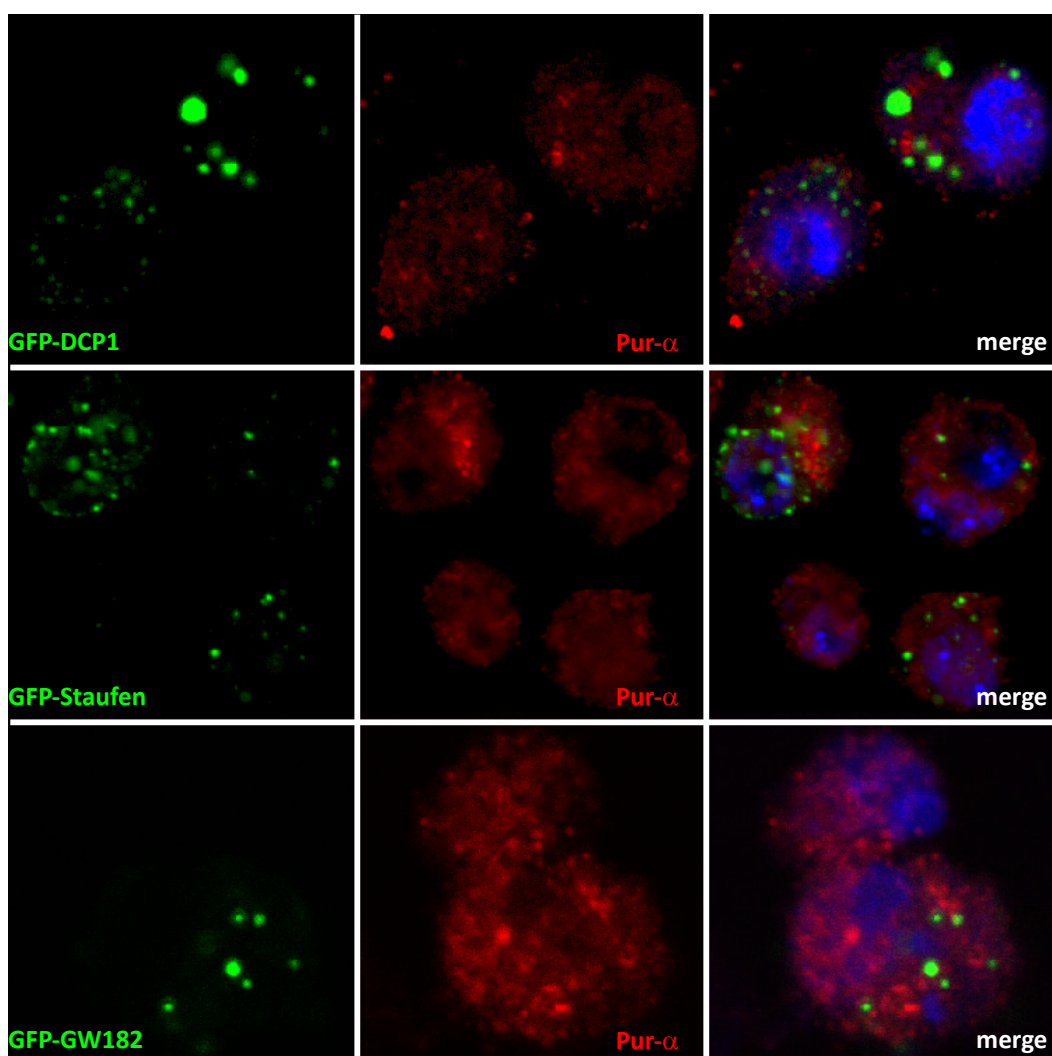


Figure 4-3: Immunostainings of P-body components and endogenous Pur-alpha in *Drosophila* Schneider cells

Schneider cells were fixed, permeabilized, stained with affinity purified α -Pur-alpha antibody and TOTO3; and visualized by confocal microscopy; green: P-body components (DCP1, Staufen, and GW182) as depicted in left panels; red: endogenous Pur-alpha, secondary antibody Cy3-conjugated α -rabbit; blue: TOTO3 stained DNA

Three different GFP-fusion constructs of well known P-body components were transiently transfected into S2 cells and endogenous Pur-alpha was stained using a polyclonal rabbit antibody. This antibody was generated against a C-terminal peptide of the Pur-alpha protein. The upper panel in Figure 4-3 shows in green color GFP-marked decapping enzyme 1 (DCP1), the middle panel GFP-Staufen and the lower panel GFP-GW182. Regarding the localization of the green foci which represent P-bodies and the red Pur-alpha particles no co-staining can be observed. Yellow spots in the merged pictures right would indicate a co-localization, respectively.

To further analyze the appearance of the Pur-alpha bodies in S2-cells different GFP-fusion proteins variants were generated and transiently transfected. The design of the different protein variants was structure-guided after (GRAEB SCH *et al.* 2009) and the GFP-fusion constructs were expressed in cell culture under the control of the constitutively active ubiquitin-promotor. Hence, a visible difference in localization would display the consequence of direct protein transport or localization and not of different expression patterns. Figure 4-4 shows the resulting Pur-alpha localizations in Schneider cells. The expression of Pur-alpha PUR repeat I and II with two point mutations R80A and R158A (Figure 4-4B), which lead to a monomeric Pur-alpha protein with decreased RNA binding capacity results in an enriched localization in the nucleus and a diffuse spreading in the cytoplasm compared to wild-type full length Pur-alpha (Figure 4-4A). Figure 4-4C shows a construct with the same point mutations like in 4-4B in the context of the full-length protein. This protein variant still has the possibility to form hetero-dimeric protein complexes with the endogenous Pur-alpha protein (Figure 4-5). Regarding the localization of this construct there is some diffuse spreading in the cytoplasm compared to wilde type (Figure 4-4A) but no enrichment in the nucleus. Figure 4-4D displays a protein version where in the full length context the according Arginine residue in the third PUR-repeat is also mutated into Alanin. The diffuse spreading in the cytoplasm gets more severe, but compared to figure 4-4B the nuclear enrichment is missing. Taken together, the correct wild-type-like localization of Pur-alpha in Schneider cells is dependent on the ability of the protein to dimerize and to bind to RNA.

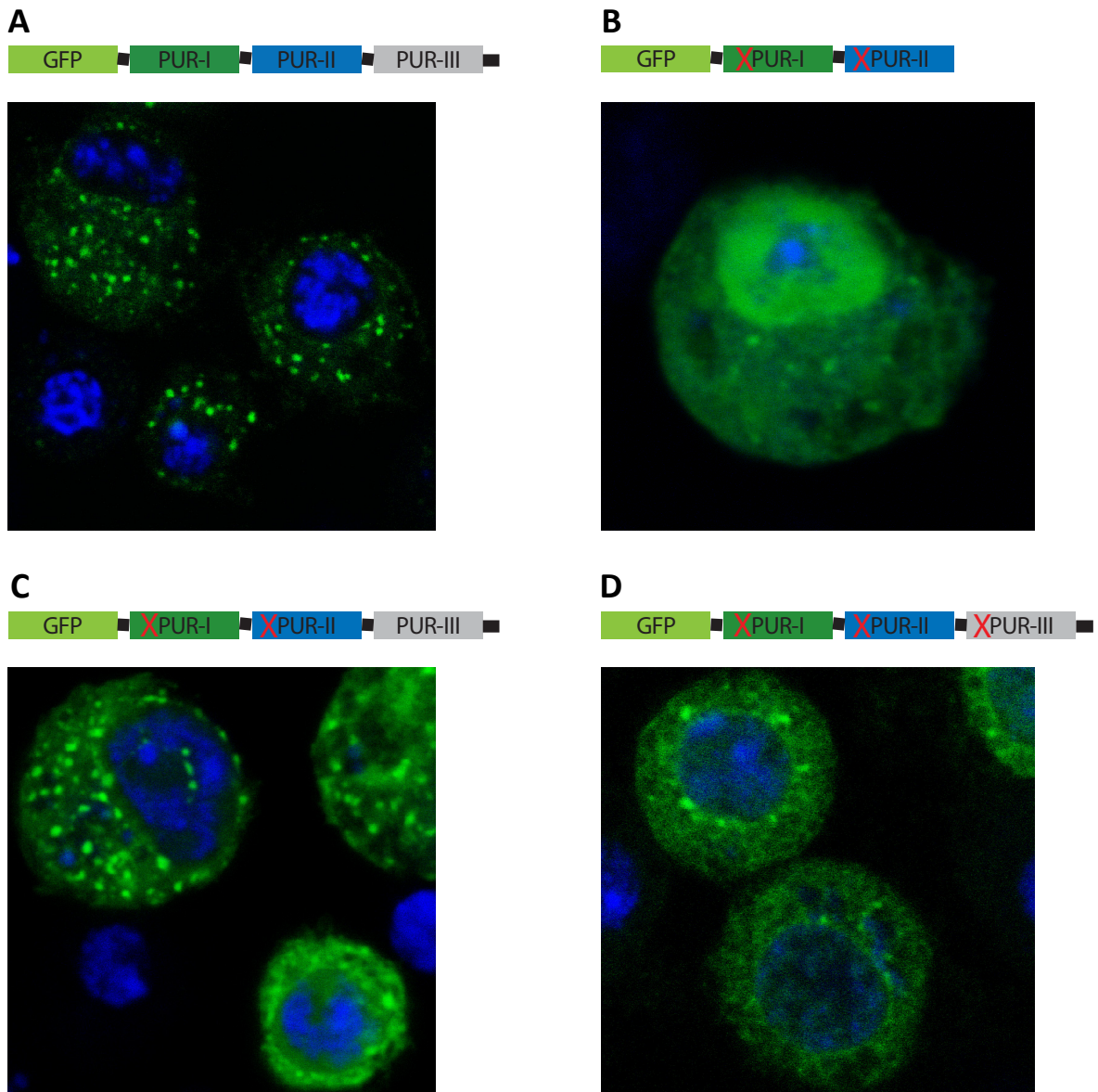


Figure 4-4: Confocal microscopy of GFP-fusion Pur-alpha constructs in *Drosophila* Schneider cells
 Schneider cells were transfected with the different GFP-constructs, fixed, permeabilized, stained with DAPI, and visualized by confocal microscopy.

A: wt full length GFP-Pur-alpha

B: GFP-Pur-alpha Repeat I+II (Aa40 to 185) R80A R158A

C: fl GFP-Pur-alpha R80A R158A

D: fl GFP-Pur-alpha R80A R158A R226A

green: GFP fluorescence, blue: DAPI stained DNA

Given that the point mutation in the PUR-repeat III would abolish RNA-binding and the capacity to protein-dimerization, the localization pattern of Pur-alpha R80A R158A R226A (Figure 4-4D) should look like Pur-alpha R80A R158A (Figure 4-4B). This was not the case and therefore the dimerization capacity of the triple mutant was investigated in a cell culture co-immunoprecipitation (CoIP) assay using transiently transfected GFP-tagged and FLAG-tagged Pur-alpha. From cell extracts GFP-trap-CoIP was performed and followed by Western Blot analysis using α -FLAG antibody to detect the potential GFP/FLAG-protein complexes (Figure 4-5). If the

third PUR-repeat is missing the dimerization capacity of the protein is almost completely lost (Figure 4-5; lane 2). The presence of mutation R226A in the third repeat has no effect on protein dimerization compared to wild type protein (Figure 4-5; lane 4 compared to lane 1). As a functional control the bottom panel shows a GFP-Western-Blot of the same membrane.

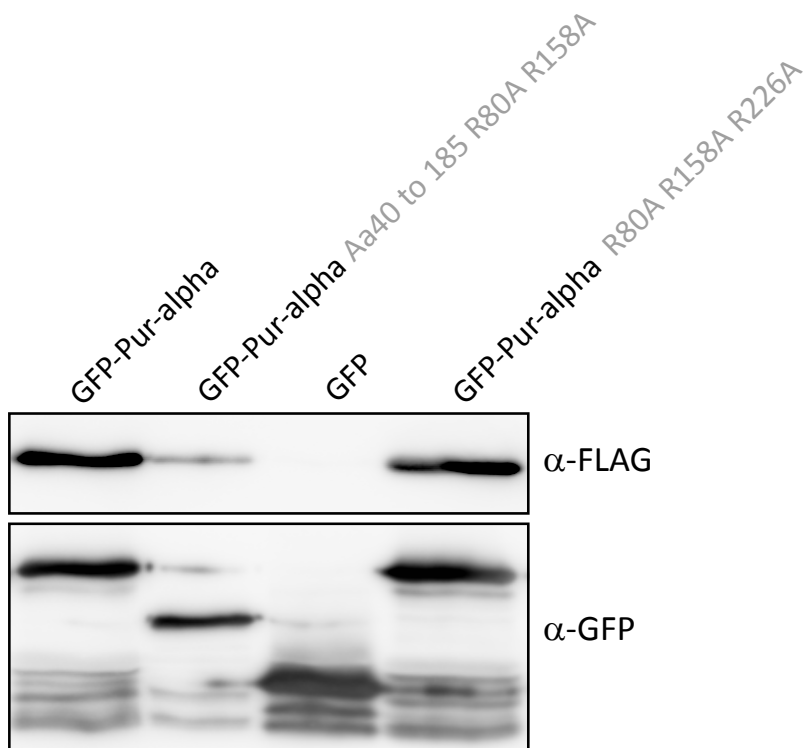


Figure 4-5: Western-Blot analysis of bound fractions after GFP-trap CoIP from Schneider cell extracts

Schneider cells were transiently transfected with FLAG-Pur-alpha and the according GFP-fused constructs named above; GFP-trap CoIP was performed and the bound fractions analyzed using SDS-PAGE and Western Blot using α -FLAG M2 (upper panel); to confirm the CoIP blot was stripped and reprobed with α -GFP (bottom panel)

4.2.1.2 Pur-alpha is associated with FMRP, Ago1 and Ago2 in Schneider cells

The identification of other cellular proteins which are also co-localized with Pur-alpha in Pur-alpha granules in Schneider cells might shed light on the physiological functions of these particles. In order to determine further proteins in the granules co-immunoprecipitation experiments were carried out and the Pur-alpha associated proteins were identified via Western Blot. Therefore a FLAG-tagged version of Pur-alpha was cloned, transiently transfected and Pur-alpha associated proteins were pulled down using a FLAG-resin. Figure 4-6 shows that FLAG-Pur-alpha is associated with Argonaute-1 and FMRP in *Drosophila*, but not with Tubulin, which serves as a control for the assay. This is in agreement with what is known for rat Pur-alpha, and indicates that *Drosophila* Pur-alpha is also a component of mRNPs.

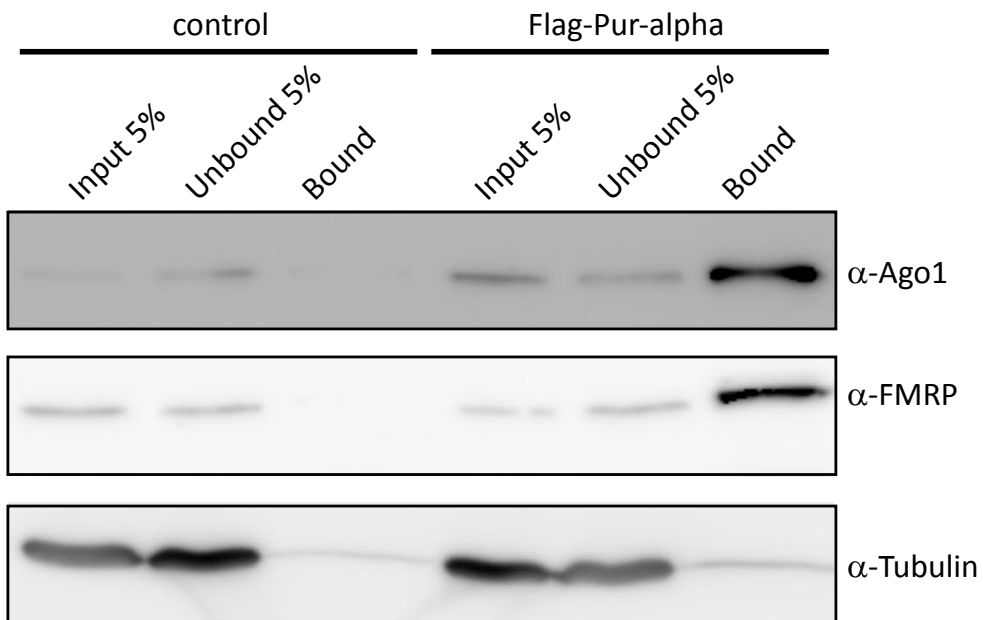


Figure 4- 6: Western-Blot analysis after FLAG-CoIP from Schneider cell extracts

Schneider cells were transiently transfected with FLAG-Pur-alpha (lane 4-5) or used not transfected as control (lane 1-3); from cell-extracts FLAG-CoIP was performed, the resulting fractions were analysed with SDS-PAGE and Western Blot using α -Ago1 (upper panel), α -FMRP (middle panel) and α -Tubulin (bottom panel)

To determine whether there is also an interaction between Pur-alpha and Argonaute-2 a different cell-culture assay was utilized. GFP-fusions of different Pur-alpha versions were transiently transfected either into untreated Schneider cells or into Schneider cells stably expressing FLAG-tagged Ago-2. Then GFP-trap co-immunoprecipitation was performed. Figure 4-7 shows that GFP-Pur-alpha is interacting with both FLAG-tagged Ago-2 and endogenous Ago-2 (Figure 4-7; lane 3 and 7). The interaction seems to be RNA independent as the truncated Pur-alpha mutant R80A R158A, which can not bind to RNA anymore, is still bound to Ago-2 (Figure 4-7; lane 5 and 9). The FLAG-Western blot serves as a control for the Ago2-stable cell line and reflects the interaction of FLAG-tagged Ago2 with Pur-alpha. The truncated Pur-alpha mutant R80A R158A also shows some unspecific binding to Tubulin (Figure 4-7; lane 5 and 9), which initially served as a control in this experiment. The association with Tubulin was actually true, as the coomassie-stained gel after transfer showed comparable “clean” bound fractions for all used Pur-alpha versions (data not shown). Anti-GFP-Western Blot confirms the immunoprecipitation of the different GFP-fused Pur-alpha constructs.

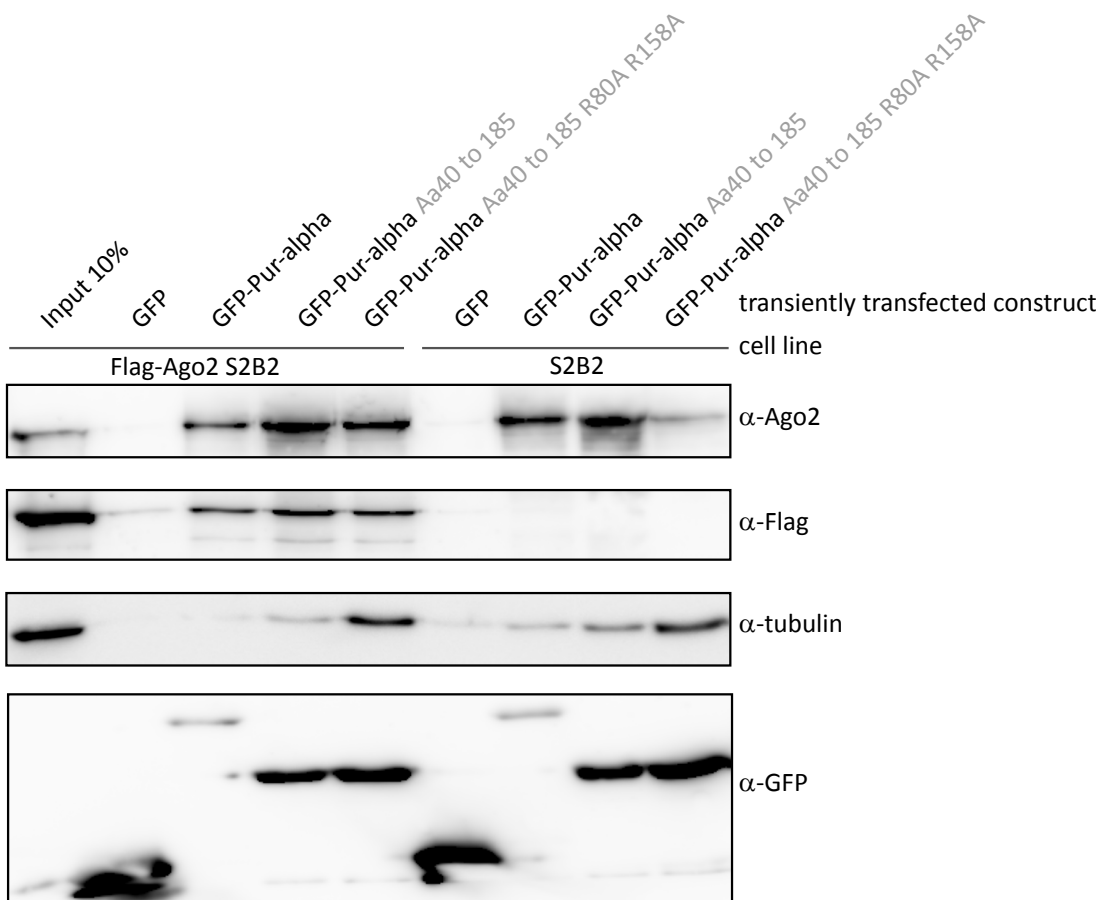


Figure 4- 7: Western-Blot analysis after GFP-trap- CoIP from Schneider cell extracts

Stably FLAG-Ago2 expressing or untreated Schneider cells were transiently transfected with different GFP-fusion constructs as indicated at the top; from cell-extracts GFP-trap-CoIP was performed, the resulting fractions were analysed with SDS-PAGE and Western Blot using α -Ago2 (upper panel), α -Flag (second panel), α -Tubulin (third panel) and as a control with α -GFP (bottom panel)

To analyze whether the truncations and mutations which affected the localization of Pur-alpha in Schneider cells also showed an effect on the protein interaction partners, further CoIP experiments were carried out. Western Blot analysis revealed PUR-repeat I and II are sufficient for the association with FMRP and Ago1 (Figure 4-8A, lane 5). If the two point mutations are present, which abolish RNA-binding, the binding is completely gone (Figure 4-8A, lane 6). Hence, the association between Pur-alpha and FMRP and Ago1 is RNA-mediated. If the two point mutations are in full-length background there is no difference visible (Figure 4-8A, lane 7). Two different point mutations R65A R142A which also affect the RNA-binding capacity of the protein, but to a lesser extent do not affect the association of Pur-alpha with FMRP and Ago1. Figure 4-8 B compares the expression levels of the different transiently transfected GFP-fusion constructs. The lower expression of GFP-Pur-alpha (Figure 4-8B, lane 2) might explain the weaker Ago1 signal after CoIP (Figure 4-8A, lane 4, α -Ago1).

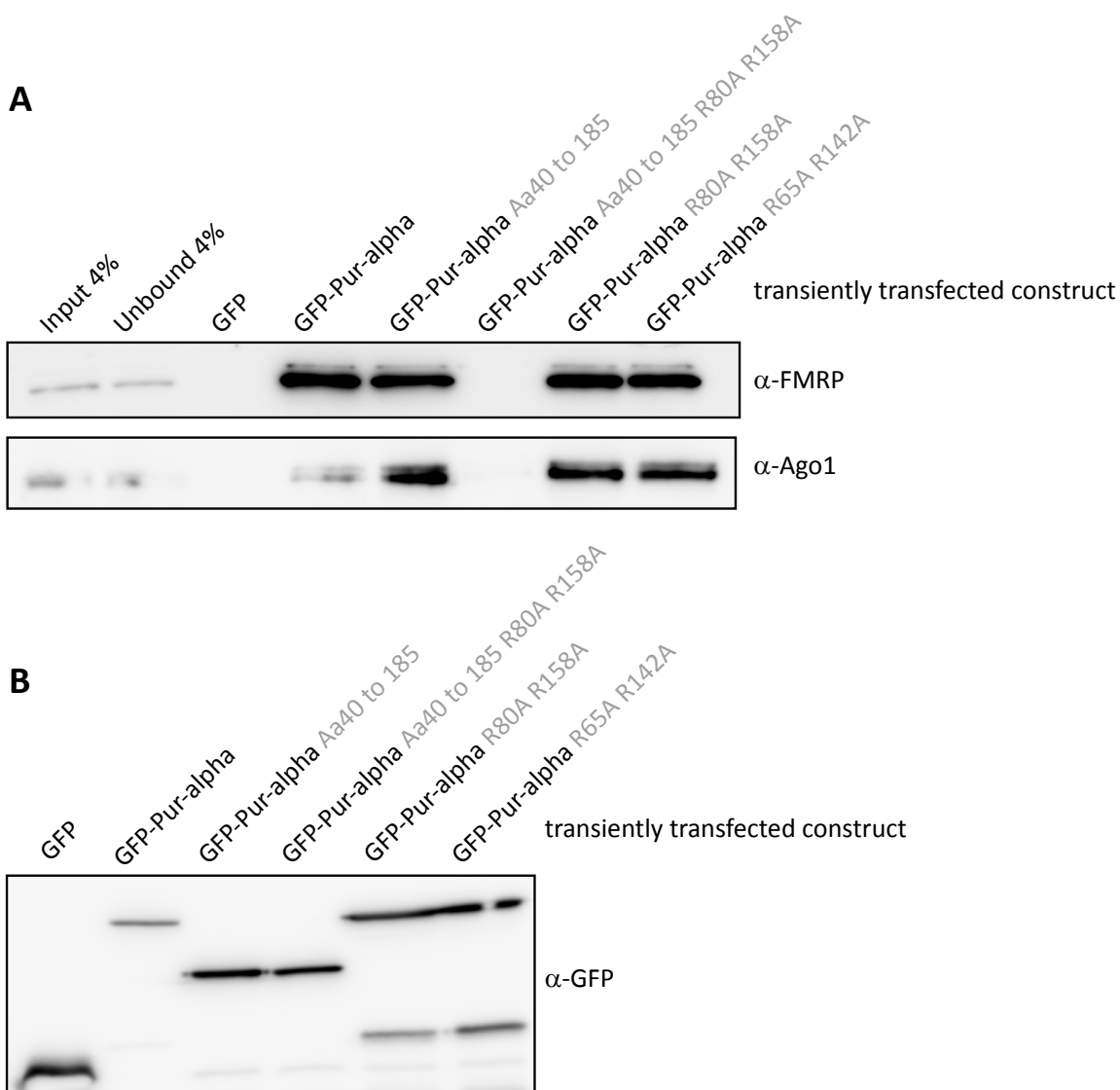


Figure 4-8: Western-Blot analysis after GFP-trap-CoIP from Schneider cell extracts

A: Schneider cells were transiently transfected with different GFP-fusion constructs as indicated at the top; from cell-extracts GFP-trap-CoIP was performed, the resulting fractions were analysed with SDS-PAGE and Western Blot using α -FMRP (upper panel) and α -Ago1 1b8 (lower panel)

B: Comparison of the expression levels of the different GFP-fusion constructs using α -GFP

4.2.2 Localisation of Pur-alpha during *Drosophila* oogenesis

As Pur-alpha is associated with RNA transport in neurons of mammals we used *Drosophila* oogenesis as an easily accessible system to study RNA transport in flies. To localize and visualize Pur-alpha during oogenesis two monoclonal rat antibodies against recombinant Pur-alpha protein (amino acids 40-255) were generated suitable for staining of wild type ovaries for confocal fluorescence microscope analysis (Elisabeth Kremmer, Helmholtz-Zentrum, München). Figure 4-9 shows an approximately stage 6 egg chamber stained with the Pur-alpha antibody and DAPI, to visualize the nuclei of the cells. A detailed examination revealed that the cells at the anterior and posterior tip of each egg chamber showed particularly strong Pur-alpha expression (Figure 4-9, white arrowheads in left picture). Staining within the cytoplasm was not uniform. The protein was distributed over many small particles or aggregates. In early egg chambers, Pur-alpha was equally abundant in follicle cells and nurse cells, but accumulated in the developing oocyte. This indicates that Pur-alpha is transported, likely as a part of RNP granules.

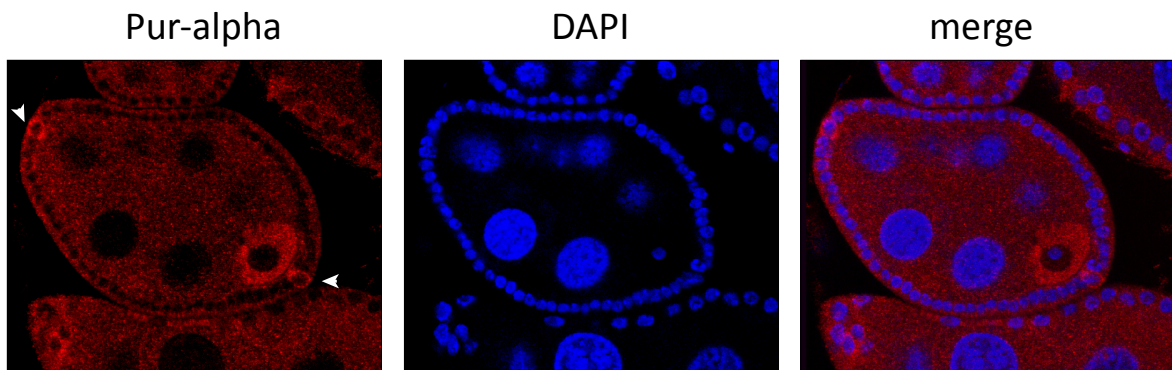


Figure 4-9: Endogenous Pur-alpha in *Drosophila* egg chamber (approximately stage 6)
confocal microscopy of a *Drosophila* egg chamber; red: endogenous Pur-alpha; blue: DAPI stained DNA, nuclei of the cells; white arrowheads: anterior and posterior cells with high Pur-alpha expression

4.2.2.1 Pur-alpha is enriched in the polar cells of the follicular epithelium

To investigate the obvious enrichment of Pur-alpha within the cells at both tips of the egg chamber in detail further fluorescent immunostainings were performed. The Pur-alpha enriched cells could be stained with α -FasciclinIII antibodies (FasIII) in Figure 4-10. FasIII is a homophilic adhesion molecule, which is expressed on a subset of neurons in the developing central nervous system (SNOW *et al.* 1989) and also strongly in the polar cells of the follicular epithelium (RUOHOLA *et al.* 1991).

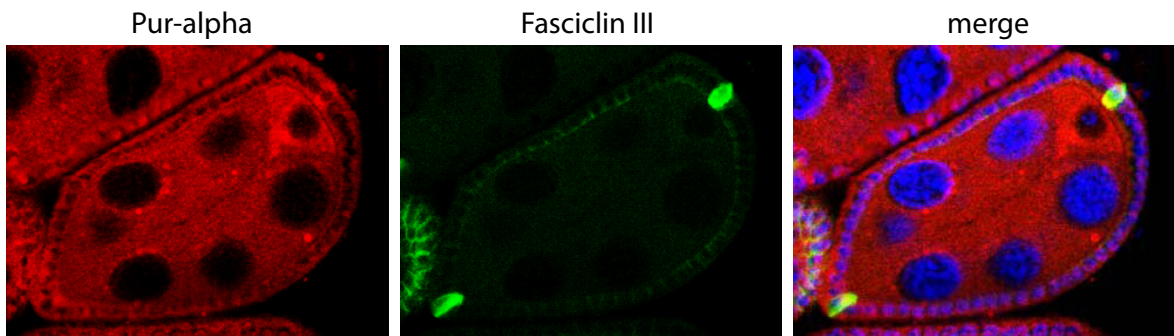
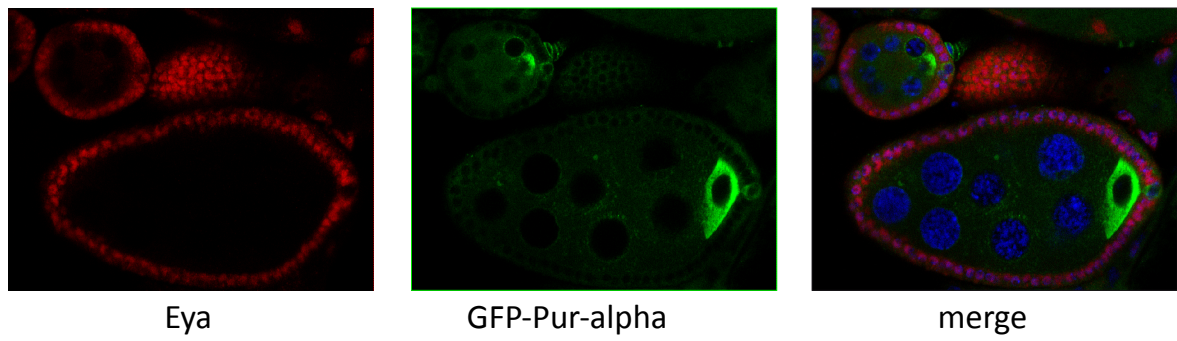


Figure 4- 10: Endogenous Pur-alpha and FasciclinIII in *Drosophila* egg chamber (approximately stage 6-7)

confocal microscopy of a *Drosophila* egg chamber; red: endogenous Pur-alpha; green FasciclinIII; blue: DAPI stained DNA, nuclei of the cells

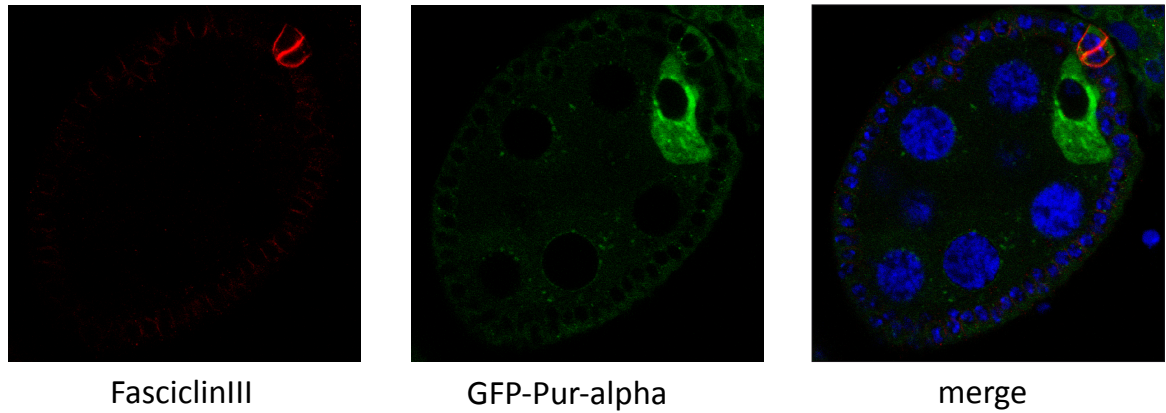
The enrichment of Pur-alpha in FasIII-positive cells was also recapitulated by the GFP-Pur-alpha fusion construct driven by the constitutively active ubiquitin promotor (Figure 4-11B), arguing that post-transcriptional regulation independent of the native mRNA 5'- and 3'-untranslated regions is responsible for this enrichment. Furthermore, these cells showed a negative staining for the transcription factor Eyes absent (eya) (Figure 4-11A). Eya is a DNA binding protein phosphatase and its expression is repressed in the polar cells by hedgehog signaling (BAI and MONTELL 2002). Based on their position, their negative staining for Eya and their positive staining for FasIII, Pur-alpha enriched cells at the extremities of the egg chamber could be identified as the polar cells. These cells play a crucial role in separation of subsequent egg chambers, migration and organization of the follicular epithelium and establishment of the anterior-posterior axis within the oocyte.

A

Eya

GFP-Pur-alpha

merge

B

FasciclinIII

GFP-Pur-alpha

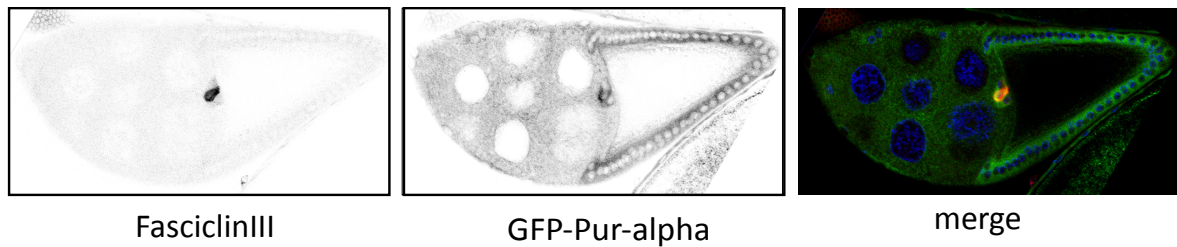
merge

Figure 4- 11: GFP-Pur-alpha enrichment in polar cells

confocal microscopy of Drosophila egg chambers (approximately stage 6); green: GFP-Pur-alpha; blue: DAPI

A: red: eya (eyes absent)

B: red: FasciclinIII



FasciclinIII

GFP-Pur-alpha

merge

Figure 4- 12: Enrichment of Pur-alpha in migrated follicle cells

Confocal microscopy of Drosophila egg chambers (approximately stage 10);

merged picture: green: GFP-Pur-alpha; blue: DAPI stained DNA, red: FasciclinIII stained polar cells

The observed enrichment of GFP- Pur-alpha in the polar cells was also visible after their migration through the nurse cells at stages 10 and later (figure 4-12).

4.2.2.2 RNA-binding and dimerization are required for correct transport of GFP-Pur-alpha during oogenesis

To analyze structural and functional requirements for Pur-alpha localization and transport during *Drosophila* oogenesis, we generated transgenic flies carrying the same GFP-Pur-alpha constructs as used in cell culture experiments. The expression of a cDNA-based, full-length GFP-Pur-alpha protein recapitulated the localization of endogenous Pur-alpha, indicating that the 3'- and 5'-untranslated regions of the endogenous *pur-alpha* mRNA are dispensable for correct Pur-alpha protein localization and enrichment during oogenesis (comparison of Pur-alpha localization in Figure 4-9 with 4-13A).

A truncation of the C-terminal pur-repeat (PUR III), leading to monomeric Pur-alpha PUR I+II which retains the ability to bind nucleic acids (GRAEBSCH *et al.* 2009) was less efficiently transported into the oocyte (Figure 4-13B, upper left panel) compared to the wild type full-length protein (Figure 4-13A). A similar reduction of transport (Figure 4-13B, lower left panel) could be detected after introduction of two point mutations (R80A, R158A) in PUR-repeat I and II of the full length protein. A combination of both, monomeric Pur-alpha and impaired nucleic acid binding was no longer transported into the oocyte (Figure 4-13B, upper right panel). Furthermore, the predominantly cytoplasmic localization of Pur-alpha was lost. The transgene with the corresponding point mutation in the third PUR-repeat (GFP-Pur-alpha R80A R158A R226A) showed almost no transport into the oocyte, and a moderate nuclear abundance (Figure 4-13B, lower right panel). The third PUR-repeat is less well conserved as the first two repeats. Nonetheless it may be capable of binding nucleic acids and providing a possible dimer interface (see also Schneider cell experiment, Figure 4-5). This led to hetero-dimerization with endogenous Pur-alpha and hence diminished correct localization of the transgenic protein.

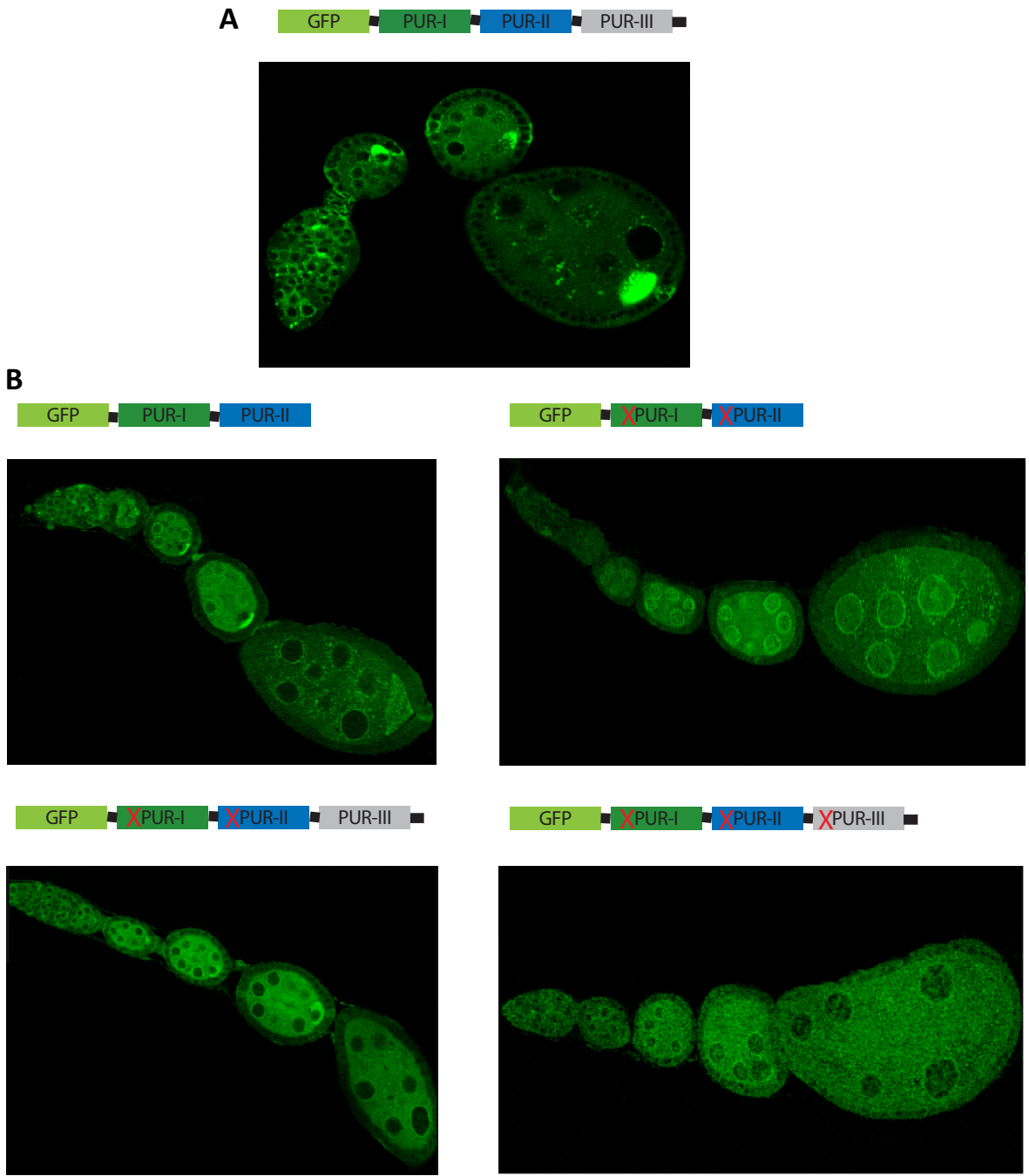


Figure 4-13: Transport of different GFP-Pur-alpha constructs during oogenesis

Confocal microscopy of *Drosophila* ovarioles, green: GFP-Pur-alpha constructs

A: full-length wild type GFP-Pur-alpha

B: top left: PUR-repeat I+II (Aa 40-185)

bottom left: fl GFP-Pur-alpha R80A R158A

top right: PUR-repeat I+II (Aa 40-185) R80A R158A

bottom right: fl GFP-Pur-alpha R80A R158A R226A

In summary, these results support the notion that Pur-alpha participates in nucleo-cytoplasmic shuttling and oocyte directed transport. For both, nuclear export and cytoplasmic transport RNA-binding seems to be crucial. Also dimerization contributes to the efficiency of these processes.

4.3 Defects in oogenesis in Pur-alpha hypomorphic alleles

To analyze Pur-alpha function in adult flies two available P-element insertion lines that affect the Pur-alpha locus on the fourth chromosome were examined. The line *pur-alpha*^{KG05177} carries an insertion in the promotor-region whereas line *pur-alpha*^{KG05743} carries an insertion within the first intron of the *pur-alpha* gene (Figure 4-14A). The effects of the P-element insertions on the protein amounts in whole fly extracts were analyzed via Western Blot using the rat monoclonal anti-Pur-alpha antibody (Figure 4-14B). Residual Pur-alpha expression was detectable in both alleles. The insertion line *pur-alpha*^{KG05743} showed a stronger reduction than the line *pur-alpha*^{KG05177} (Figure 4-14B).

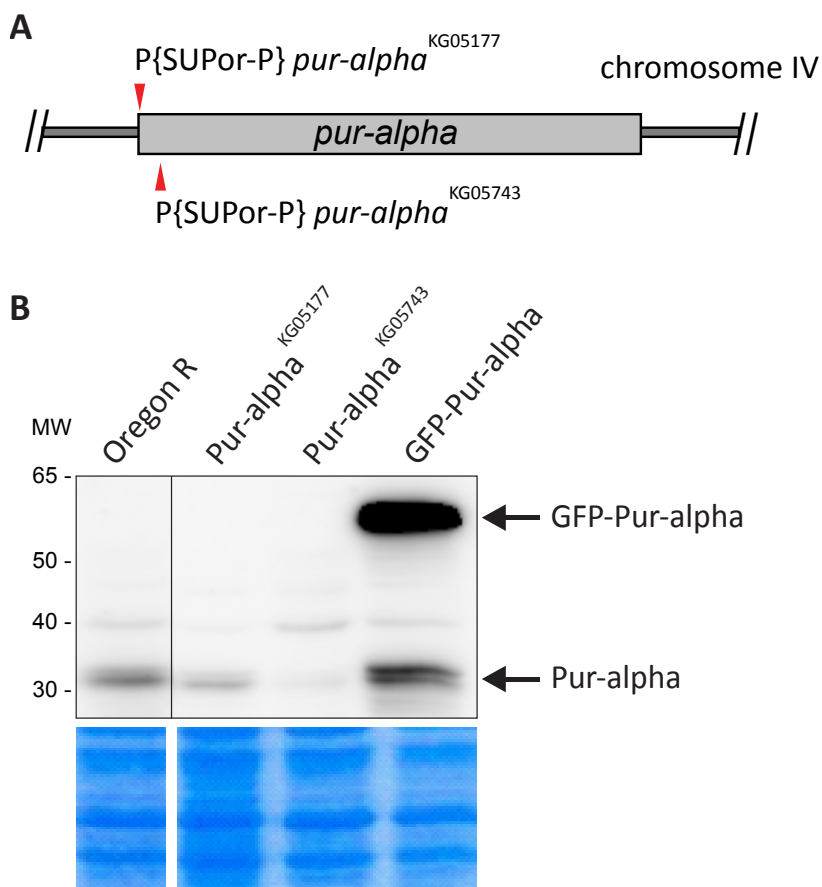


Figure 4-14: Pur-alpha hypomorphic alleles

A: Scheme of *pur-alpha* locus on chromosome IV; red arrow heads: P-Element insertion sites ; *pur-alpha*^{KG05177}: promoter region; *pur-alpha*^{KG05743}: first intron

B: Western Blot of whole fly extracts : rat monoclonal α -Pur-alpha, Pur-alpha 31 kDa; GFP-Pur-alpha 57 kDa; Bottom panel: coomassie staining of the SDS-Gel after transfer as loading control

The localization pattern of Pur-alpha during oogenesis is not affected by reduced amounts of Pur-alpha protein in the insertion lines (Figure 4-15). Regarding Figure 4-15 the fact has to be considered that microscope's photo-multipliers were modulated to obtain pictures with comparable intensities in order to visualize the localization of endogenous Pur-alpha. Using comparable photo-multiplier settings the intensity of Pur-alpha staining was reflecting the results of the Western Blot analysis as depicted above (Figure 4-14B) (data not shown).

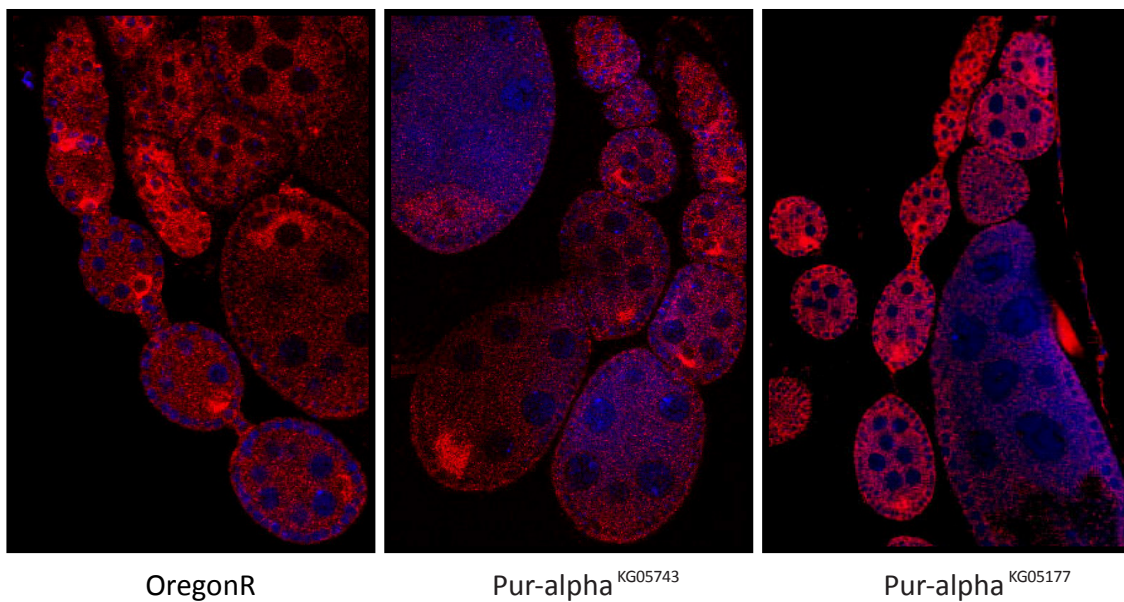


Figure 4-15: Endogenous Pur-alpha in Drosophila ovarioles

Confocal microscopy of *Drosophila* ovarioles of wildtype and hypomorphic allele-flies kept under normal conditions; red: endogenous Pur-alpha; blue: TOTO3 stained DNA, nuclei of the cells

Furthermore it could be observed, that pur-alpha mutant ovarioles were in a wild type shape if the female flies were kept at standard conditions before ovary dissection.

4.3.1 Decreased egg laying in Pur-alpha hypomorphic alleles

Both alleles *pur-alpha*^{KG05177} and *pur-alpha*^{KG05743} are homozygous viable and fertile at 25°C standard conditions. However, when placed at 30°C for 96 hours, Pur-alpha mutant females laid fewer eggs than their wild-type counterparts. This was true for both homozygous hypomorphic alleles as well as for trans-heterozygous mutants (Figure 4-16). Heterozygous animals of both alleles showed a wild type like egg-laying phenotype.

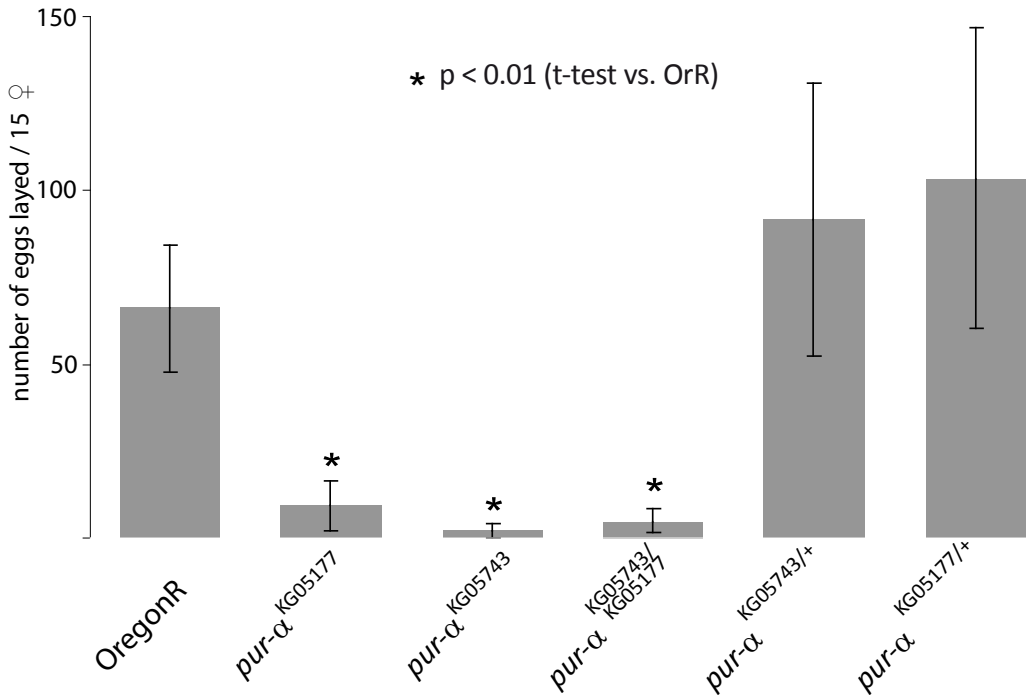


Figure 4-16: Quantification of egg laying of *pur-alpha* mutant and wild type flies

Flies were kept for 4 days at 30°C after hatching; number of eggs laid on grape juice agar per 15 flies after 16 hours was determined. Bar chart displays mean egg-numbers after three experiments, error bars indicate the standard deviations, p-values < 0,01 are depicted with asterisks

4.3.2 Malformation of follicular epithelium in Pur-alpha hypomorphic alleles

To determine the cause for the reduced egg production wild type and mutant ovaries were examined in detail after four days at 30°C by staining the nuclear DNA with DAPI, followed by confocal microscopy. In wild type ovarioles, egg chambers are surrounded by a monolayer of follicle cells when they emerge from the germarium (Figure 4-17, left panel). In this experimental setting the large, polyploid nurse cell nuclei could be easily distinguished from the much smaller nuclei of the follicle cells which surround them. Until stage 9 of oogenesis the follicle cells surround the nurse cells and the oocyte, then at stage 10 the border and polar cells start to migrate through the nurse cells to enclose the anterior side of the oocyte. This process depends on many signaling and differentiation events involving the polar cells. The right panel in Figure 4-17 shows that the follicle cells of a *pur-alpha*^{KG05743} ovariole after four days at 30°C could not migrate properly and failed to encircle the nurse cells and the oocyte during early oogenesis (until approximately stage 8). Rather, they seemed to form a lump of cells on one side of the egg chamber (white arrows, Figure 4-17B).

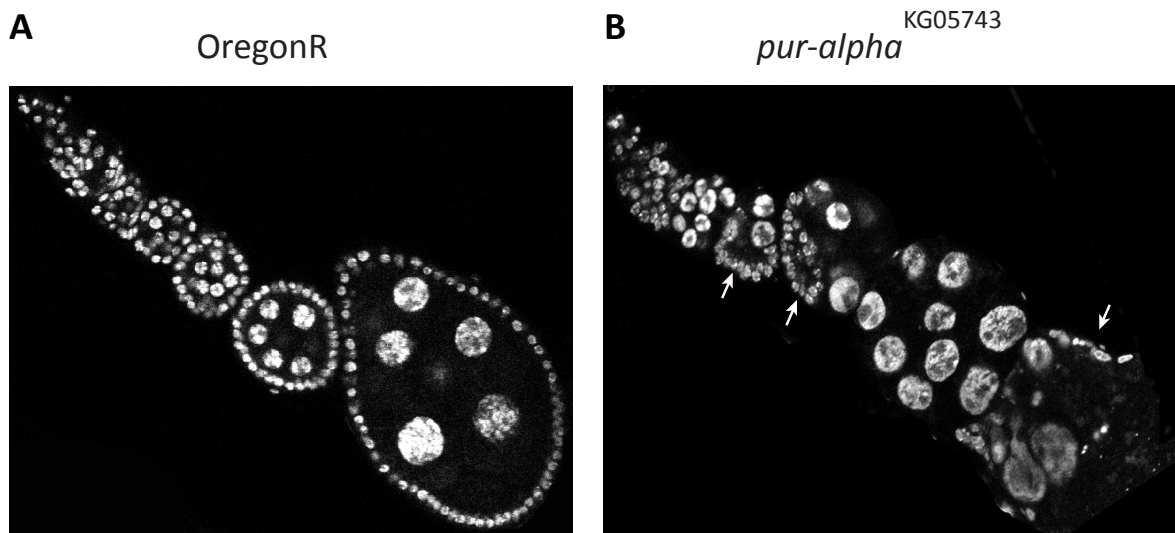


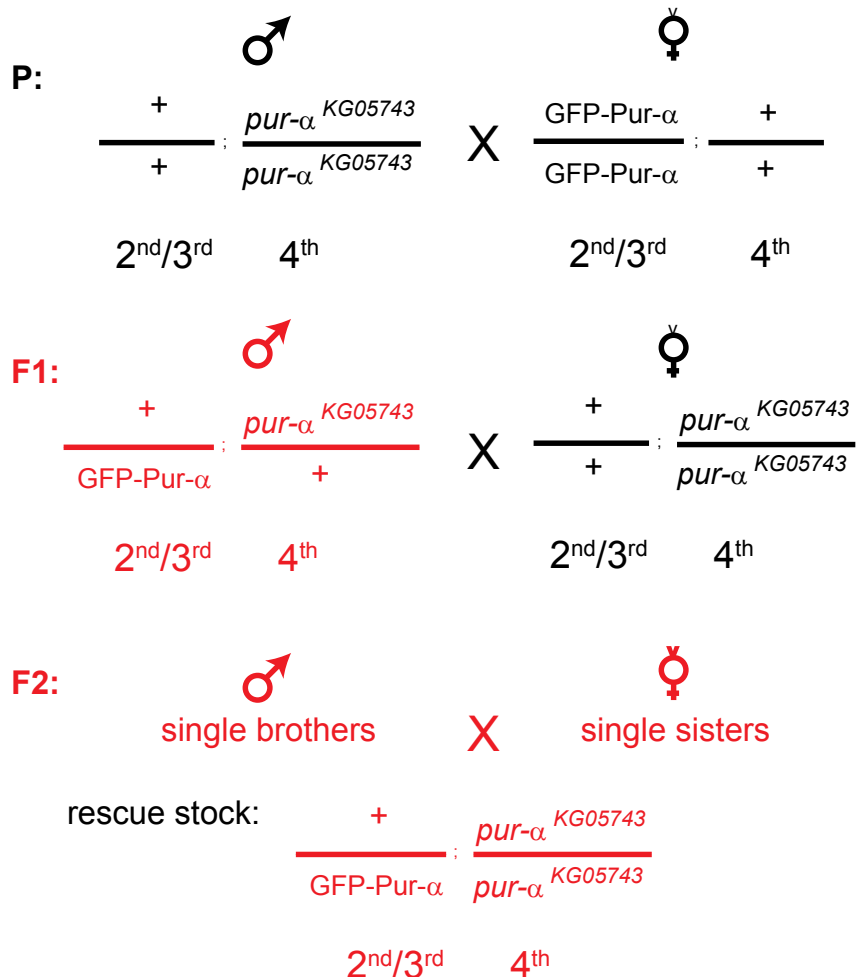
Figure 4-17: DAPI staining of OregonR and *pur-alpha*^{KG05743} ovarioles after four days at 30°C
 Flies were kept for 4 days at 30°C after hatching; the ovaries were dissected, fixed, permeabilized, stained with DAPI and visualized by confocal microscopy;
A: wild-type (OregonR) ovariole
B: *pur-alpha*^{KG05743} ovariole; white arrows: lump of follicle cells

	Ovarioles	Stage 10 egg chambers	Percentage (%)
Wild type (OregonR)	104	63	61
<i>pur-alpha</i> ^{KG05743}	43	0	0
<i>pur-alpha</i> ^{KG05177}	97	21	22
<i>pur-alpha</i> ^{KG05177} / <i>pur-alpha</i> ^{KG05743}	169	30	18

Table 4-1: Stage 10 egg chambers after four days at 30°C
 Flies were kept for 4 days at 30°C after hatching; the ovaries were dissected, fixed, permeabilized, stained with DAPI and visualized by confocal microscopy; the number of stage 10 containing egg chambers was counted

In the weaker P-element insertion allele $pur-\alpha^{KG05177}$, where more protein was still remaining (Western Blot, Figure 4-14 B) the early follicle cell migration phenotype or the formation of follicle cell lumps could not be observed after keeping the flies at 30 °C. But also a reduced egg laying was measured (Figure 4-16). To find out the reason why also the $pur-\alpha^{KG05177}$ flies laid fewer eggs staged 10 egg chambers were counted after four days at 30°C (Table 4-1). In 63 out of 104 wild-type ovarioles a stage 10 egg chamber could be observed. Homozygous the $pur-\alpha^{KG05177}$ ovaries had 22% stage ten egg chambers (n=97, stage 10: 21) and 18% of trans-heterozygous $pur-\alpha^{KG05177}/pur-\alpha^{KG05743}$ ovarioles contained stage 10 egg chambers (n=169, stage 10: 30). In the strong allele $pur-\alpha^{KG05743}$ no stage 10 egg chambers could be identified after keeping the flies at the restrictive conditions.

To make sure that the phenotype of reduced egg-laying and the malformation of the ovarioles was really due to the P-element insertions in the *pur-alpha* gene and not caused by any unknown background mutations we tried to rescue the phenotype by giving back transgenic GFP-Pur-alpha fusion constructs. Therefore flies were crossed to obtain new fly stocks which express different GFP-fusion constructs in the background of the homozygous $pur-\alpha^{KG05743}$ allele. As there are hardly any functional markers available for genetics on the fourth chromosome, fly crossing was carried out without marker and the obtained new lines were checked via a PCR-assay for their correct phenotype (Figure 4-18). PCR primers were designed that the presence or absence of a PCR product specifically distinguished between presence and absence of the P-element insertion in the *pur-alpha* gene.



Identification via GFP fluorescence and PCR analysis

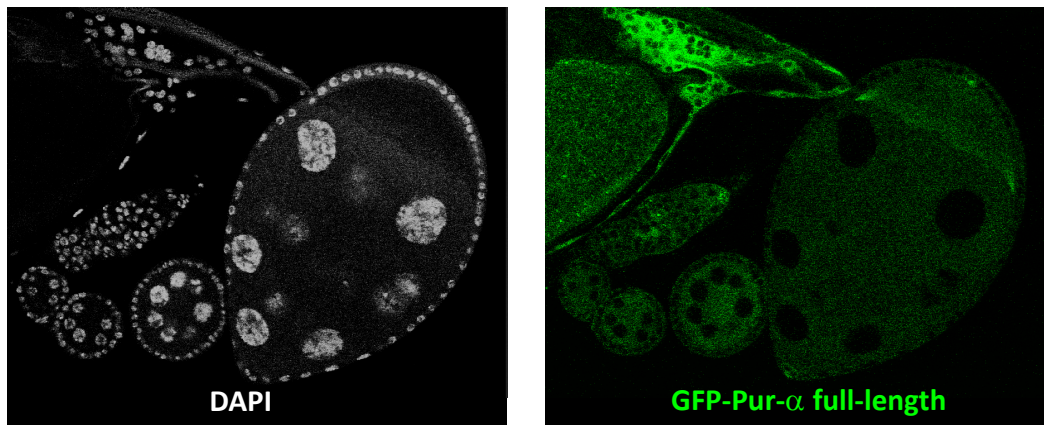
Figure 4-18: Fly crossing scheme for rescue experiment

Flies were crossed according to their genotypes for 2nd/3rd and 4th chromosome as depicted in the scheme; red color in F1 indicates the progeny which was used from the previous for the next crossing step; to obtain for the P-element homozygous flies the flies of the F2 generation were crossed individually; the presence of the GFP-pur-alpha transgene in the F3 generation was verified with a fluorescence stereomicroscope; it was further analyzed via PCR, whether the P-element insertion was homozygous

The newly generated rescue fly stocks were kept at 30°C for four days after hatching to induce the earlier observed egg laying defect. Their ovaries were dissected, fixed and stained with DAPI to visualize the resulting morphology (Figure 4-19). Only the flies carrying the full-length GFP-Pur-alpha construct were able to produce correctly shaped ovarioles (Figure 4-19 A). The lower panel in Figure 4-19 A shows out crossed homozygous *pur-alpha^{KG05743}* ovaries which were negative for the GFP-Pur-alpha full length protein which had also malformed ovarioles. This served as a control for the functionality of the rescue experiment and to exclude other background genetic defects. The GFP-Pur-alpha construct repeat I+II R80A R158A that lacks the ability to bind to RNA was not able to rescue the phenotype (Figure 4-19 B). GFP alone, used as control, could also not revert the malformation of the ovarioles in *pur-alpha^{KG05743}* flies (Figure 4-19 C).

A

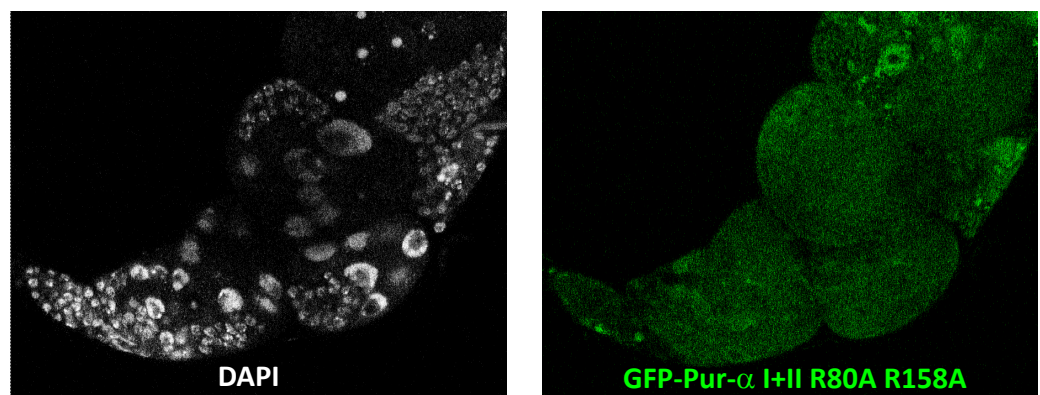
GFP-Pur- α full-length; $pur-\alpha^{KG05743}$



GFP-Pur- α -/-; $pur-\alpha^{KG05743}$

B

GFP-Pur- α I+II R80A R158A; $pur-\alpha^{KG05743}$



C

GFP; $pur-\alpha^{KG05743}$

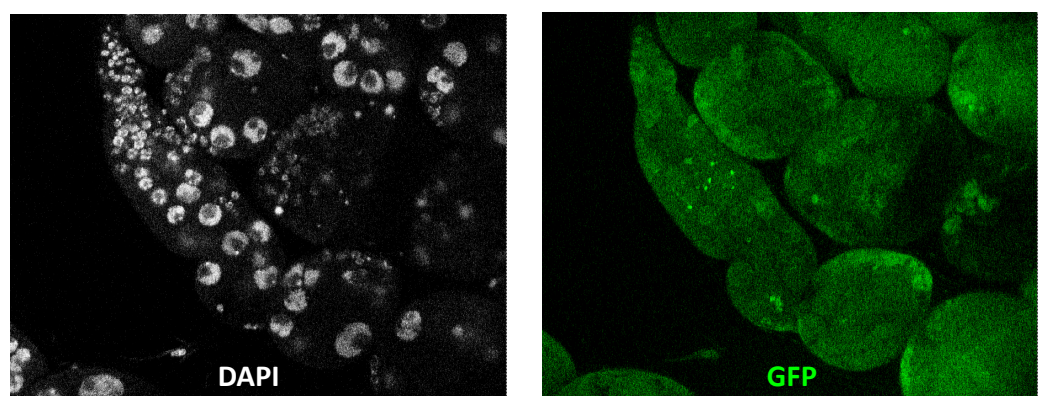


Figure 4- 19: DAPI staining and GFP fluorescence of rescue fly stocks

Fly stocks were generated according to crossing scheme in Figure 18; flies were kept for 4 days at 30°C after hatching; the ovaries were dissected, fixed, permeabilized, stained with DAPI and GFP and DAPI fluorescence visualized by confocal microscopy;

A: GFP-Pur-alpha in mutant background; lower panel:outcrossed homozygous *pur-alpha*^{KG05743} ovariole;

B: GFP-Pur-alpha I+II R80A R158A in mutant background;

C: GFP in mutant background

We further asked whether the decreased egg laying could also be rescued by giving back the transgenic expressed GFP-Pur-alpha versions. To test this, the same egg-laying experiment as in Figure 4-16 was performed and eggs were counted after keeping the flies for four days at 30°C. Neither the GFP-only control (Figure 4-20, first bar) nor the mutated and truncated GFP-Pur-alpha I+II R80A R158A protein (Figure 4-20, third bar) could rescue the phenotype. An increased wild type like egg laying could only be observed by giving back the wild type full length protein (Figure 4-20, second bar). As a control out crossed homozygous *pur-alpha*^{KG05743} flies were also used in this experimental setup (Figure 4-20, bar 4). The better egg laying performance of these lines compared to the initial *pur-alpha*^{KG05743} line (Figure 4-16) can be interpreted by the “refreshed” genome of the flies which came from the out crossing procedure.

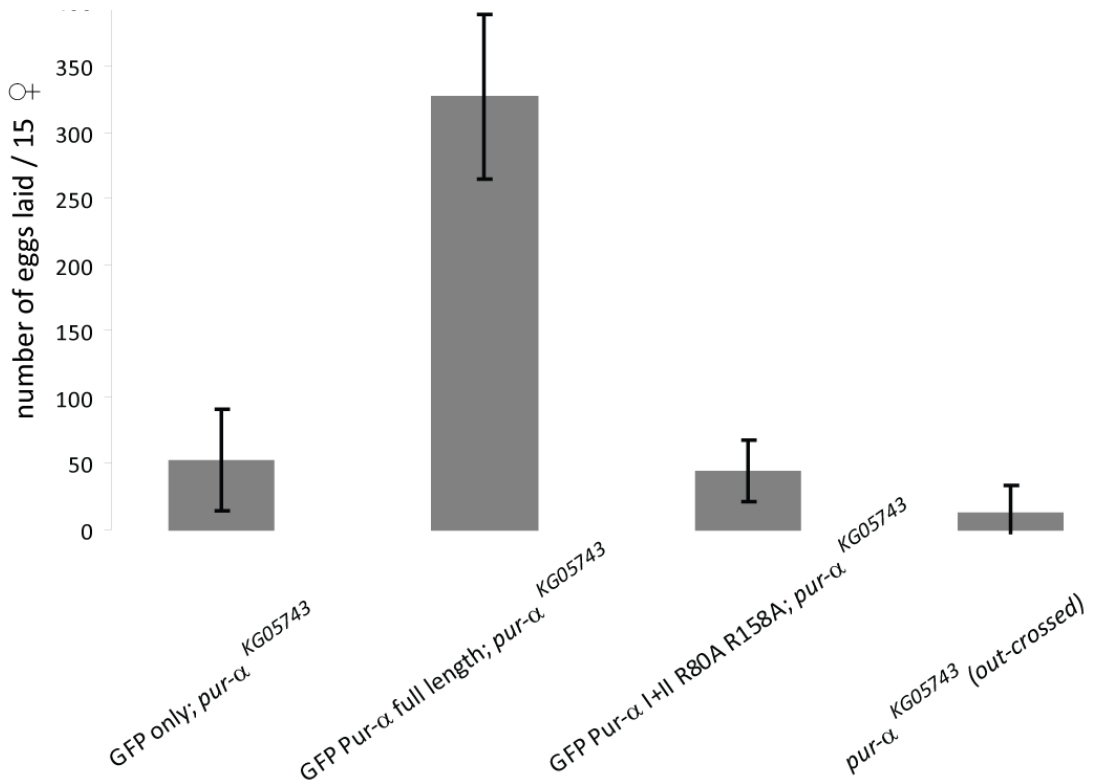


Figure 4- 20: Quantification of egg laying of *pur-alpha* mutant and rescue flies

Flies were kept for 4 days at 30°C after hatching; number of eggs laid on grape juice agar per 15 flies after 16 hours was determined. Bar chart displays mean egg-numbers after three experiments, genotypes are indicated below the bars respectively; error bars indicate the standard deviations

4.3.3 Knock-down of Pur-alpha in follicle cells

Another possibility to check whether the observed *pur-alpha* phenotype results from the decreased amounts of Pur-alpha protein due to the insertion of the transposable elements is RNA-interference (RNAi). By the use of tissue-specific GAL4-driver lines which are crossed with flies expressing small hairpin RNAs under the control of UAS-sites, a tissue specific knock down of a gene of interest can be achieved (mechanism, see Figure 4-21).

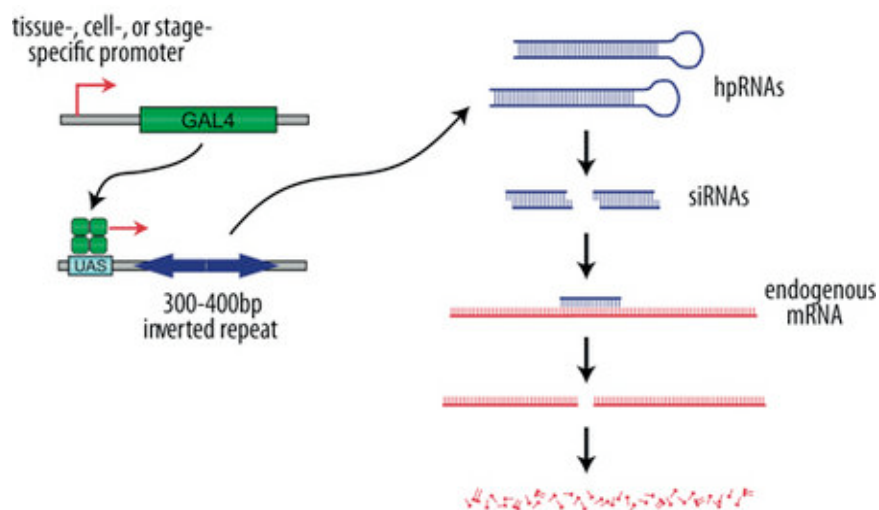


Figure 4-21: Transgenic RNAi in Drosophila

The generic GAL4/UAS system is used to drive the expression of a hairpin RNA (hpRNAs). These double-stranded RNAs are processed by Dicer into siRNAs which direct sequence-specific degradation of the target mRNA (picture and text taken from <http://stockcenter.vdrc.at/control/rnailibrary>)

To accomplish a knock down of pur-alpha in follicle cells the VDRC line 101363 was used and driven by a traffic-jam GAL4 driver line (OLIVIERI *et al.* 2010). The expression pattern in follicle cells via the traffic jam GAL4 construct was checked using UAS-GFP expressing flies (data not shown) and the knock down of Pur-alpha was visualized by an immunofluorescent staining of endogenous Pur-alpha in knock down and wild type ovaries (Figure 4-22). The follicular epithelium which surrounds the egg chamber shows a weaker red staining (Figure 4-22, right picture) compared to wild type (Figure 4-22, left picture). This staining also served as a further specificity control for the generated rat anti-Pur-alpha antibody.

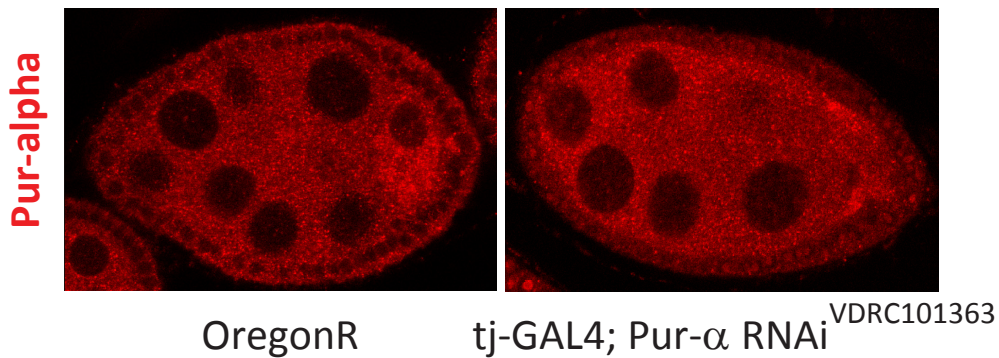


Figure 4-22: Knock down of Pur-alpha in follicle cells

Ovaries from wild type and Pur-alpha knock down flies (traffic jam (tj) GAL4; VDRC101363) were dissected, fixed, permeabilized, stained with rat α -Pur-alpha antibody and α -rat-Cy3 conjugated secondary antibody and visualized by confocal microscopy

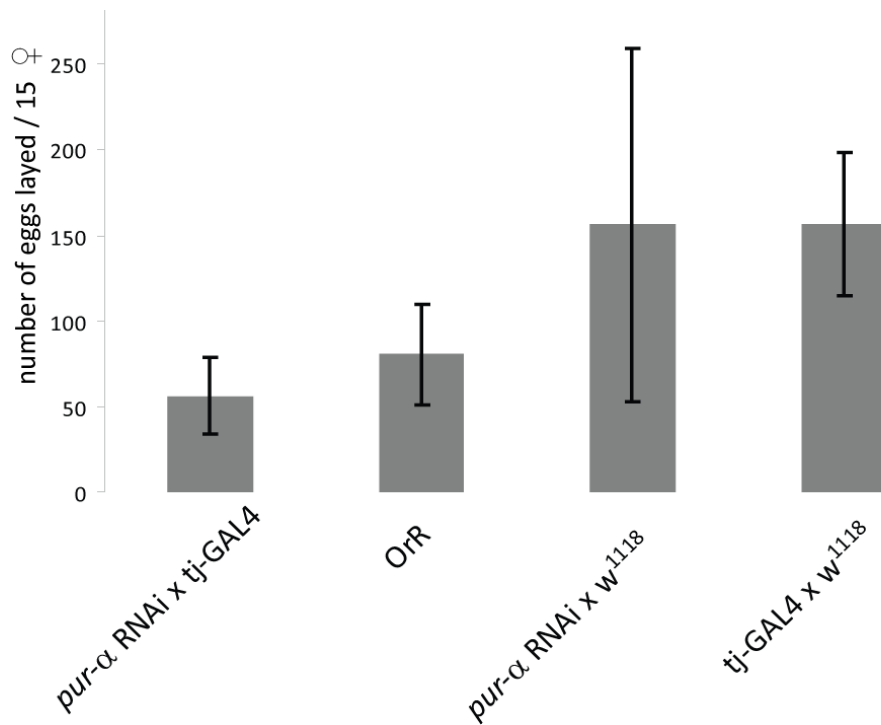


Figure 4-23: Quantification of egg laying of pur-alpha knock down and control flies

Flies were kept for 4 days at 30°C after hatching; number of eggs laid on grape juice agar per 15 flies after 16 hours was determined. Bar chart displays mean egg-numbers after two or three experiments, error bars indicate the standard deviations, crossing of the UAS-line and the GAL4-driver-line with w¹¹¹⁸ and OrR flies served as controls

The egg laying experiment with the knock down flies couldn't show the same phenotype which was observed with the P-element insertion flies. The number of laid eggs was not significantly affected by the knock down of Pur-alpha in the follicle cells (Figure 4-23).

However, the appearance of the laid eggs and embryos from the Pur-alpha knock down flies was different compared to the control and wild type flies. The embryos looked loose and perforated. To analyze whether this observation had an effect on the outcome of the progeny, the hatching of larvae from these embryos was monitored. 80% of control flies were able to hatch (103 out of 129), but only 33% (45 out of 135) of the Pur-alpha knock down larvae (Table 4-2). Compared to the severe egg laying phenotype of *pur- α* ^{KG05743} flies (Figure 4-16) the effect of reduced amounts of pur-alpha protein in follicle cells seemed to be less dramatic but still measurable.

	embryos	hatched larvae	percentage (%)
Control (w^{1118} x Pur-α-RNAi)	129	103	80
Pur- α knock down (tj-GAL4 x Pur-α-RNAi)	135	45	33

Table 4-2: Hatching of larvae

Embryos were collected approximately 8 hours after egg laying and placed on a standard grape juice plate and incubated for 24 hours at standard conditions, hatched larvae were counted

4.3.4 Morphological analysis of main ovary components in *pur-alpha*^{KG05743} flies

4.3.4.1 Oocyte and polar cell determination

Not only the polar cells showed an accumulation of Pur-alpha, but also the oocyte itself is enriched with Pur-alpha protein (see Figure 4-9). To test whether the reduced Pur-alpha levels lead to defects in oocyte specification in the ovarioles of *pur-alpha*^{KG05743} flies, an antibody staining against the RNA binding protein Orb was used. The cytoplasmic poly-A binding protein Orb is strongly enriched in early oocytes and required for the establishment of polarity (CHRISTERSON and MCKEARIN 1994; LANTZ *et al.* 1994), thus allowing the identification of the oocyte. The anti orb staining was performed after *pur-alpha*^{KG05743} mutant females were kept 4 days at 30°C, the same experimental setup as used for the egg laying-experiment earlier in this study. Figure 4-24 shows that in general one oocyte was present per developing egg chamber, which indicates that oocyte specification was not fundamentally disturbed. However, in infrequent cases it was difficult to distinguish individual egg chambers because they were incompletely separated by the follicle cells, a phenotype sometimes referred to as extra oocyte specification.

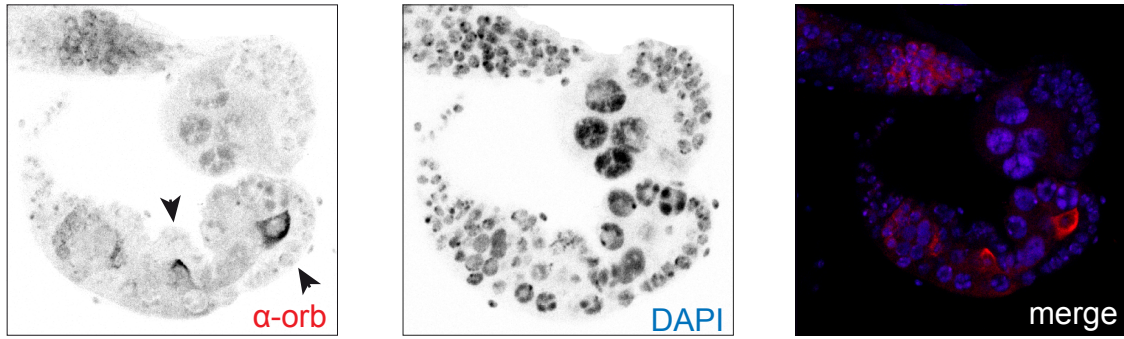


Figure 4-24: Orb and DAPI staining of *pur-alpha*^{KG05743} ovarioles

Flies were kept for 4 days at 30°C after hatching; the ovaries were dissected, fixed, permeabilized, stained with α -orb as primary antibody and α -mouse Cy3 conjugated secondary antibody and DAPI; and visualized by confocal microscopy; red: orb; blue: DAPI-stained DNA; white arrows: lump of follicle cells

The other cell type where a strong Pur-alpha enrichment could be observed was the polar follicle cells (Figure 4-11). In *pur-alpha*^{KG05743} flies the correct migration of the follicle cells is disturbed. This migration is dependent on the organizer function of the polar cells (BECCARI *et al.* 2002). To reveal whether there are no polar cells determined or all follicle cells have polar cell character in the Pur-alpha mutants, their ovaries were stained with FasciclinIII antibody (RUOHOLA *et al.* 1991) after keeping them at the restrictive temperature (Figure 4-25).

Despite the lump formation of the follicle cells in *pur-alpha*^{KG05743} ovaries there were always two pairs of polar follicle cells determined. The polar cells could be identified by their strong FasciclinIII staining (Figure 4-25). In contrast to wild type (OregonR, top panel) the polar cell pairs in *pur-alpha*^{KG05743} ovaries did not lie at the anterior and posterior pole of the egg chamber, they were rather randomly distributed in the bunch of follicle cells.

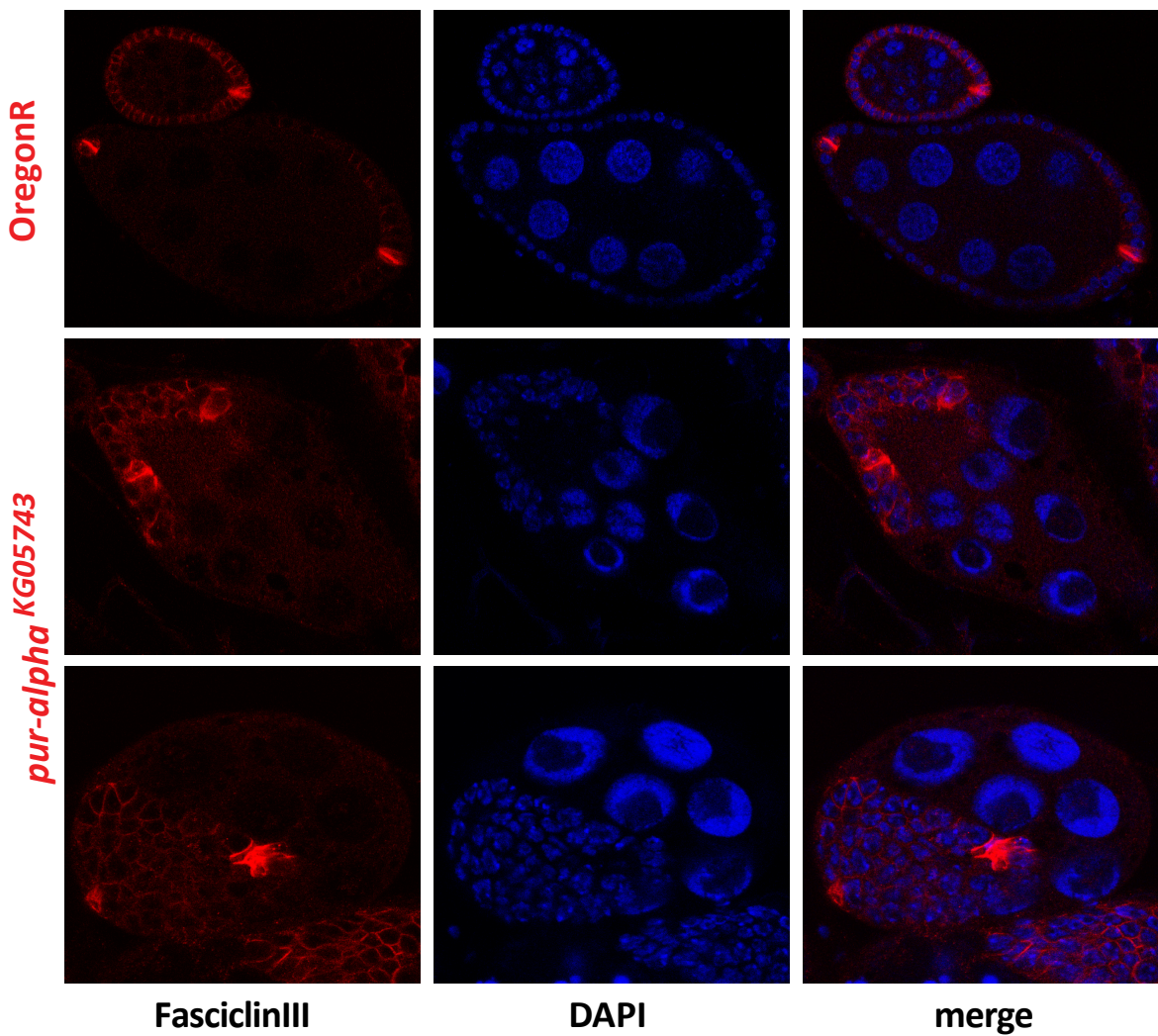


Figure 4-25: FasciclinIII and DAPI staining of OregonR and *pur-alpha*^{KG05743} ovarioles
 Flies were kept for 4 days at 30°C after hatching; the ovaries were dissected, fixed, permeabilized, stained with α -fasciclinIII as primary antibody and α -mouse Cy3 conjugated secondary antibody and DAPI; and visualized by confocal microscopy; red: FasciclinIII; blue: DAPI-stained DNA

4.3.4.2 Adherens junctions and ring canals

To answer the question whether other main structural features of the ovarioles were affected by the *pur-alpha*^{KG05743} hypomorphic allele, more immunostainings were carried out. The protein armadillo, which is the *Drosophila* homolog to vertebrate beta-catenin, is a main component of the adherens junction protein complex. Adherens junctions mediate cell-cell-adhesion and organization of cells into epithelia (Cox *et al.* 1996; PEIFER *et al.* 1993). The malformation of the follicle epithelium in *pur-alpha*^{KG05743} ovaries might be due to a dysfunction of adherens junctions. Therefore an immunostaining using α -armadillo antibody was performed after keeping the flies at

the restrictive conditions (Figure 4-26, top panel). Armadillo is generally localized polarized at the inner side of the follicle cells which is the connection surface side to the nurse cells. This was true for wild type egg chambers (Figure 4-26, left picture) as well as for *pur-alpha*^{KG05743} mutant egg chambers (Figure 4-26, right picture). Hence, the polarized pattern of Armadillo seemed to be not interrupted by the defects in follicle epithelium caused by the P-Element insertion in the *pur-alpha* gene.

In *Drosophila* egg chambers the nurse cells and the oocyte are connected by cytoplasmic bridges called ring canals. Through these canals the nurse cells transfer maternal components like proteins, mRNAs, ribosomes and mitochondria into the developing oocyte. There are 15 ring canals in each egg chamber, which can be visualized by staining with an antibody against hu-li tai shao (hts). Hts is a structural protein required for ring canal formation (ROBINSON *et al.* 1994). The lower panel of Figure 4-26 shows hts-stained wild type (left picture) and Pur-alpha mutant ovarioles (right picture). The number and structure of ring canals appeared similar in the mutant ovarioles compared to wild type. A precise quantification is challenging due to the grossly perturbed morphology of pur-alpha mutant ovaries.

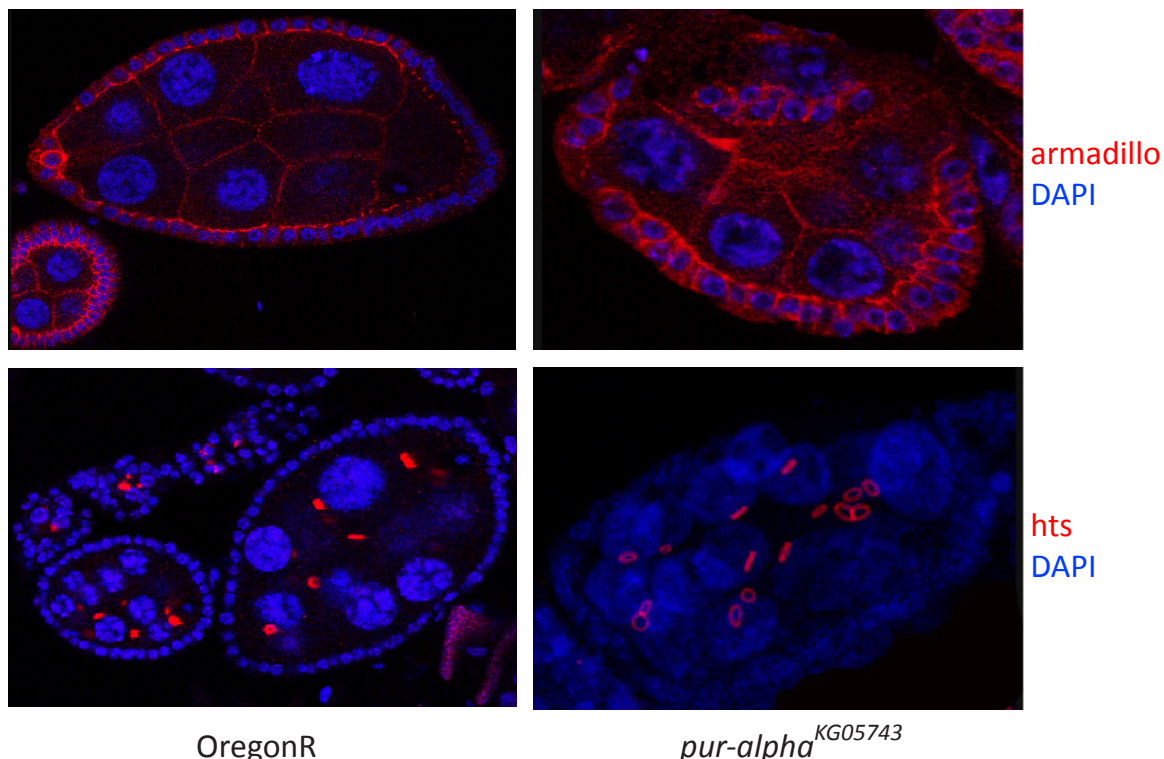


Figure 4-26: Armadillo, hts and DAPI staining of OregonR and *pur-alpha*^{KG05743} ovarioles
Flies were kept for 4 days at 30°C after hatching; the ovaries were dissected, fixed, permeabilized, stained with anti either α -armadillo or α -hts as primary antibody and α -mouse Cy3 conjugated secondary antibody and DAPI; and visualized by confocal microscopy; red: top panel: armadillo, bottom panel: hts; blue: DAPI-stained DNA

4.4 Pur-alpha associated proteins

In order to investigate the underlying molecular mechanism for the follicle cell phenotype of the *pur-alpha* hypomorphic alleles we analyzed Pur-alpha associated proteins from *Drosophila* ovary extracts. Co-immunoprecipitation from GFP-Pur-alpha transgenic ovaries was performed using GFP-trap® affinity-beads. As a control and to distinguish between specific and unspecific interaction partners, ovaries expressing GFP only were used. The purified GFP-containing protein complex fractions were separated on a SDS-PAGE gradient gel. The gel was cut in a size distribution visualized by the white lines in Figure 4-27 and the slices were separately analyzed using LC-MS/MS to identify the binding partners.

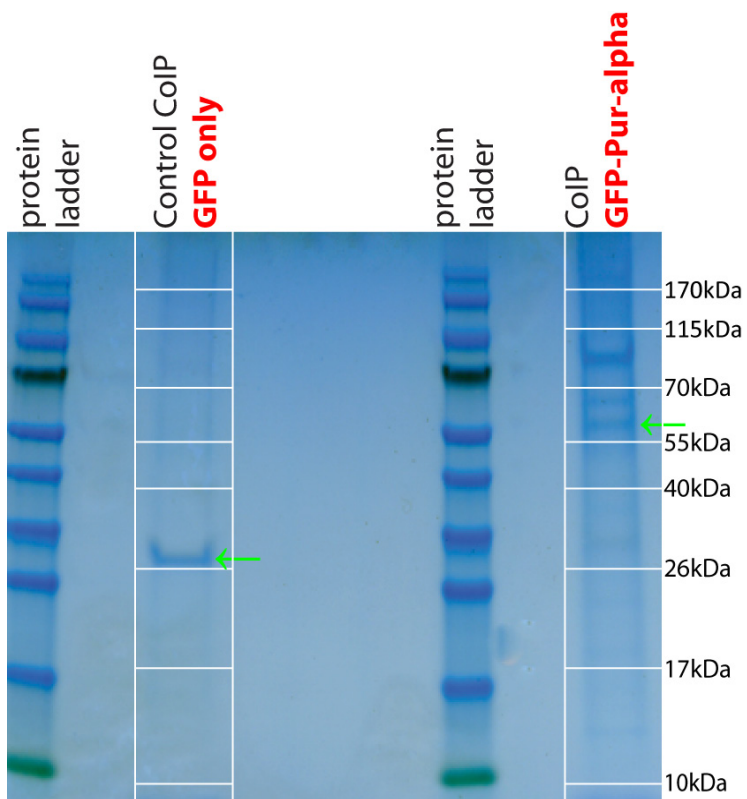


Figure 4-27: Mass-Spectrometry of Pur-alpha associated proteins in ovary extracts
Ovaries from GFP and GFP-Pur-alpha expressing flies were dissected, ovary extracts were prepared in lysis buffer and co-immunoprecipitation was performed from 2 mg ovary extract using GFP-trap A beads; the bound fractions were loaded on a precise protein gradient gel (20-4%) and stained with colloidal coomassie. Gel pieces were sliced as depicted above with white lines and analyzed using LC-MS/MS. Green arrows show the primarily pulled down proteins GFP (left side) and GFP-fused Pur-alpha (right side).

Table 4-3 shows the proteins which were specifically found in the Pur-alpha bound fraction and their abundance over a threshold of 20 % sequence coverage of the peptides regarding the whole protein sequence. In this list Me31B, Growl, Cup, Exuperantia, Trailer hitch and Ypsilon Schachtel were proteins specifically associated with Pur-alpha which are already known to be part of transported mRNPs during *Drosophila* oogenesis.

Protein	Number of peptides	Sequence coverage
Pur-alpha	20	67%
Me31B	28	63%
Growl	19	42%
Cup	32	41%
Exuperantia	16	35%
Trailer hitch	24	34%
Stress-sensitive B	9	27%
PABP	13	25%
Hsc4	15	25%
Dj-1beta	4	25%
Hsp26	4	24%
Ypsilon Schachtel	6	23%

Table 4-3: Mass-spectrometry of Pur-alpha associated proteins

Table shows mass spec results after CoIP, left column: name of associated protein, middle column: number of measured peptides, right column: sequence coverage of peptide sequence in relation to protein sequence, cut off was 20% sequence coverage, bold: proteins known to be associated with transported RNPs during *Drosophila* oogenesis

To validate the results of the mass spectrometry analysis the GFP affinity purification was repeated, followed by Western Blotting. This approach also allowed us to examine the interactions established by the mutated or truncated GFP-Pur-alpha variants described earlier.

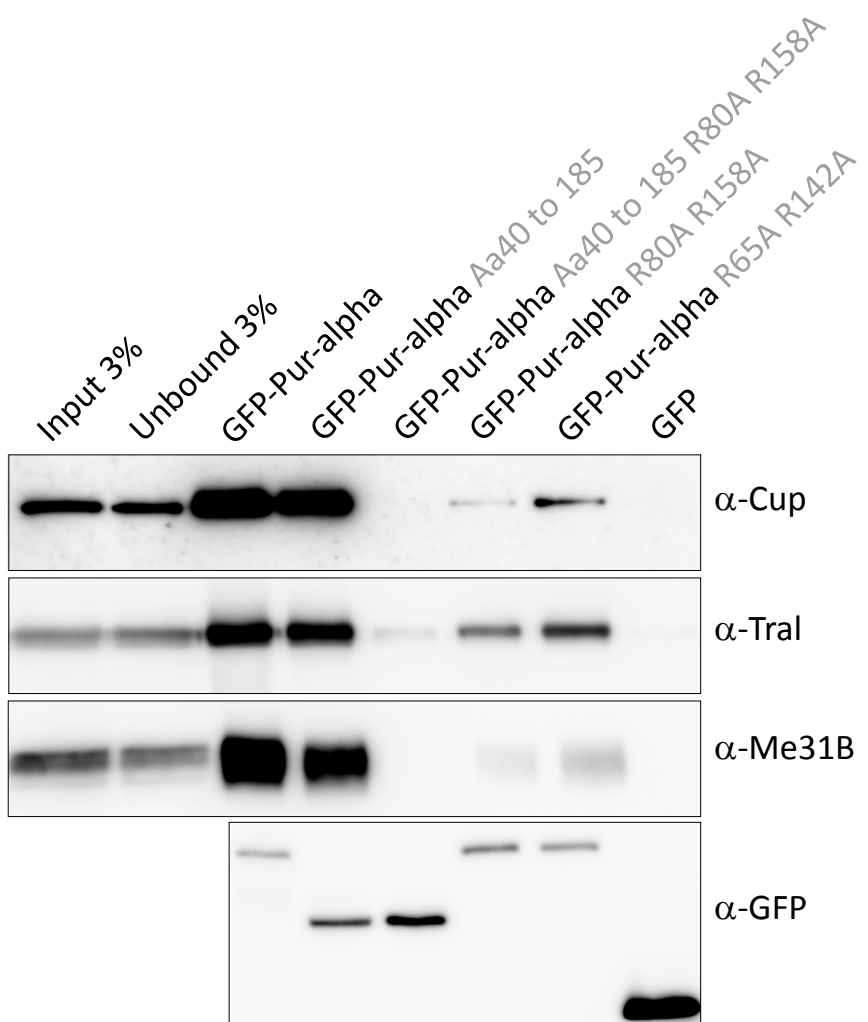


Figure 4-28: Verification of mass-spec results with Western Blotting

Ovaries from GFP and different GFP-Pur-alpha variants expressing flies (depicted above) were dissected, ovary extracts were prepared in lysis buffer and Co-Immunoprecipitation was performed from ovary extracts using GFP-trap A beads; 10 %-SDS-gel was loaded with the resulting fractions as depicted above; Western Blot analysis was performed using α -Cup, α -Tral and α -Me31B- antibody; bottom panel shows α -GFP Western Blot for comparison of pull down efficiency of the differently expressed GFP-fused-constructs

The association of full length GFP-Pur-alpha with Cup, Trailer hitch (Tral) and Me31B was nicely reproduced via Western Blot (Figure 4-28, lane 3) with available antibodies. For monomeric GFP-Pur-alpha repeat I and II the same association behaviour was visible (Figure 4-28, lane 4) indicating that dimerization was not required for this association. If the RNA binding capacity of Pur-alpha repeat I and II was impaired by the introduction of the two point mutations R80A and R158A the association with Cup and Me31B was completely abolished (Figure 4-28, lane 5). This leads to the assumption that these interactions are RNA-mediated. The association with Tral was diminished but not completely prevented. Thus, the interaction seemed to be at least partly direct. If the point mutations were introduced in full length background of the protein the association with the three tested factors was also diminished but still reasonable. The

dimerization of transgenic mutated GFP-Pur-alpha with the natural endogenous Pur-alpha via the third Pur-repeat is a possible reason for the observed association. The same was true for the two point mutations R65A R142A which impair the nucleic acid binding capacity of Pur-alpha to a lesser extent (Figure 4-28, lane 6). Taken together, these results suggested that the association of Pur-alpha with mRNP transport components is likely mediated through mRNAs bound by Pur-alpha. As a control GFP-only ovary extract was used in the initial mass spectrometry analysis (Figure 4-28, lane 7). The control anti-GFP-Western blot (Figure 4-28, bottom panel) shows that the GFP-fusion proteins could all be successfully immunoprecipitated.

4.5 Pur-alpha associated RNAs

4.5.1 Pur-alpha associated messengerRNAs

4.5.1.1 microArray and GO-Analysis

To get global information of Pur-alpha associated mRNAs a microarray analysis was carried out. Therefore GFP-trap co-immunoprecipitation was performed from GFP-Pur-alpha expressing ovary extracts as well as from flies expressing only GFP as a control. Bound and Input RNA was prepared and 100 ng were analyzed with Affymetrix Drosophila genome 2.0 arrays. Four arrays were performed, one array hybridization for each input and immunoprecipitated RNA sample. For normalization and data analysis R! / Bioconductor was applied. A broad range of transcripts (6340 in total) were detectable in the immunoprecipitate as well as in the control. Although total RNA recovery was higher with GFP-Pur-alpha than with GFP alone, it was not possible to distinguish a small subgroup of genes with a particularly high recovery in the GFP-Pur-alpha immunoprecipitate. To identify groups of functionally related factors all detected mRNAs were ranked according to their GFP-Pur-alpha vs. control ratio, and then a gene ontology (GO) analysis was performed. We employed GOrilla (EDEN *et al.* 2009), a software tool that allows searching for GO-term categories enriched at the top of a ranked list relative to the total list of detected genes (5300 genes were employed in the analysis). As a control, the mRNAs isolated from the protein extracts used as input in the Immunoprecipitation were also analyzed and ranked according to their GFP-Pur-alpha vs. control expression ratio, followed by gene ontology analysis. In order to get insights into Pur-alpha's role in specific localizations of proteins and mRNA transport, the GOrilla analysis was applied concentrating on cellular component terms. As shown in table 4-4,

GO-terms involving cell junctions (anchoring junction, cell junction, adherens junction) were significantly enriched in the ranked list after co-immunoprecipitation but not in the list ranked for the input ratio (Table 4-5).

Description (GO-term)	P-value Bound	P-value Input	Number of genes
<i>anchoring junction</i>	9.43E-6	-	19
<i>cell junction</i>	2.33E-5	-	25
plasma membrane part	2.34E-5	1.02E-4	46
apical part of cell	2.84E-5	-	9
axon	2.84E-5	-	9
<i>adherens junction</i>	2.87E-5	-	18
chromatin	6.49E-5	-	22
plasma membrane	7.45E-5	-	53
<i>cell projection</i>	1.1E-4	6.45E-4	16

Table 4-4: List according to Bound ratio

Description (GO-term)	P-value Input	P-value Bound	Number of genes
external encapsulating structure	3.41E-19	-	12
chorion	1.11E-15	-	10
membrane	9.09E-10	-	142
integral to membrane	1.03E-08	-	92
intrinsic to membrane	2.59E-08	-	94
plasma membrane	1.55E-06	-	61
vitelline envelope	5.04E-06	-	3
extracellular region	1.83E-05	-	17
membrane part	7.17E-05	-	134
plasma membrane part	1.02E-04	2.34E-5	45

Table 4-5: List according to Input ratio

4.5.1.2 Analysis of Pur-alpha associated mRNAs with qRT-PCR

To verify and analyze the results of the microarray data in more detail qRT-PCR experiments were carried out. We therefore repeated the immunoprecipitation procedure and analyzed the bound as well as the input mRNA by qRT-PCR for a set of candidate genes taken from the top of the microarray list together with several other genes with a known function during oogenesis and GAPDH, actin 5C and rp49 as controls. Through comparison of the ct-values of input and bound fractions the ratio of bound to input for GFP-Pur-alpha and for the GFP only control could be determined. Generally, the recovery was higher in GFP-Pur-alpha immunoprecipitates compared with GFP only, confirming that the GFP-Pur-alpha fusion protein retained its RNA binding capacity. Figure 4-29 and 4-30 show the results of three independent co-immunoprecipitation experiments ordered by the recovery-rate, respectively. Argonaute-2 (Ago2), diego (dgo), lerp, notch (N), CG4570 and disheveled (dsh) mRNA were significantly associated with Pur-alpha. The binding of mRNAs to the GFP only control is shown in figure 4-30.

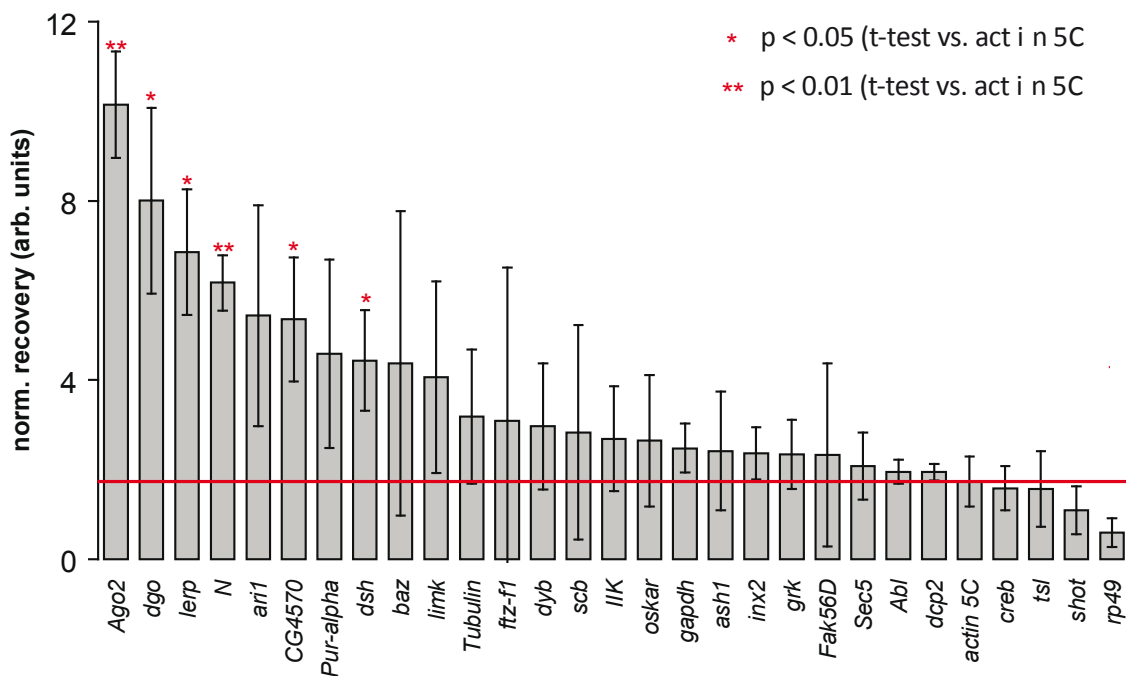


Figure 4-29: mRNA recovery after Co-IP of GFP-Pur-alpha ovaries

Bar chart depicts results from three individual qRT-PCR experiments with GFP-trap beads from GFP-Pur-alpha ovary extract, association with actin 5C mRNA serves as threshold (red line); red stars indicate p-values determined with student's t-test, significant p-values are depicted with red asterisks

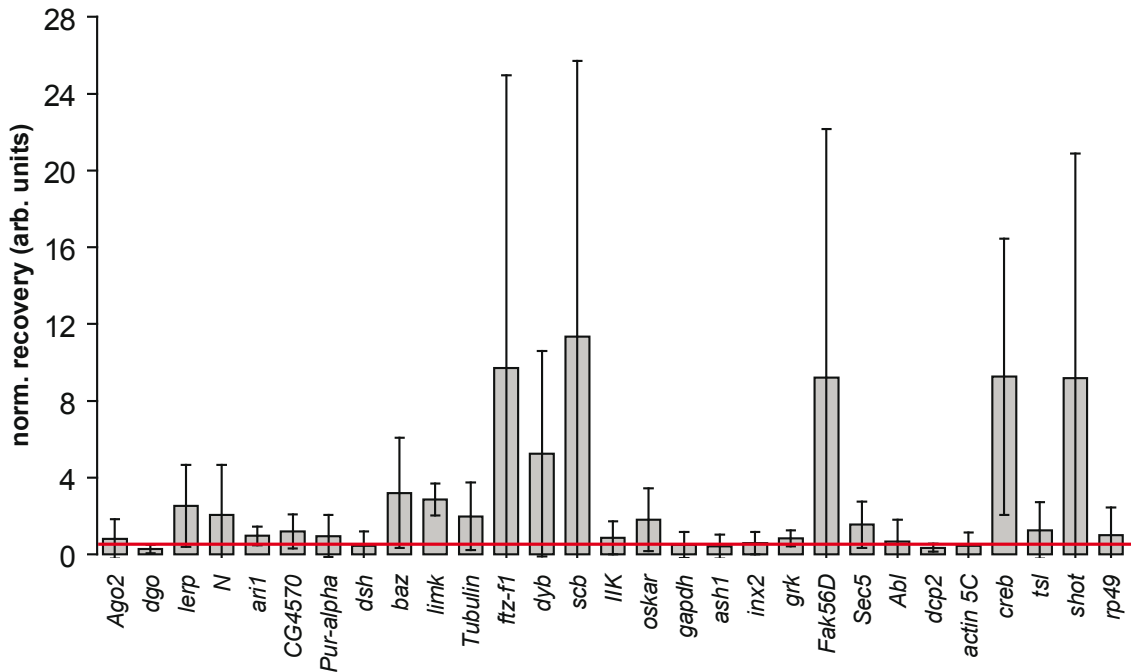


Figure 4-30: mRNA recovery after Co-IP of GFP-only (control) ovaries

Bar chart depicts results from three individual qRT-PCR experiments with GFP-trap beads from GFP ovary extract, red line indicates threshold (association with actin 5C mRNA)

4.5.1.3 Pur-alpha binds to sequences similar to the *opa* sequence

It is known that Pur-alpha binds to purine rich sequences so called PUR-elements in DNA and to CGG repeats in the Fmr1 mRNA. To analyze whether there is also a common sequence motif within the identified mRNAs from Drosophila ovary extracts, a sequence alignment was performed. Figure 5-1 (chapter 5.5) shows the sequence alignment with the *opa* sequence depicted on top. This sequence motif was identified within the notch mRNA sequence and consists predominantly of the triplets CAG (red, Figure 5-1) and CAA (green, Figure 5-1). It can be found in many other developmentally regulated transcripts (WHARTON *et al.* 1985). The predominantly with Pur-alpha associated mRNAs ago2, dsh, bazooka (baz) and ftz-f1 share opa-like sequences.

4.5.1.4 Recombinant Pur-alpha binds to (CAG)₄ and (CAG)₃CAA RNA *in vitro*

To verify the binding capacity of Pur-alpha *in vitro* electrophoretic mobility shift assays (EMSA) were performed. Therefore Fluorescein-labeled 12mer RNA oligos with (CGG)₄ as a positive control, (CAG)₄, (CAG)₃CAA and (CAA)₄ were used and titrated with increasing amounts of either recombinant Pur-alpha PUR-repeat I+II or Pur-alpha PUR-repeat I+II+III. Figure 4-31 shows the EMSA of (CAG)₄ with Pur-alpha PUR-repeat I+II+III. The ratio between bound and total RNA oligo was determined and the resulting binding curves fitted with the Dose Response (Logistic) fitting function (Figure 4-32). The half maximal effective concentration (EC50) values displayed in Table 4-6 specify the μ M binding constant of each protein variant to the RNA oligos, respectively. The binding constants of the full-length protein to the three RNAs (CGG)₄, (CAG)₄ and (CAG)₃CAA range between 1,2 and 1,6 μ M, with the highest affinity to (CAG)₃CAA RNA. The truncated protein, which consists of a single PUR-domain (Pur-alpha I+II) shows the highest binding affinity (0,7 μ M) to (CGG)₄ RNA, but also binds to (CAG)₄ and (CAG)₃CAA RNA. These results could verify the earlier in the microarray and the qRT-PCR observed results.

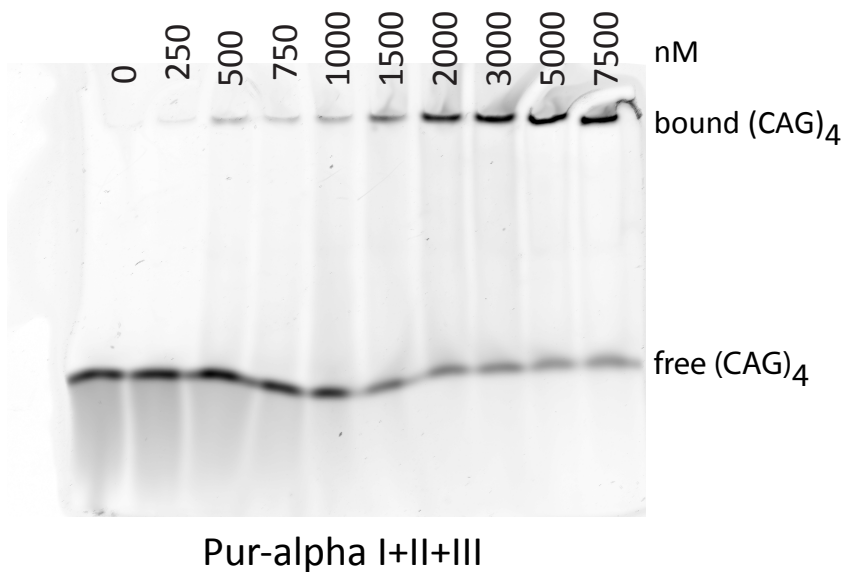
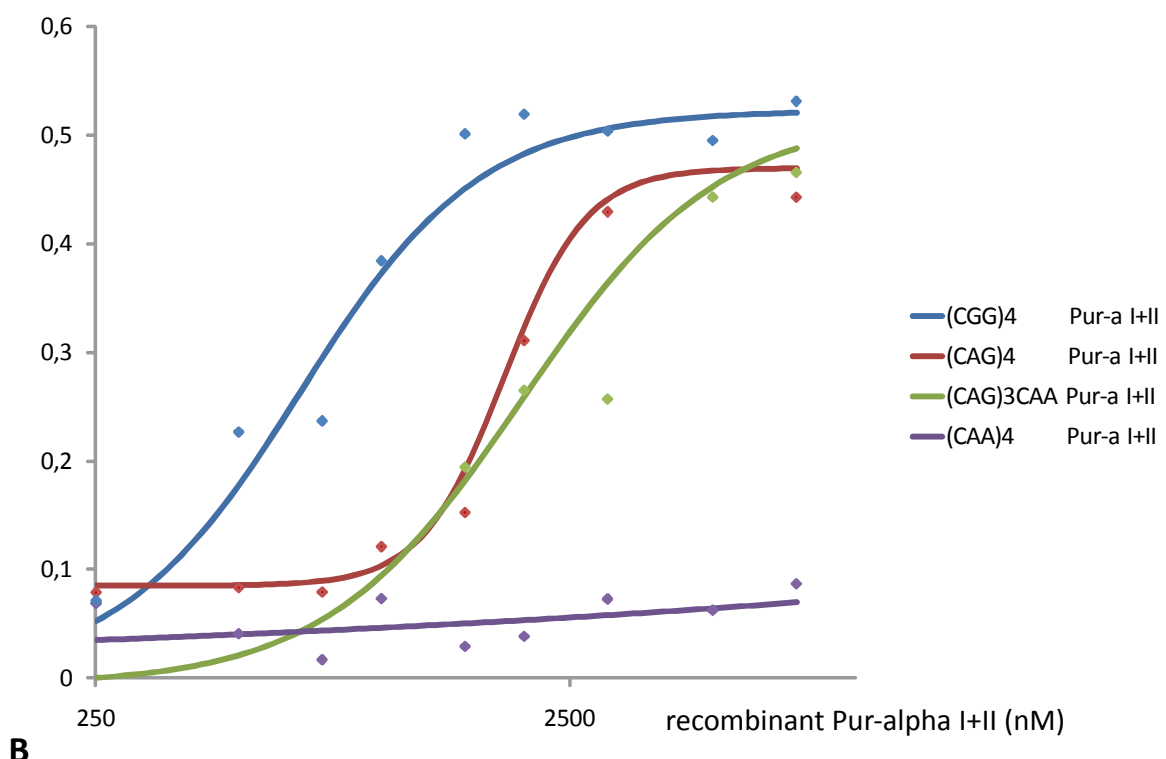
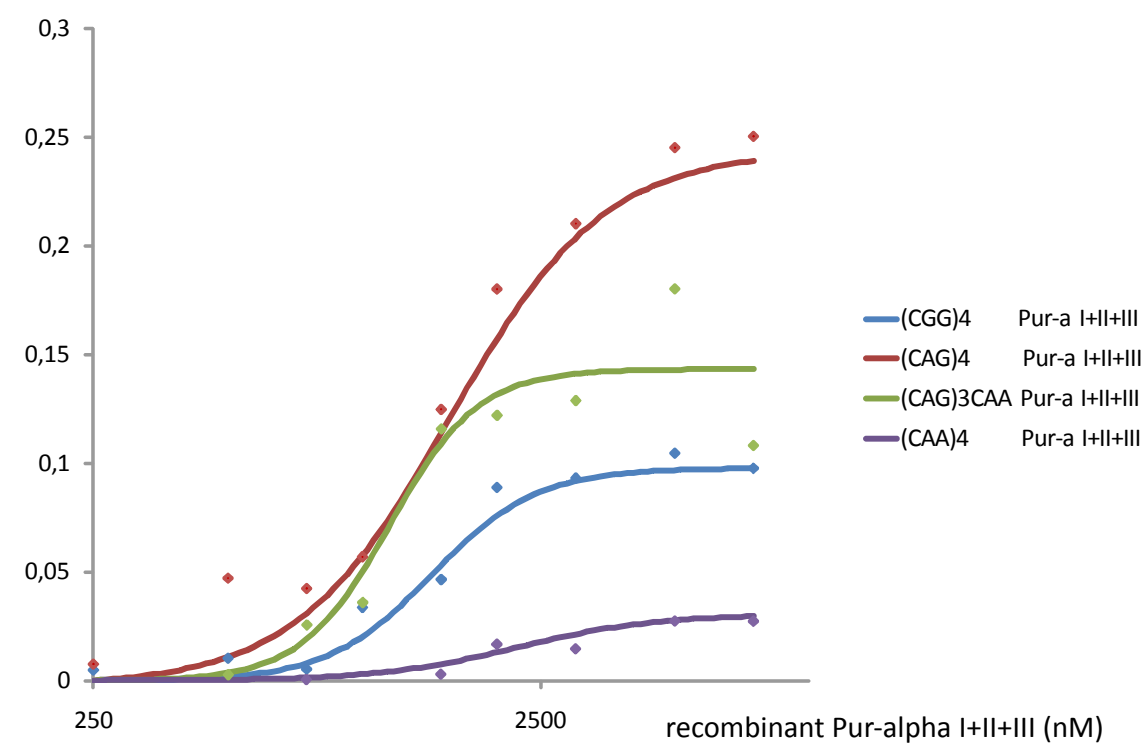


Figure 4-31: Pur-alpha binds to (CAG)₄ RNA

EMSA with recombinant Pur-alpha I+II+III and Flourescein-labeled (CAG)₄ RNA; c((CAG)₄)=100 nM, protein was titrated as depicted above the lanes

A**B****Figure 4-32: Binding curves of recombinant Pur-alpha**

A: Binding curves of recombinant Pur-alpha I+II to (CGG)₄ (blue), (CAG)₄ (dark red), (CAG)3CAA (green) and (CAA)₄ (violet) RNA 12mer

B: Binding curves of recombinant Pur-alpha I+II+III to (CGG)₄ (blue), (CAG)₄ (dark red), (CAG)3CAA (green) and (CAA)₄ (violet) RNA 12mer

RNA oligo	Pur-alpha I+II	Pur-alpha I+II+III
r(CGG) ₄	0,68 µM	1,43 µM
r(CAG) ₄	1,81 µM	1,56 µM
r(CAG) ₃ CAA	1,97 µM	1,15 µM
r(CAA) ₄	not determined	2,22 µM

Table 4-6: EC50 values/binding constants of recombinant Pur-alpha to RNA oligos

4.5.2 Pur-alpha associated microRNAs

4.5.2.1 Pur-alpha associated microRNAs from FLAG-Pur-alpha transfected Schneider cells

If Pur-alpha is associated with mRNP particles, then microRNAs should also be found in Pur-alpha immunoprecipitates. As easily accessible first experimental setting co-immunoprecipitations from Schneider cells transfected with FLAG-tagged Pur-alpha were performed. The pulled down RNAs were purified with TRizol and then the small RNA content was analyzed regarding the four microRNAs miR-277, bantam, miR-34 and miR-317 via Northern Blotting (Figure 4-33). As control probe the ribosomal 2S-RNA was used (Figure 4-33, bottom panel). The Argonaute-1 IP (Figure 4-33, lane 3) served as a control for the functionality of the assay; all four tested microRNAs were associated with the RISC component Ago1. The IP of the FLAG-tagged (Figure 4-33, lane 4) as well as of the endogenous (Figure 4-33, lane 5) Pur-alpha resulted in purification of all four tested microRNAs. And the endogenous Pur-alpha also seemed to be associated with the ribosomal S2-RNA (Figure 4-33, lane 5, bottom panel). This was not surprising as there might also be ribosomes associated with mRNPs. As the fact was known from earlier experiments during this thesis that Pur-alpha interacts with Ago1 in Schneider cells (Figure 4-6) the pulled down microRNAs might be associated with the co-purified Ago1 protein. Thus, Pur-alpha is associated likely in an indirect manner with several microRNAs in cell culture.

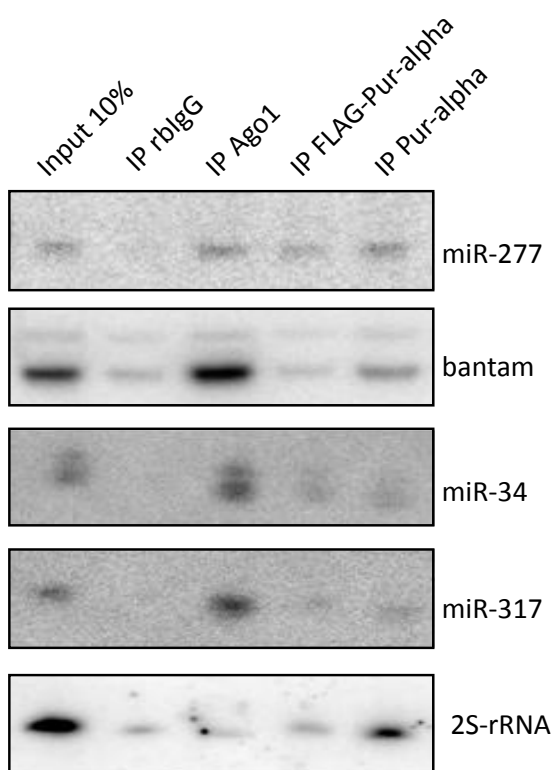


Figure 4-33: Analysis of Pur-alpha associated microRNAs in cell-culture

Drosophila Schneider cells were transfected with FLAG-Pur-alpha, after three days cells were harvested and CoIP using α -rabbit-IgG, α -Ago1 1b8, α -FLAG and polyclonal rb α -Pur-alpha antibody from cell extracts was performed. RNA from bound fractions was purified with TRIZOL and Northern Blot analysis was performed using as-RNA probes against mir-277, bantam, miR-34 and mi-317; 2S-rRNA served as a control.

4.5.2.2 Pur-alpha associated microRNAs from GFP-Pur-alpha transgenic ovary-extracts

After the cell culture experiments revealed that Pur-alpha complexes contain microRNAs, the Pur-alpha associated microRNAs from *Drosophila* ovary extracts were analyzed in a more global fashion. Therefore a compendium of 80 microRNAs was tested. These microRNAs were compiled based on deep sequencing data from various life stages covering the development of *Drosophila* from embryo to adult fly (ModEncode Consortium). Together, the analyzed microRNAs cover at least 95% of the microRNA-matching reads for any of the life stages examined.

Again GFP associated complexes were purified from ovaries from GFP-Pur-alpha- and GFP-only-expressing flies using GFP-trap® affinity-beads. The RNA content from the obtained complexes was purified with Trizol, reverse transcribed and analyzed with qRT-PCR using the miScript system. From the cDNA the levels of the 80 microRNAs were determined. Figure 4-34 shows a heatmap of the measured levels of the microRNAs of two independent experiments (A and B). Comparing the microRNA levels of the GFP-Pur-alpha extracts to the miRNAs recovered after

immunoprecipitation of GFP-Pur-alpha, especially miR-252, miR-133 and miR-124 were enriched (Figure 4-34). This is indicated by the green color in the two input fractions (Input A and B) which represents a low abundance compared to the red color in the two bound fractions (Bound A and B) which represents a high abundance (Figure 4-34, top three lanes). Other microRNAs like e.g. mir-306, miR-278 and miR-282 were depleted from the bound fractions in the two experiments; indicated by the color changes from red in the input fractions to green in the bound fractions. Control-co-immunoprecipitations from extracts harboring only GFP contained much lower levels of microRNAs which are indicated by the bright green colors (Figure 4-34, 'Bound control'-column).

Consequently, this change in the relative abundance of certain microRNAs between the input fractions and Pur-alpha-co-immunoprecipitated fractions is indicating that not all mRNP particles are equally associated with GFP-Pur-alpha.

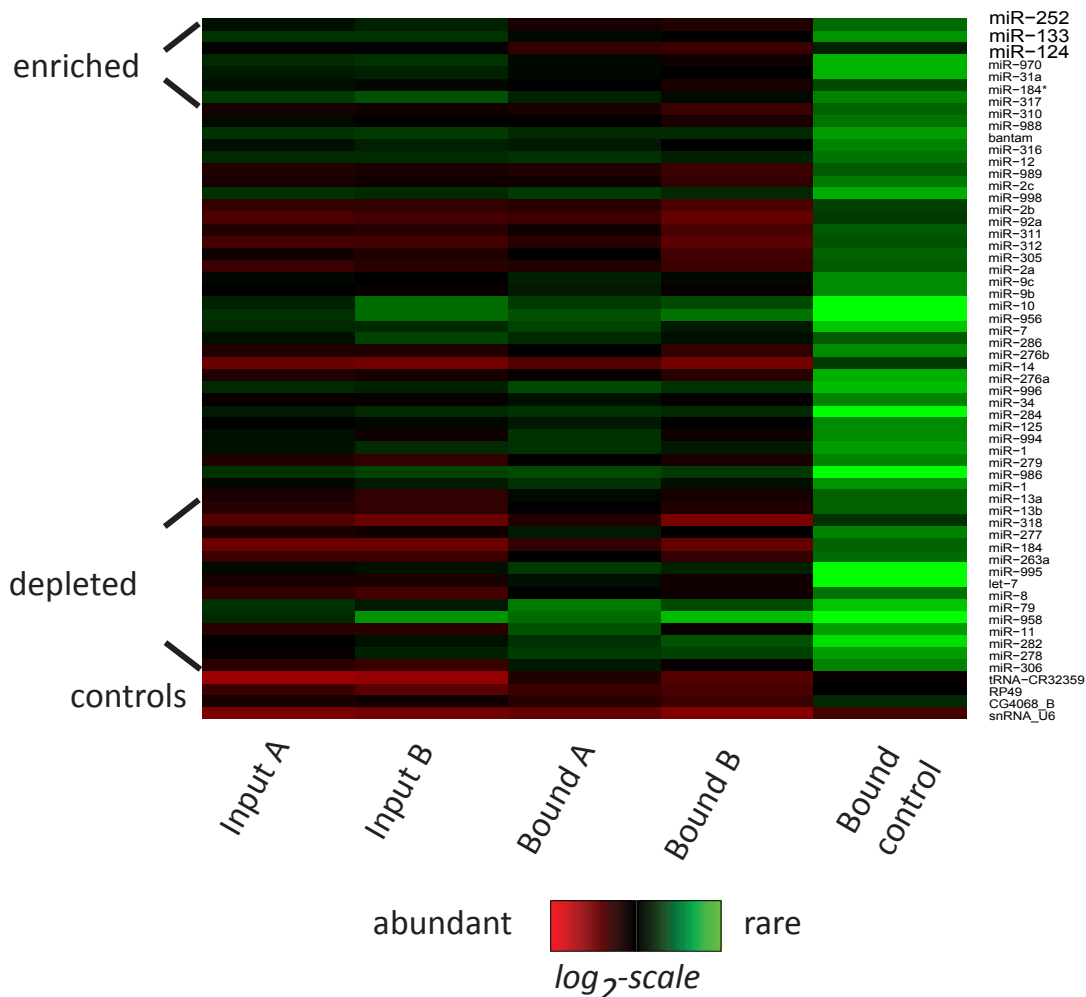


Figure 4-34: Heatmap of Pur-alpha associated microRNAs in Drosophila ovary extracts

Two independent CoIP-experiments A and B were performed, microRNA levels were determined with qRT-PCR using the Qiagen miScript-System; red color: abundant RNAs; green color: rare RNAs

To verify the results from the global microRNA analysis of Pur-alpha ovary precipitates, qRT-PCR experiments were carried out, analyzing especially the Pur-alpha associated or depleted microRNAs again using the miScript system. The result is depicted by the bar chart in Figure 4-35 and confirmed the earlier observed results, namely that miR-252, miR-133 and miR-124 were preferentially associated with Pur-alpha; and miR-282, miR-278 and miR-306 were not.

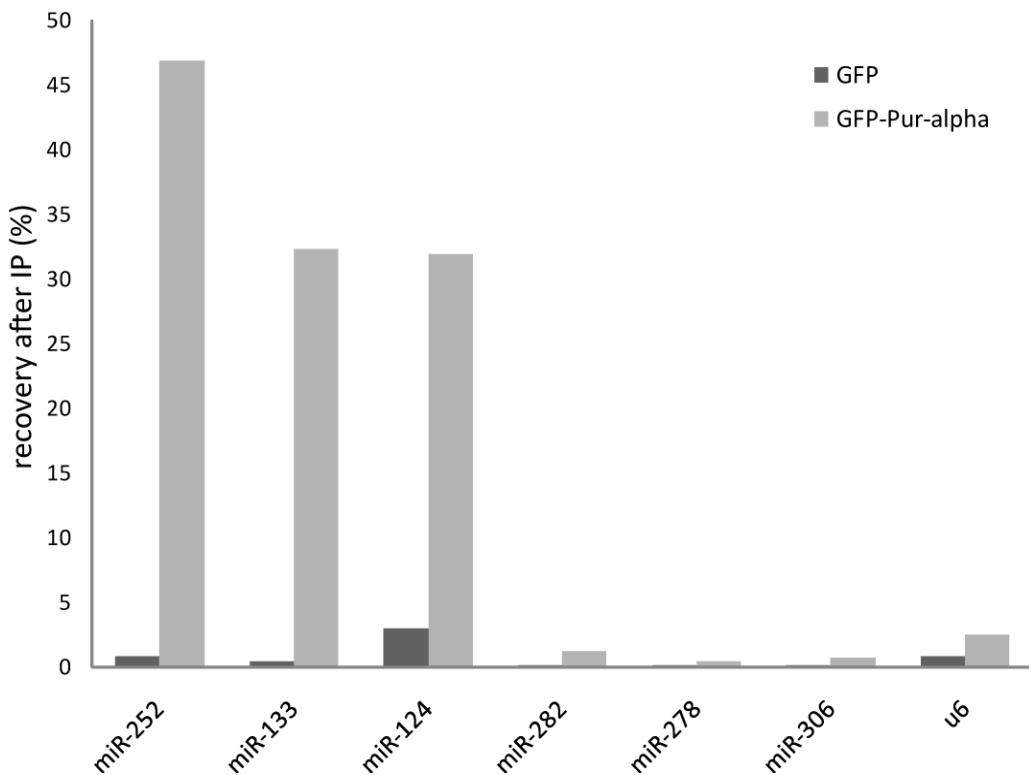


Figure 4-35: miScript qRT-PCR after CoIP of GFP-/GFP-Pur-alpha expressing ovary extracts

Single microRNA levels were measured with qRT-PCR using the Qiagen miScript-System, and recovery after CoIP was determined using the $2^{-\Delta\Delta Ct}$ -method, dark grey bars indicate the pulled down microRNAs from GFP-only ovary extracts, light grey bars the GFP-Pur-alpha pulled down microRNAs

4.5.2.3 GO-term analysis of top three enriched or depleted microRNA predicted targets

In certain cases, miRNAs co-regulate genes that function within a common theme. Therefore another analysis of the cellular component GO-terms was performed, this time asking for enrichment among the predicted targets of the top 3 enriched or depleted miRNAs. To avoid introducing a bias by the origin of the material, the 5300 mRNAs, which had been earlier detected in the microarray experiments from ovary extracts, were used as control population. Again, the GO-terms for cell junction and membrane localization were clearly overrepresented among the

predicted targets of miR-252 and miR-124, which were found preferentially associated with GFP-Pur-alpha (Table 4-7). This finding is consistent with the results of the GO-term analysis for the mRNAs (Table 4-4). For miR-133 there are no predicted targets.

Taken together, this data suggests that Pur-alpha is associated with a variety of mRNAs and microRNAs but appears to preferentially bind transcripts coding for cell-cell junction components.

miR-252

GO-term	P-value
integral to membrane	1.03E-14
intrinsic to membrane	-
membrane part	-
plasma membrane	-
membrane	3.45E-5
plasma membrane part	1.83E-4
extracellular region part	4.4E-4
myosin complex	-
endocytic vesicle	-
integral to plasma membrane	

miR-124

GO-term	P-value
plasma membrane part	2.56E-5
focal adhesion	3.34E-5
cell-substrate adherens junction	7.03E-5
cell-substrate junction	9.7E-5
membrane part	3.67E-4
cell junction	4.41E-4

Table 4-7: GO-term analysis of predicted miRNA targets of miR-252 and miR-124

5. DISCUSSION

In *Drosophila*, the division of a germ line stem cell is the beginning of a program that turns a cystoblast into a mature egg containing nutrients, pattern information and an egg shell for mechanical protection. This production requires a precisely defined and coordinated interaction between the germ line descendants and the somatic follicle cells that surround them.

During this thesis the nucleic acid binding protein Pur-alpha was identified as a novel player in this process. It was shown that its function is essential for the first encapsulation of a germ line cyst and furthermore, for the migration of the border cells prior to stage 10. Pur-alpha is part of mRNP complexes. The transported mRNAs are enriched for cell junction and adhesion molecules, likely associated with miRNAs repressing their translation. Transport of these mRNAs to their appropriate location within the cell may be required for cell migration and/or recognition of the neighboring cells at the destination.

5.1 Pur-alpha's structure to function relation

The *Drosophila* Pur-alpha protein consists of three so called PUR-repeats. Structurally the first two repeats form a whirly like fold, which makes up an autonomous nucleic acid binding domain, the PUR-domain (GRAEB SCH *et al.* 2009). A homo-dimerization of the protein is achieved via the third PUR-repeat, which itself forms a PUR-domain together with another third PUR-repeat from a second Pur-alpha protein. The *in vivo* studies during this thesis could show that Pur-alpha is transported early into the developing oocyte during *Drosophila* oogenesis. The generation of transgenic flies with different GFP-fused truncated and mutated Pur-alpha protein versions helped to reveal the requirements for correct localization of different modified mutated or truncated proteins. The analysis of GFP-Pur-alpha R80A R158A transgenic ovaries showed that RNA binding and dimerization of the protein are crucial for optimal transport into the oocyte (Chapter 4.2.2). The recruitment of more than one RNA binding domain onto a cargo mRNA is a common strategy among RNA transport factors, likely to increase affinity, specificity or the chance for the cargo to remain bound throughout the entire transport time (VALVERDE *et al.* 2008). Introduction of the point mutation R229A in the third Pur-repeat leads to diminished but not completely abolished transport (Chapter 4.2.2; Figure 4-13) of the full-length protein with mutations in every PUR-repeat (GFP-Pur-alpha R80A R158A R229A). The residual transport can be explained by the possible dimerization of a transgenic protein with an endogenous wild type

protein which can still bind to RNA and is therefore transported correctly. The dimerization capacity of triple mutant Pur-alpha protein was shown in the Co-IP experiment from *Drosophila* Schneider cells extract with GFP- and FLAG-tagged Pur-alpha (Chapter 4.2.1.1; Figure 4-5). A further observation from cell-culture experiments (Chapter 4.2.2.1) as well as from *in vivo* studies of transport during oogenesis (Chapter 4.2.2.2) was that mutant Pur-alpha with diminished nucleic acid binding started to accumulate in the nucleus of Schneider cells or nurse cells. This might be an indication that under normal circumstances, Pur-alpha shuttles between nucleus and cytoplasm considering the assembly of Pur-alpha containing mRNPs at least in part in the nucleus. Stable binding to RNA is required for efficient nuclear export of Pur-alpha and its potential cargo. The accumulation of Pur-alpha in the nucleus was also observed during neurodegeneration in FXTAS, where nuclear inclusions in neurons and astrocytes containing the mutation carrying *FMR1* mRNA and Pur-alpha bound to this wrong RNA were observed (JIN *et al.* 2007). The export from the nucleus appeared to be independent from Exportin 1 (CRM1) and Importin-alpha 3 (D-Cas). This was analyzed in cell culture experiments using LeptomycinB (FASKEN *et al.* 2000) and RNA-interference against D-Cas (TEKOTTE *et al.* 2002) (data not shown).

Analogous shuttling between nucleus and cytoplasm has been described for Cup (ZAPPAVIGNA *et al.* 2004), one of the Pur-alpha protein interaction partners which was identified in this thesis in chapter 4.4. RNA binding of Pur-alpha is also required for the association of Pur-alpha with its protein interaction partners. The interaction of Pur-alpha from ovary extracts with Cup, Trailor hitch and Me31b was abolished if RNA binding was impaired (Chapter 4.4; Figure 4-28) and the same was true for cell-culture experiments where the interaction with Ago1, FMRP and partly Ago2 was prevented (Chapter 4.2.1.2, Figure 4-7 and 4-8), if the two point mutations R80A and R158A where present in Pur-alpha PUR-repeat I+II.

5.2 Identified Pur-alpha associated proteins

The most abundant Pur-alpha associated protein found by mass spectrometry analysis in *Drosophila* ovary extracts in this study was Me31B. Altogether, 28 peptides derived from Me31B were found, which covered 63 % of the protein sequence (Chapter 4.4; Table 4-3). Me31B is a DEAD-box-helicase protein and involved in the formation of cytoplasmic mRNP complexes together with Exuperantia (Exu) and oocyte-localizing RNAs (NAKAMURA *et al.* 2001). If Me31B is lost during early oogenesis, translation of the associated mRNAs *oskar* and *BicD* starts before they reach their final destinations. Me31B was also found in Staufen- and FMRP containing RNPs in *Drosophila* neurons (BARBEE *et al.* 2006), where it was shown to act together with Trailor hitch

(Tral) in FMRP-driven, Argonaute protein dependent translational repression. The proteins Exu (SCHUPBACH and WIESCHAUS 1986) and Tral (WILHELM *et al.* 2005) were also found in Pur-alpha immunoprecipitates with 16 peptides for Exu and 24 peptides for Tral, corresponding to 35% and 24% sequences coverage, respectively (Chapter 4.4; Table 4-3). Exu is known to be a main sponge body component in *Drosophila* oogenesis. These structures are intracellular compartments for the assembly and transport of maternal products involved in RNA localization (WILSCH-BRAUNINGER *et al.* 1997). Taken together, the association of Pur-alpha with these proteins and their known functions, allowed us to conclude that Pur-alpha is part of transported mRNPs during oogenesis. The translational silencing during transport appears to be at least in part achieved by microRNAs. These findings fit nicely together with the observed microRNA content in Pur-alpha co-immunoprecipitates (Chapter 4.5.2).

Another Pur-alpha associated protein identified is Cup (32 peptides and 41 % sequence coverage; Chapter 4.4; Table 3). Together with Nanos, Cup functions in the maintenance of germ-line stem cells during oogenesis (VERROTTI and WHARTON 2000). Through its interaction with the translation initiation factor eIF4E Cup controls the translation of *oskar*, *gurken* and *nanos* mRNA (CLOUSE *et al.* 2008; NAKAMURA *et al.* 2004; WILHELM *et al.* 2003). On the protein level Cup is associated with the mRNA binding protein Staufen and the adaptor protein Miranda, which is indicating a function for Cup mediated translational repression during mRNA transport (PICCIONI *et al.* 2009). The observed association between Cup and Pur-alpha argues for a further role of Pur-alpha in transport of translationally silenced mRNAs during oogenesis. Interestingly, the abundant transport protein Staufen (reviewed in (ROEGIERS and JAN 2000)) was not found among the Pur-alpha associated proteins in this study. Therefore, Pur-alpha mediated transport might be independent of the Staufen dependent transport machinery.

Cup mutant flies lay eggs with incompletely closed egg shells (SCHUPBACH and WIESCHAUS 1991). For the proper production of the egg shell the differentiation of follicle cells, correct follicle cell migration and many complex protein modification and trafficking events are necessary (reviewed in (WARING 2000)). If Pur-alpha is knocked down in the follicle cells of the ovary with a UAS-RNAi line against Pur-alpha and a traffic jam-GAL4 driver line (Chapter 4.3.3), the eggs appear flask and perforated and the hatching of the larvae is decreased to 33 % (Chapter 4.3.3, Table 4-2). The knock down did not produce the same severe phenotype which was observed in *pur-alpha*^{KG05743} mutant ovaries, probably due to the remaining Pur-alpha level in the germline cells. However, the observed phenotype suggests a functional interaction between Cup and Pur-alpha mutant flies, which must be confirmed and further analyzed in future genetic experiments.

It is known that in mouse brain extracts, Pur-alpha associates with the Fragile-X mental retardation protein (FMRP) (JOHNSON *et al.* 2006; OHASHI *et al.* 2002). This association was

confirmed during this thesis with *Drosophila* Pur-alpha and the homologous dFMR1 protein in Schneider cells (Chapter 4.2.1.2; Figure 4-6). The dFMR1-interacting protein Ago2 also co-purifies with Pur-alpha (Chapter 4.2.1.2; Figure 4-7) (JIN *et al.* 2004). Both *fmr1* and *ago2* mutant flies show a multiple oocyte phenotype at low penetrance (PEPPER *et al.* 2009). This phenotype could also be present in some of the *pur-alpha*^{KG05743} ovaries. Since the Pur-alpha protein forms a complex with Ago2 and the *ago2* mRNA was found associated with Pur-alpha, it is not possible to distinguish whether this may be connected to the follicle cell migration defect because the Ago2-Pur-alpha protein complex is missing, or because the corresponding mRNAs are no longer properly localized in *pur-alpha* mutants.

5.3 Pur-alpha mutant flies display a new early follicle cell phenotype

In mutant flies carrying the allele *pur-alpha*^{KG05743} the follicle cells fail to surround the germline cyst, which is budding from the germarium at stage 1 during early *Drosophila* oogenesis. The initial encapsulation of the germline cyst is achieved by mesenchymal to epithelial transition of precursor follicle cells (MARGOLIS and SPRADLING 1995). In the following differential adhesion of these follicle cells to their neighboring cells drives the encapsulation of the germline cyst (for a review see (STEINBERG 2007)). The reduced amount of Pur-alpha protein seems to interfere with these up to now not very well studied early differentiation events, indicating a crucial role for Pur-alpha in mesenchymal to epithelial transition or differential adhesion.

Female flies carrying the weaker allele *Pur-alpha*^{KG05177} have more Pur-alpha protein left than the flies with the *pur-alpha*^{KG05743} allele (Chapter 4.3; Figure 4-14). They have reduced numbers of stage 10 egg chambers in their ovarioles (Chapter 4.3.2; Table 4-1), a defect that occurs later during oogenesis. For the correct establishment of a stage 10 egg chamber centripetal migration of the follicle cells is necessary at stage 10 B of oogenesis. The centripetally migrating follicle cells form the later operculum and ventral collar of the eggshell. For centripetal migration events Decapentaplegic (Dpp) and Notch signaling is crucial (DOBENS *et al.* 2005; DOBENS *et al.* 2000). If the Pur-alpha level is decreased due to the P-element insertion in the *pur-alpha*^{KG05177} allele, the centripetal migration is impaired. This argues for an important function of Pur-alpha in either Dpp or Notch signaling.

Another observed phenotype in flies with Pur-alpha knock down in follicle cells displays perforated and loose embryos with reduced hatching of larvae (Chapter 4.3.3, Table 4-2), which might be due to a leaky egg shell and defects during egg shell development. In germline cells with wild type levels of Pur-alpha, the migration events of the follicle cells which are necessary for the

first encapsulation or centripetal migration remain unaffected. Hence, signaling events between somatic follicle cells and germline cells are crucial for these migration steps, which require a certain amount of Pur-alpha protein to be completely functional.

Taken together, the severity and the time point of manifestation of the different observed phenotypes seem to correlate with the residual Pur-alpha protein levels and affected cell types. Although the occurrence of the phenotypic defects is different for the two P-element insertions and the Pur-alpha knock down, all defects are linked to follicle cell functions. Consequently, Pur-alpha plays a central role in correct follicle cell function and their associated responsibilities during the course of development.

Other well known follicle cell phenotypes are compound follicles, which have two or more germline cysts in one egg chamber. For example, mutations in hedgehog (hh) signaling cause defects in cyst encapsulation with two cysts in one egg chamber (FORBES *et al.* 1996). The JAK-STAT signaling pathway also plays important roles in the development of a correct follicular epithelium. If Domeless, which functions upstream of the Unpaired signal, is mutated early in oogenesis egg chambers show incomplete encapsulation or fusion and if the onset of the mutation is later border cell migration is impaired (GHIGLIONE *et al.* 2002). Similar phenotypes were observed in *toucan* mutants (GRAMMONT *et al.* 1997), and in *brainiac* and *egghead* flies, which also have epithelial discontinuities, e.g. multilayered egg chambers or compound egg chambers (GOODE *et al.* 1996a; GOODE *et al.* 1996b; GOODE *et al.* 1992).

The notch signaling pathway is also a main organizer of correct follicle cell development during *Drosophila* oogenesis. Changes in notch level induce stalk abnormalities and later defects in axis formation of the oocyte (LARKIN *et al.* 1996; RUOHOLA *et al.* 1991). Correct function of fringe, which modulates the ability of the Notch receptor to be activated by its ligands, is especially important for the determination of the polar cells, which are the main organizers in the follicular epithelium (GRAMMONT and IRVINE 2001; GRAMMONT and IRVINE 2002). The protein Cut, a genetic interactor of Notch also affects the fate of the follicular cells and if mutated leads to egg chambers containing fewer than 15 nurse cells with incorrect and incomplete encapsulation by follicle cells (JACKSON and BLOCHLINGER 1997).

A comparison of all known follicle cell phenotypes with egg chambers from flies carrying the *pur-alpha*^{KG05743} allele shows that the appearance of follicle cell lumps at one side of the egg chamber is a new and up to now not described very early phenotype during *Drosophila* oogenesis caused by decreased levels of Pur-alpha protein.

5.4 Cell fates appear unchanged in *pur-alpha* mutant ovaries

Migration defects might be caused by problems within the migrating cells or because the target cells are no longer recognizable for the migrating cells. Cell fate changes along the migration path or at the final destination site may lead to changes in the specific set of cell-surface molecules and receptor ligands, with the result that the migrating cells get lost or do not start migrating at all. A series of well defined signaling events ensures that position-dependent differentiation events occur at the appropriate times as the egg chamber matures. Specifically, the germ line induces Notch signaling in the prepolar cells via expression of the ligand Delta on its surface. Together with the expression of Fringe on neighboring follicle cells, this induces polar cell fate and expression of the ligand Unpaired, activating the JAK/STAT pathway in the adjacent cells and differentiating those into stalk cells (Chapter 2.2.2) (ASSA-KUNIK *et al.* 2007; GRAMMONT and IRVINE 2001; GRAMMONT and IRVINE 2002; LOPEZ-SCHIER and ST JOHNSTON 2001).

The observed migration defect in *pur-alpha*^{KG05177} and *pur-alpha*^{KG05743} flies could be explained if polar cells or the oocyte are no longer specified correctly. But interestingly this does not appear to be the case. One single oocyte per egg chamber is specified, the oocyte-nurse cell ratio remains normal and the nurse cells are undergoing polyplloidization as in wild type (Chapter 4.3.4.1; Figure 4-24). The specification of two pairs of polar cells is also not affected in the malformed egg chambers. The Fasciclin-III positive polar cell pairs even seem to be lying at opposite sides instead of along the anterior posterior axis of the egg chamber (Chapter 4.3.4.1; Figure 4-25). There may nonetheless be changes in the fate of other cells indirectly affecting patterning and migration. In addition, due to the highly disorganized ovariole structure in *pur-alpha*^{KG05743} mutants it cannot be assessed whether the observed specification of oocyte and polar cells occurs at the correct time points during *Drosophila* oogenesis.

The maintenance of adherens junctions is also a crucial process during oogenesis and for correct development of the follicular epithelium (ROPER and BROWN 2003; TANENTZAPF *et al.* 2000). Armadillo, which is the *Drosophila* homolog to vertebrate beta-catenin, is a main component of the adherens junction protein complex (COX *et al.* 1996; PEIFER *et al.* 1993). The level of armadillo protein and the polarized localization at the apical surface of the follicle cells remains unaffected in *pur-alpha*^{KG05743} mutants indicating correct assembly of adherens junctions in Pur-alpha mutants (Chapter 4.3.4.2, Figure 4-26).

5.5 Pur-alpha's RNA cargoes

The developing *Drosophila* oocyte has been intensively studied as a model system for the localization of mRNAs. The majority of maternally provided mRNAs shows a specific localization pattern in the embryo (LECUYER *et al.* 2007) and Pur-alpha may be required to transport at least a portion of these maternal transcripts. Since the earlier defect in the follicle cells in *pur-alpha* mutants halts oocyte maturation, the localization of e.g. *oskar* or *bicoid* mRNA could not be assessed directly, but is unaffected in flies kept at non restrictive temperature (data not shown). However, eggs laid by mutant mothers kept at the restrictive temperature develop normally when placed back at 25°C (data not shown); indicating that any defect imposed at the restrictive temperature is reversible.

In the *Drosophila* ovary, Pur-alpha is expressed in both, the follicle cells and the germline cells, and it is reasonable to assume that the Pur-alpha containing complexes may differ in their detailed composition between those two lineages with respect to the associated proteins and mRNAs. Furthermore, the co-immunoprecipitation experiments in this thesis likely captured all mRNAs contained in entire Pur-alpha mRNPs, not all of which are necessarily bound by Pur-alpha directly. Finally, Pur-alpha is a RNA binding protein and it might be possible that some of the detected RNAs are bound to Pur-alpha only after cell lysis. To deal with this problem an *in vivo* cross linking step of the whole ovaries before cell lysis would help and also allow more extensive washing steps after the co-immunoprecipitation to get rid of unspecific binders. The prepared ovary extracts are most likely predominated by the germ-line form of Pur-alpha complexes, simply because the mature eggs contribute the greatest part. The identification of Cup and Me31B as prominent protein interaction partners emphasizes this fact because both proteins are expressed only in the germ line cells (KEYES and SPRADLING 1997; NAKAMURA *et al.* 2001).

Even though the phenotype is most evident in follicle cells, it is difficult to directly identify the mRNAs bound to Pur-alpha in follicle cells, which are required for proper follicle cell migration, due to the small fraction of follicle cells compared to germline cells in ovary extracts used for the co- immunoprecipitations. Nonetheless, the mRNAs coding for *notch* (*N*), *ago-2*, *disheveled* (*dsh*), *diego* (*dgo*) and *larp*, which are significantly associated with Pur-alpha, were identified in the co-immunoprecipitation assay in this study (Chapter 4.5.1, Figure 4-29). Diego regulates the frizzled pathway of planar cell polarity signaling by binding to dsh (JENNY and MŁODZIK 2006). Dsh, in turn, functions in the ovary as part of the DWnt4/Fz-2 signaling cascade. This system controls the mobility of somatic apical cells while they surround the germarium (COHEN *et al.* 2002), an event that occurs even earlier than the strongest phenotype which was observed in *pur-alpha*^{KG05743} flies.

Regarding the sequences of Pur-alpha associated mRNAs it is interesting to note that the notch mRNA contains a common sequence motif called *opa*-sequence. The *opa*-sequence element is a 93 bp repeated sequence consisting predominantly of the triplets CAG and CAA and can be found in many other developmentally regulated transcription units (WHARTON *et al.* 1985). Our electrophoretic mobility shift assays (Chapter 4.5.1, Figure 4-32) could confirm the binding of Pur-alpha to a $(CAG)_4$ 12mer RNA and to $(CAG)_3CAA$ RNA *in vitro*, while binding to a $(CAA)_4$ 12mer RNA could not be observed. The mRNAs of notch, ago2, dsh, bazooka (baz) and ftz-f1 which were found to be associated with Pur-alpha also contain CAG rich sequences (Figure 5-1).

Figure 5-1: putative RNA-binding sites of Pur-alpha

Comparison of sequences of Pur-alpha associated mRNAs; green: CAA; red: CAG

This argues for a new RNA binding motif of Pur-alpha in addition to the already known binding to the known CGG repeat RNA motif. In contrast to these results, Jin and colleagues found in their *in vitro* studies with fly brain lysates that CAG repeat RNA is not bound by Pur-alpha (JIN *et al.* 2007). In detail, they could not compete the binding of Pur-alpha to rCGG repeat RNA with a 100 fold excess of rCAG repeat RNA (Figure 5-2). This might be due to differences in affinity if rCGG RNA is bound by Pur-alpha of whole fly brain lysate stronger than by purified recombinant Pur-alpha. Another explanation might be that another unknown factor within the undefined lysates is either interfering with the binding of Pur-alpha to r(CAG)_n or promotes binding to r(CGG)_n.

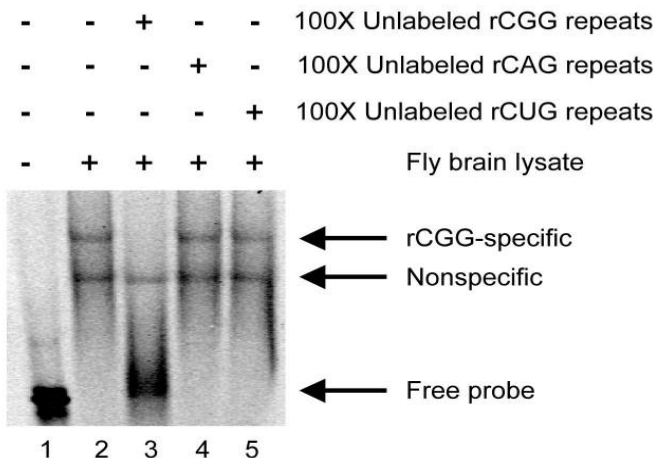


Figure 5-2: Gel-shift competition assay with fly brain lysates

Lane 1: rCGG probe only; lane 2: rCGG probe with fly brain lysates; lanes 3–5: rCGG probe and fly brain lysates in the presence of 100-fold unlabeled triplet repeat RNA, as indicated (molar ratio) (figure taken from Jin et al., 2007)

The global analysis of Pur-alpha associated mRNAs with GOrilla revealed that mRNAs with GO-terms involving cell-cell junctions (anchoring junction, cell junction and adherens junction) are enriched in GFP-Pur-alpha co-immunoprecipitates (Chapter 4.5.1; Table 4-4). Considering the follicle cell phenotype of *pur-alpha* mutant flies these cellular functions fit nicely to the role of Pur-alpha in the establishment of a correctly formed follicular epithelium.

Taken together the findings support the notion that during *Drosophila* oogenesis, Pur-alpha mediates the mRNA transport that is required for cellular recognition and orientation in a three-dimensional cellular context by localizing mRNAs of cell-cell junction factors and the multiple bound mRNAs may be synergistically responsible for the observed mutant phenotype.

The main part of the small RNA content in the germline is piRNAs. These RNAs protect the germline from selfish mobile genetic elements to ensure a correct transfer of the genetic material to the progeny (for a review see (KHURANA and THEURKAUF 2010)). But there are also a few studies of microRNA function in the *Drosophila* ovary. Iovino and colleagues revealed that miR-184 has important functions during oogenesis and early embryogenesis, and if its function is impaired the whole egg production is defective (IOVINO *et al.* 2009). Self-renewal of the germline stem cells also requires microRNA function (PARK *et al.* 2007). Furthermore, Reich and colleagues observed that transgenes with synthetic sites of miR-317 undergo microRNA-machinery mediated repression in the ovary (REICH *et al.* 2009).

During this study Pur-alpha associated microRNAs were identified; with miR-252, miR-133 and miR-124 as “top 3” bound microRNAs (Chapter 4.5.2; Figure 4-34). A GO-analysis of the predicted targets of these microRNAs revealed that GO-terms for cell-cell junction and membrane

localization were clearly overrepresented (Chapter 4.5.2.3; Table 4-7). This observation correlates with the functional terms of Pur-alpha associated mRNAs (Chapter 4.5.1.1; Table 4-4). Altogether, this suggests a role for Pur-alpha in transport of translationally silenced mRNAs of cell-cell-junction and localization factors during *Drosophila* oogenesis.

5.6 Implication of Pur-alpha for metastasis and neurodegeneration

Border cells undergo an epithelial to mesenchymal transition before they start migrating through the nurse cells during oogenesis. This is closely related to the transition from a solid primary tumor to migrating and metastasis forming cancer cells. Compared to tumor cells which form metastases, border cells never lose their apical-basal polarity during the process of migration. Human *Pur-alpha* was described as a tumor suppressor (chapter 2.4.3) due to its role in transcriptional regulation and to its associated protein binding partners (DARBINIAN *et al.* 2001b; LEZON-GEYDA *et al.* 2001; WANG *et al.* 2008). This thesis describes that *Drosophila* Pur-alpha is an important player in cell migration considering a new aspect of how Pur alpha might be implicated in cancer and the formation of metastases.

Sequestration of Pur-alpha into nuclear inclusion in neurons and astrocytes by binding to overrepresented r(CGG)_n repeat RNA is one of the molecular mechanisms responsible for the development of FXTAS in a *Drosophila* disease model (JIN *et al.* 2007). There are many neurodegeneration diseases which derive from toxic RNA transcripts with expanded triplet repeats (for a review see (TODD and PAULSON 2010)).

This study identified that Pur-alpha binds as well as to CGG repeat RNA to CAG repeat RNA (Chapter 4.5.1.4; Figure 4-32). The triplet repeat expansion disorder spinocerebellar ataxia type 3, also known as Machado-Joseph Disease (TEIVE 2009), is a consequence of a triplet repeat expansion of r(CAG)_n in the *ataxin 3* gene (LI *et al.* 2008). Also the overrepresentation of CAG repeats in the antisense transcripts of a non coding gene ATXN8, which is responsible for the development of spinocerebellar ataxia type 8 (SCA8), seems to be a reason for the disease (MOSELEY *et al.* 2006). Binding of Pur-alpha to the overrepresented r(CAG)_n repeats might be a new aspect for the molecular mechanism underlying these diseases.

5.7 Conclusion

This study revealed *Drosophila melanogaster* as a very versatile model organism to study the multiple functions of the protein Pur-alpha *in vivo*. New functions for Pur-alpha during oogenesis were identified which include the ensheathment of the developing egg chamber during early oogenesis, the migration of border cells to overcome stage 10 of oogenesis and a further function during the development of a proper egg shell. All the observed Pur-alpha phenotypes suggest a crucial role for Pur-alpha in the somatic follicle cells of the *Drosophila* ovary.

Furthermore, an early yet undescribed oogenesis phenotype was discovered, namely a formation of a lump of follicle cells at one side of the egg chambers.

Pur-alpha associated mRNAs could be identified, which in common share CGG and CAG repeat rich sequences, which are similar to the opa-sequence and can be related to the GO term cell junction.

The functions of Pur-alpha during follicle cell migration might help to obtain further insights into metastasis formation in cancer. The new RNA binding motif of Pur-alpha might help to understand the molecular mechanisms of triplet repeat expansion RNA associated diseases like FXTAS and spinocerebellar ataxia in more detail.

6. APPENDIX

6.1 Abbreviations

63N1	endo-siRNA cell culture reporter cell line
67-1D	siRNA cell culture reporter cell line
A	Alanine, Adenine
Aa	Amino acid
Ago	Argonaute protein
Amp	Ampicillin
APS	Ammonium peroxodisulfate
ATP	Adenosine triphosphate
bp	Base pair(s)
BSA	Bovine serum albumine
C	Cytosine
cDNA	complementary DNA
Co-IP	co-immunoprecipitation
CT-value	cycle of threshold value in qPCR
d	day(s)
Da	Dalton
<i>dm</i> , <i>D. melanogaster</i>	<i>Drosophila melanogaster</i>
DMSO	Dimethyl sulfoxide
DNA	Desoxy-ribonucleic acid
dNTP	Desoxy-nucleotide-tri-phosphate
DPP	Decapentaplegic
ds	double-stranded
DTT	Dithiothreitol
EC50	half maximal effective concentration
ECL	Enhanced Chemiluminescence
<i>E. coli</i>	<i>Escherichia coli</i>
EGFP	Enhanced Green Fluorescent protein
EMSA	electrophoretic mobility shift assay
endo-	endogenous

exo-	exogenous
Eya	eyes absent
FACS	Fluorescence Activated Cell Sorting
FBS	Fetal Bovine Serum
fl	full length
FMRP	Fragile Mental Retardation Protein
for	forward
G	Guanine
g	gram, standard acceleration
GFP	Green Fluorescent Protein
GO	gene ontology
h	hour(s)
hh	hedgehog
HEPES	(4-(2-hydroxyethyl)-1-piperazineethanesulfonic acid
HRP	Horseradish Peroxidase
hts	hu-li tai shao
Hygro	Hygromycin
IgG	immunoglobulin protein G
inp.	input
IP	immunoprecipitation
IPTG	Isopropyl- β -D-thiogalactopyranosid
k	kilo
Kana	Kanamycin
k.d.	knock down
KIF	Kinesin superfamily protein
k.o.	knock-out
MCS	Multiple Cloning Site
mg	milligram
min	minute
miR	micro RNA
ml	milliliter
mRNA	messenger RNA
mRNP	messenger ribonucleoprotein
nc	non coding
Neo	Neomycin

ng	nanogram
nt	nucleotide(s)
NTP	nucleotide-tri-phosphate
ORF	open reading frame
OrR	Oregon R fly wild type strain
p.a.	pro analysis
PAGE	Polyacrylamide Gel Electrophoresis
PCR	Polymerase Chain Reaction
piRNA	Piwi-interacting RNA
Poly-A	polyadenylation
PVDF	Polyvinylidenefluoride
qPCR	quantitative Polymerase Chain Reaction
R	Arginine
rb	rabbit
rel	relative
rev	reverse
RNA	ribonucleic acid
RNAi	RNA interference
RNP	ribonucleoprotein particle
rpm	runs per minute
rRNA	ribosomal RNA
RT	reverse transcription or real-time
S2 cell	Schneider-2 cell
SAXS	small angle X-ray scattering
SDS	sodium doceetyl sulfate
siRNA	small interfering RNA
SOB	Super Optimal Broth
ss	single stranded
SSC	sodium chloride/sodium citrate
SV40	Simian Virus 40
T	thymine
TRIS	Tris(hydroxymethyl)-aminomethane
TRBP	TAR RNA binding protein
tub	tubulin
U	uracil

UAS	yeast Upstream Activating Sequence
UTR	untranslated region
V	Volt
Δ	deletion
α	anti
$^{\circ}\text{C}$	degrees Celsius
μ	micro

6.2 Acknowledgements

Ich bedanke mich herzlich bei meinem Doktorvater, Klaus Förstemann, der es mir ermöglicht hat an diesem spannenden, herausfordernden und vor allem sehr abwechslungsreichen Projekt zu arbeiten. Vor allem für die nie endenden neuen Ideen, Denkanstöße und Lösungen für alle aufkommenden Probleme und die immer positiven aufmunternden Worte möchte ich mich bedanken.

Meinem Thesis Advisory Komitee, Gaia Tavosanis und Dierk Niessing, danke ich für fruchtbare Diskussionen und hilfreiche Tipps für den Fortschritt zu Beginn der Doktorarbeit.

Prof. Dr. Dietmar Martin möchte ich für die freundliche Übernahme des Zweitgutachtens danken.

Almut Graebsch und Sabine Ströbl danke ich für die Zusammenarbeit, die Lösung der Proteinstruktur und das zur Verfügung stellen von Plasmiden. Kerstin Maier und Björn Schwalb danke ich für die Durchführung und Auswertung der microArray-Experimente.

Für die Mitarbeit am Projekt möchte ich Maresa Grundhuber und Andreas Hader danken, die durch ihr Praktikum, bzw. ihre Bachelorarbeit am Fortgang der Arbeit mitgewirkt haben. Katharina Michalik danke ich für das Bereitstellen von Fliegenfutter, Puffern und Laborverbrauchsmaterialien, durch das das Arbeiten im Labor um vieles leichter wurde.

Der ganzen Arbeitsgruppe vor allem Steffi1, Steffi2, Stephanie, Romy, Katha und Milijana, danke ich für die super Zusammenarbeit im Labor. Auch in schlechten Zeiten, hat man mit euch nie den Humor und das Lachen verloren. Die Freundschaft und Unternehmungen, die über den Laboralltag hinaus gehen, haben vieles einfacher und vor allem lustiger gemacht.

Britta Flach und Stephanie Fesser danke ich für das Korrekturlesen der Arbeit.

Meinen Eltern und Freunden danke ich für die Unterstützung und Aufmunterungen während der ganzen Zeit von Studium und Doktorarbeit, ohne die das alles bestimmt nicht möglich gewesen wäre.

6.3 Curriculum Vitae

Verena Nicole Aumiller

Personal Data:

Date of Birth: November 28th, 1981

Place of Birth: Dachau, Germany

Nationality: German

Family status: unmarried

Academic training:

2007-2011 Graduate studies at the Gene Center, Ludwigs-Maximilians-Universität, München

2006-2007 Helmholtz-Zentrum, München, Clinical Cooperation Group HCT

2001-2006 Biology Studies at the Ludwigs-Maximilians-Universität, München and Friedrich-Alexander-Universität, Erlangen-Nürnberg

Diploma degree in biology

Education:

1999-2001 Holbein Gymnasium, Augsburg

1992-1999 A.B. von Stetten'sches Institut, Gymnasium, Augsburg

1988-1992 Luitpold Grundschule, Augsburg

7. References

- ALTING-MEES, M. A., J. A. SORGE and J. M. SHORT, 1992 pBluescriptII: multifunctional cloning and mapping vectors. *Methods Enzymol* **216**: 483-495.
- ANDERSON, P., and N. KEDERSHA, 2009 RNA granules: post-transcriptional and epigenetic modulators of gene expression. *Nat Rev Mol Cell Biol* **10**: 430-436.
- ASSA-KUNIK, E., I. L. TORRES, E. D. SCHEJTER, D. S. JOHNSTON and B. Z. SHILO, 2007 Drosophila follicle cells are patterned by multiple levels of Notch signaling and antagonism between the Notch and JAK/STAT pathways. *Development* **134**: 1161-1169.
- BAI, J., and D. MONTELL, 2002 Eyes absent, a key repressor of polar cell fate during Drosophila oogenesis. *Development* **129**: 5377-5388.
- BARBEE, S. A., P. S. ESTES, A. M. CZIKO, J. HILLEBRAND, R. A. LUDEMAN *et al.*, 2006 Staufen- and FMRP-containing neuronal RNPs are structurally and functionally related to somatic P bodies. *Neuron* **52**: 997-1009.
- BASTOCK, R., and D. ST JOHNSTON, 2008 Drosophila oogenesis. *Curr Biol* **18**: R1082-1087.
- BECCARI, S., L. TEIXEIRA and P. RORTH, 2002 The JAK/STAT pathway is required for border cell migration during Drosophila oogenesis. *Mech Dev* **111**: 115-123.
- BEHM-ANSMANT, I., J. REHWINKEL, T. DOERKS, A. STARK, P. BORK *et al.*, 2006 mRNA degradation by miRNAs and GW182 requires both CCR4:NOT deadenylase and DCP1:DCP2 decapping complexes. *Genes Dev* **20**: 1885-1898.
- BERGEMANN, A. D., and E. M. JOHNSON, 1992 The HeLa Pur factor binds single-stranded DNA at a specific element conserved in gene flanking regions and origins of DNA replication. *Mol Cell Biol* **12**: 1257-1265.
- BERRY-KRAVIS, E., L. ABRAMS, S. M. COFFEY, D. A. HALL, C. GRECO *et al.*, 2007 Fragile X-associated tremor/ataxia syndrome: clinical features, genetics, and testing guidelines. *Mov Disord* **22**: 2018-2030, quiz 2140.
- BRAND, A. H., and N. PERRIMON, 1993 Targeted gene expression as a means of altering cell fates and generating dominant phenotypes. *Development* **118**: 401-415.
- CHEN, N. N., and K. KHALILI, 1995 Transcriptional regulation of human JC polyomavirus promoters by cellular proteins YB-1 and Pur alpha in glial cells. *J Virol* **69**: 5843-5848.
- CHEPENIK, L. G., A. P. TRETIKOVA, C. P. KRACHMAROV, E. M. JOHNSON and K. KHALILI, 1998 The single-stranded DNA binding protein, Pur-alpha, binds HIV-1 TAR RNA and activates HIV-1 transcription. *Gene* **210**: 37-44.
- CHRISTERSON, L. B., and D. M. MCKEARIN, 1994 orb is required for anteroposterior and dorsoventral patterning during Drosophila oogenesis. *Genes Dev* **8**: 614-628.

- CLOUSE, K. N., S. B. FERGUSON and T. SCHUPBACH, 2008 Squid, Cup, and PABP55B function together to regulate gurken translation in Drosophila. *Dev Biol* **313**: 713-724.
- COHEN, E. D., M. C. MARIOL, R. M. WALLACE, J. WEYERS, Y. G. KAMBEROV *et al.*, 2002 DWnt4 regulates cell movement and focal adhesion kinase during Drosophila ovarian morphogenesis. *Dev Cell* **2**: 437-448.
- Cox, R. T., C. KIRKPATRICK and M. PEIFER, 1996 Armadillo is required for adherens junction assembly, cell polarity, and morphogenesis during Drosophila embryogenesis. *J Cell Biol* **134**: 133-148.
- DARBINIAN, N., J. CUI, A. BASILE, L. DEL VALLE, J. OTTE *et al.*, 2008 Negative regulation of AbetaPP gene expression by pur-alpha. *J Alzheimers Dis* **15**: 71-82.
- DARBINIAN, N., G. L. GALLIA and K. KHALILI, 2001a Helix-destabilizing properties of the human single-stranded DNA- and RNA-binding protein Puralpha. *J Cell Biochem* **80**: 589-595.
- DARBINIAN, N., G. L. GALLIA, J. KING, L. DEL VALLE, E. M. JOHNSON *et al.*, 2001b Growth inhibition of glioblastoma cells by human Pur(alpha). *J Cell Physiol* **189**: 334-340.
- DARBINIAN, N., G. L. GALLIA, M. KUNDU, N. SHCHERBIK, A. TRETIKOVA *et al.*, 1999 Association of Pur alpha and E2F-1 suppresses transcriptional activity of E2F-1. *Oncogene* **18**: 6398-6402.
- DARBINIAN, N., B. E. SAWAYA, K. KHALILI, N. JAFFE, B. WORTMAN *et al.*, 2001c Functional interaction between cyclin T1/cdk9 and Puralpha determines the level of TNFalpha promoter activation by Tat in glial cells. *J Neuroimmunol* **121**: 3-11.
- DOBENS, L., A. JAEGER, J. S. PETERSON and L. A. RAFTERY, 2005 Bunched sets a boundary for Notch signaling to pattern anterior eggshell structures during Drosophila oogenesis. *Dev Biol* **287**: 425-437.
- DOBENS, L. L., J. S. PETERSON, J. TREISMAN and L. A. RAFTERY, 2000 Drosophila bunched integrates opposing DPP and EGF signals to set the operculum boundary. *Development* **127**: 745-754.
- EDEN, E., R. NAVON, I. STEINFELD, D. LIPSON and Z. YAKHINI, 2009 GOrilla: a tool for discovery and visualization of enriched GO terms in ranked gene lists. *BMC Bioinformatics* **10**: 48.
- ELVIRA, G., S. WASIAK, V. BLANDFORD, X. K. TONG, A. SERRANO *et al.*, 2006 Characterization of an RNA granule from developing brain. *Mol Cell Proteomics* **5**: 635-651.
- EULALIO, A., I. BEHM-ANSMANT, D. SCHWEIZER and E. IZAURRALDE, 2007 P-body formation is a consequence, not the cause, of RNA-mediated gene silencing. *Mol Cell Biol* **27**: 3970-3981.
- FASKEN, M. B., R. SAUNDERS, M. ROSENBERG and D. W. BRIGHTY, 2000 A leptomycin B-sensitive homologue of human CRM1 promotes nuclear export of nuclear export sequence-containing proteins in Drosophila cells. *J Biol Chem* **275**: 1878-1886.

- FORBES, A. J., H. LIN, P. W. INGHAM and A. C. SPRADLING, 1996 hedgehog is required for the proliferation and specification of ovarian somatic cells prior to egg chamber formation in *Drosophila*. *Development* **122**: 1125-1135.
- FORSTEMANN, K., M. D. HORWICH, L. WEE, Y. TOMARI and P. D. ZAMORE, 2007 *Drosophila* microRNAs are sorted into functionally distinct argonaute complexes after production by dicer-1. *Cell* **130**: 287-297.
- FORSTEMANN, K., Y. TOMARI, T. DU, V. V. VAGIN, A. M. DENLI *et al.*, 2005 Normal microRNA maturation and germ-line stem cell maintenance requires Loquacious, a double-stranded RNA-binding domain protein. *PLoS Biol* **3**: e236.
- GALLIA, G. L., E. M. JOHNSON and K. KHALILI, 2000 Puralpha: a multifunctional single-stranded DNA- and RNA-binding protein. *Nucleic Acids Res* **28**: 3197-3205.
- GHIGLIONE, C., O. DEVERGNE, E. GEORGENTHUM, F. CARBALLES, C. MEDIONI *et al.*, 2002 The *Drosophila* cytokine receptor Domeless controls border cell migration and epithelial polarization during oogenesis. *Development* **129**: 5437-5447.
- GODT, D., and U. TEPPASS, 1998 *Drosophila* oocyte localization is mediated by differential cadherin-based adhesion. *Nature* **395**: 387-391.
- GOODE, S., M. MELNICK, T. B. CHOU and N. PERRIMON, 1996a The neurogenic genes egghead and brainiac define a novel signaling pathway essential for epithelial morphogenesis during *Drosophila* oogenesis. *Development* **122**: 3863-3879.
- GOODE, S., M. MORGAN, Y. P. LIANG and A. P. MAHOWALD, 1996b Brainiac encodes a novel, putative secreted protein that cooperates with Grk TGF alpha in the genesis of the follicular epithelium. *Dev Biol* **178**: 35-50.
- GOODE, S., D. WRIGHT and A. P. MAHOWALD, 1992 The neurogenic locus brainiac cooperates with the *Drosophila* EGF receptor to establish the ovarian follicle and to determine its dorsal-ventral polarity. *Development* **116**: 177-192.
- GRAEB SCH, A., S. ROCHE and D. NIESSING, 2009 X-ray structure of Pur-alpha reveals a Whirly-like fold and an unusual nucleic-acid binding surface. *Proc Natl Acad Sci U S A* **106**: 18521-18526.
- GRAMMONT, M., B. DASTUGUE and J. L. COUDERC, 1997 The *Drosophila* toucan (toc) gene is required in germline cells for the somatic cell patterning during oogenesis. *Development* **124**: 4917-4926.
- GRAMMONT, M., and K. D. IRVINE, 2001 fringe and Notch specify polar cell fate during *Drosophila* oogenesis. *Development* **128**: 2243-2253.
- GRAMMONT, M., and K. D. IRVINE, 2002 Organizer activity of the polar cells during *Drosophila* oogenesis. *Development* **129**: 5131-5140.

- GRECO, C. M., R. F. BERMAN, R. M. MARTIN, F. TASSONE, P. H. SCHWARTZ *et al.*, 2006 Neuropathology of fragile X-associated tremor/ataxia syndrome (FXTAS). *Brain* **129**: 243-255.
- GRECO, C. M., R. J. HAGERMAN, F. TASSONE, A. E. CHUDLEY, M. R. DEL BIGIO *et al.*, 2002 Neuronal intranuclear inclusions in a new cerebellar tremor/ataxia syndrome among fragile X carriers. *Brain* **125**: 1760-1771.
- GUPTA, M., V. SUEBLINVONG, J. RAMAN, V. JEEVANANDAM and M. P. GUPTA, 2003 Single-stranded DNA-binding proteins PURalpha and PURbeta bind to a purine-rich negative regulatory element of the alpha-myosin heavy chain gene and control transcriptional and translational regulation of the gene expression. Implications in the repression of alpha-myosin heavy chain during heart failure. *J Biol Chem* **278**: 44935-44948.
- HAAS, S., P. THATIKUNTA, A. STEPLEWSKI, E. M. JOHNSON, K. KHALILI *et al.*, 1995 A 39-kD DNA-binding protein from mouse brain stimulates transcription of myelin basic protein gene in oligodendrocytic cells. *J Cell Biol* **130**: 1171-1179.
- HAASE, A. D., L. JASKIEWICZ, H. ZHANG, S. LAINE, R. SACK *et al.*, 2005 TRBP, a regulator of cellular PKR and HIV-1 virus expression, interacts with Dicer and functions in RNA silencing. *EMBO Rep* **6**: 961-967.
- HARTIG, J. V., S. ESSLINGER, R. BOTTCHER, K. SAITO and K. FORSTEMANN, 2009 Endo-siRNAs depend on a new isoform of loquacious and target artificially introduced, high-copy sequences. *EMBO J* **28**: 2932-2944.
- INOUE, T., E. S. LEMAN, D. B. YEATER and R. H. GETZENBERG, 2008 The potential role of purine-rich element binding protein (PUR) alpha as a novel treatment target for hormone-refractory prostate cancer. *Prostate* **68**: 1048-1056.
- IOVINO, N., A. PANE and U. GAUL, 2009 miR-184 has multiple roles in Drosophila female germline development. *Dev Cell* **17**: 123-133.
- ITOH, H., M. J. WORTMAN, M. KANOFSKY, R. R. USON, R. E. GORDON *et al.*, 1998 Alterations in Pur(alpha) levels and intracellular localization in the CV-1 cell cycle. *Cell Growth Differ* **9**: 651-665.
- JACKSON, S. M., and K. BLOCHLINGER, 1997 cut interacts with Notch and protein kinase A to regulate egg chamber formation and to maintain germline cyst integrity during Drosophila oogenesis. *Development* **124**: 3663-3672.
- JAMBHEKAR, A., and J. L. DERISI, 2007 Cis-acting determinants of asymmetric, cytoplasmic RNA transport. *RNA* **13**: 625-642.
- JENNY, A., and M. MLODZIK, 2006 Planar cell polarity signaling: a common mechanism for cellular polarization. *Mt Sinai J Med* **73**: 738-750.

- JIN, P., R. DUAN, A. QURASHI, Y. QIN, D. TIAN *et al.*, 2007 Pur alpha binds to rCGG repeats and modulates repeat-mediated neurodegeneration in a *Drosophila* model of fragile X tremor/ataxia syndrome. *Neuron* **55**: 556-564.
- JIN, P., D. C. ZARNESCU, S. CEMAN, M. NAKAMOTO, J. MOWREY *et al.*, 2004 Biochemical and genetic interaction between the fragile X mental retardation protein and the microRNA pathway. *Nat Neurosci* **7**: 113-117.
- JOHNSON, E. M., 2003 The Pur protein family: clues to function from recent studies on cancer and AIDS. *Anticancer Res* **23**: 2093-2100.
- JOHNSON, E. M., P. L. CHEN, C. P. KRACHMAROV, S. M. BARR, M. KANOVSKY *et al.*, 1995 Association of human Pur alpha with the retinoblastoma protein, Rb, regulates binding to the single-stranded DNA Pur alpha recognition element. *J Biol Chem* **270**: 24352-24360.
- JOHNSON, E. M., Y. KINOSHITA, D. B. WEINREB, M. J. WORTMAN, R. SIMON *et al.*, 2006 Role of Pur alpha in targeting mRNA to sites of translation in hippocampal neuronal dendrites. *J Neurosci Res* **83**: 929-943.
- KAMINSKI, R., A. DARBINIAN, N. MERABOVA, S. L. DESHMANE, M. K. WHITE *et al.*, 2008 Protective role of Puralpha to cisplatin. *Cancer Biol Ther* **7**: 1926-1935.
- KANAI, Y., N. DOHMAE and N. HIROKAWA, 2004 Kinesin transports RNA: isolation and characterization of an RNA-transporting granule. *Neuron* **43**: 513-525.
- KELM, R. J., JR., P. K. ELDER and M. J. GETZ, 1999 The single-stranded DNA-binding proteins, Puralpha, Purbeta, and MSY1 specifically interact with an exon 3-derived mouse vascular smooth muscle alpha-actin messenger RNA sequence. *J Biol Chem* **274**: 38268-38275.
- KEYES, L. N., and A. C. SPRADLING, 1997 The *Drosophila* gene fs(2)cup interacts with otu to define a cytoplasmic pathway required for the structure and function of germ-line chromosomes. *Development* **124**: 1419-1431.
- KHALILI, K., L. DEL VALLE, V. MURALIDHARAN, W. J. GAULT, N. DARBINIAN *et al.*, 2003 Puralpha is essential for postnatal brain development and developmentally coupled cellular proliferation as revealed by genetic inactivation in the mouse. *Mol Cell Biol* **23**: 6857-6875.
- KHURANA, J. S., and W. THEURKAUF, 2010 piRNAs, transposon silencing, and *Drosophila* germline development. *J Cell Biol* **191**: 905-913.
- KIEBLER, M. A., and G. J. BASSELL, 2006 Neuronal RNA granules: movers and makers. *Neuron* **51**: 685-690.
- KIM, K., J. CHOI, K. HEO, H. KIM, D. LEVENS *et al.*, 2008 Isolation and characterization of a novel H1.2 complex that acts as a repressor of p53-mediated transcription. *J Biol Chem* **283**: 9113-9126.

- KINDLER, S., H. WANG, D. RICHTER and H. TIEDGE, 2005 RNA transport and local control of translation. *Annu Rev Cell Dev Biol* **21**: 223-245.
- KING, R. C., 1970 *Ovarian development in Drosophila melanogaster*. Academic Press, New York,.
- KLASE, Z., P. KALE, R. WINOGRAD, M. V. GUPTA, M. HEYDARIAN *et al.*, 2007 HIV-1 TAR element is processed by Dicer to yield a viral micro-RNA involved in chromatin remodeling of the viral LTR. *BMC Mol Biol* **8**: 63.
- KNAPP, A. M., J. E. RAMSEY, S. X. WANG, K. E. GODBURN, A. R. STRAUCH *et al.*, 2006 Nucleoprotein interactions governing cell type-dependent repression of the mouse smooth muscle alpha-actin promoter by single-stranded DNA-binding proteins Pur alpha and Pur beta. *J Biol Chem* **281**: 7907-7918.
- KOBAYASHI, S., K. AGUI, S. KAMO, Y. LI and K. ANZAI, 2000 Neural BC1 RNA associates with pur alpha, a single-stranded DNA and RNA binding protein, which is involved in the transcription of the BC1 RNA gene. *Biochem Biophys Res Commun* **277**: 341-347.
- KRACHMAROV, C. P., L. G. CHEPENIK, S. BARR-VAGELL, K. KHALILI and E. M. JOHNSON, 1996 Activation of the JC virus Tat-responsive transcriptional control element by association of the Tat protein of human immunodeficiency virus 1 with cellular protein Pur alpha. *Proc Natl Acad Sci U S A* **93**: 14112-14117.
- LANTZ, V., J. S. CHANG, J. I. HORABIN, D. BOPP and P. SCHEDL, 1994 The *Drosophila* orb RNA-binding protein is required for the formation of the egg chamber and establishment of polarity. *Genes Dev* **8**: 598-613.
- LARKIN, M. K., K. HOLDER, C. YOST, E. GINIGER and H. RUOHOLA-BAKER, 1996 Expression of constitutively active Notch arrests follicle cells at a precursor stage during *Drosophila* oogenesis and disrupts the anterior-posterior axis of the oocyte. *Development* **122**: 3639-3650.
- LECUYER, E., H. YOSHIDA, N. PARTHASARATHY, C. ALM, T. BABAK *et al.*, 2007 Global analysis of mRNA localization reveals a prominent role in organizing cellular architecture and function. *Cell* **131**: 174-187.
- LEZON-GEYDA, K., V. NAJFELD and E. M. JOHNSON, 2001 Deletions of PURA, at 5q31, and PURB, at 7p13, in myelodysplastic syndrome and progression to acute myelogenous leukemia. *Leukemia* **15**: 954-962.
- LI, L. B., and N. M. BONINI, 2010 Roles of trinucleotide-repeat RNA in neurological disease and degeneration. *Trends Neurosci* **33**: 292-298.
- LI, L. B., Z. YU, X. TENG and N. M. BONINI, 2008 RNA toxicity is a component of ataxin-3 degeneration in *Drosophila*. *Nature* **453**: 1107-1111.

- LIN, D., T. V. PESTOVA, C. U. HELLEN and H. TIEDGE, 2008 Translational control by a small RNA: dendritic BC1 RNA targets the eukaryotic initiation factor 4A helicase mechanism. *Mol Cell Biol* **28**: 3008-3019.
- LIU, H., S. M. BARR, C. CHU, D. S. KOHTZ, Y. KINOSHITA *et al.*, 2005 Functional interaction of Puralpha with the Cdk2 moiety of cyclin A/Cdk2. *Biochem Biophys Res Commun* **328**: 851-857.
- LIVAK, K. J., and T. D. SCHMITTGEN, 2001 Analysis of relative gene expression data using real-time quantitative PCR and the 2(-Delta Delta C(T)) Method. *Methods* **25**: 402-408.
- LOPEZ-SCHIER, H., and D. ST JOHNSTON, 2001 Delta signaling from the germ line controls the proliferation and differentiation of the somatic follicle cells during *Drosophila* oogenesis. *Genes Dev* **15**: 1393-1405.
- MA, Z. W., A. D. BERGEMANN and E. M. JOHNSON, 1994 Conservation in human and mouse Pur alpha of a motif common to several proteins involved in initiation of DNA replication. *Gene* **149**: 311-314.
- MARGOLIS, J., and A. SPRADLING, 1995 Identification and behavior of epithelial stem cells in the *Drosophila* ovary. *Development* **121**: 3797-3807.
- MARTIN, K. C., and A. EPHRUSSI, 2009 mRNA localization: gene expression in the spatial dimension. *Cell* **136**: 719-730.
- MOSELEY, M. L., T. ZU, Y. IKEDA, W. GAO, A. K. MOSEMILLER *et al.*, 2006 Bidirectional expression of CUG and CAG expansion transcripts and intranuclear polyglutamine inclusions in spinocerebellar ataxia type 8. *Nat Genet* **38**: 758-769.
- MURALIDHARAN, V., T. SWEET, Y. NADRAGA, S. AMINI and K. KHALILI, 2001 Regulation of Puralpha gene transcription: evidence for autoregulation of Puralpha promoter. *J Cell Physiol* **186**: 406-413.
- NAKAMURA, A., R. AMIKURA, K. HANYU and S. KOBAYASHI, 2001 Me31B silences translation of oocyte-localizing RNAs through the formation of cytoplasmic RNP complex during *Drosophila* oogenesis. *Development* **128**: 3233-3242.
- NAKAMURA, A., K. SATO and K. HANYU-NAKAMURA, 2004 Drosophila cup is an eIF4E binding protein that associates with Bruno and regulates oskar mRNA translation in oogenesis. *Dev Cell* **6**: 69-78.
- O'DONNELL, W. T., and S. T. WARREN, 2002 A decade of molecular studies of fragile X syndrome. *Annu Rev Neurosci* **25**: 315-338.
- OHASHI, S., S. KOBAYASHI, A. OMORI, S. OHARA, A. OMAE *et al.*, 2000 The single-stranded DNA- and RNA-binding proteins pur alpha and pur beta link BC1 RNA to microtubules through binding to the dendrite-targeting RNA motifs. *J Neurochem* **75**: 1781-1790.

- OHASHI, S., K. KOIKE, A. OMORI, S. ICHINOSE, S. OHARA *et al.*, 2002 Identification of mRNA/protein (mRNP) complexes containing Puralpha, mStaufen, fragile X protein, and myosin Va and their association with rough endoplasmic reticulum equipped with a kinesin motor. *J Biol Chem* **277**: 37804-37810.
- OKAMURA, K., A. ISHIZUKA, H. SIOMI and M. C. SIOMI, 2004 Distinct roles for Argonaute proteins in small RNA-directed RNA cleavage pathways. *Genes Dev* **18**: 1655-1666.
- OLIVIERI, D., M. M. SYKORA, R. SACHIDANANDAM, K. MECHTLER and J. BRENNCKE, 2010 An in vivo RNAi assay identifies major genetic and cellular requirements for primary piRNA biogenesis in *Drosophila*. *EMBO J* **29**: 3301-3317.
- ONO, M., T. MURAKAMI, A. KUDO, M. ISSHIKI, H. SAWADA *et al.*, 2001 Quantitative comparison of anti-fading mounting media for confocal laser scanning microscopy. *J Histochem Cytochem* **49**: 305-312.
- ORR, H. T., and H. Y. ZOGHBI, 2007 Trinucleotide repeat disorders. *Annu Rev Neurosci* **30**: 575-621.
- PARK, J. K., X. LIU, T. J. STRAUSS, D. M. MCKEARIN and Q. LIU, 2007 The miRNA pathway intrinsically controls self-renewal of *Drosophila* germline stem cells. *Curr Biol* **17**: 533-538.
- PEIFER, M., S. ORSULIC, D. SWEETON and E. WIESCHAUS, 1993 A role for the *Drosophila* segment polarity gene armadillo in cell adhesion and cytoskeletal integrity during oogenesis. *Development* **118**: 1191-1207.
- PEPPER, A. S., R. W. BEERMAN, B. BHOGAL and T. A. JONGENS, 2009 Argonaute2 suppresses *Drosophila* fragile X expression preventing neurogenesis and oogenesis defects. *PLoS One* **4**: e7618.
- PICCIONI, F., C. OTTONE, P. BRESCIA, V. PISA, G. SICILIANO *et al.*, 2009 The translational repressor Cup associates with the adaptor protein Miranda and the mRNA carrier Staufen at multiple time-points during *Drosophila* oogenesis. *Gene* **428**: 47-52.
- REICH, J., M. J. SNEE and P. M. MACDONALD, 2009 miRNA-dependent translational repression in the *Drosophila* ovary. *PLoS One* **4**: e4669.
- ROBINSON, D. N., K. CANT and L. COOLEY, 1994 Morphogenesis of *Drosophila* ovarian ring canals. *Development* **120**: 2015-2025.
- ROEGIERS, F., and Y. N. JAN, 2000 Staufen: a common component of mRNA transport in oocytes and neurons? *Trends Cell Biol* **10**: 220-224.
- ROPER, K., and N. H. BROWN, 2003 Maintaining epithelial integrity: a function for gigantic spectraplakin isoforms in adherens junctions. *J Cell Biol* **162**: 1305-1315.
- ROTH, S., and J. A. LYNCH, 2009 Symmetry breaking during *Drosophila* oogenesis. *Cold Spring Harb Perspect Biol* **1**: a001891.

- RUOHOLA, H., K. A. BREMER, D. BAKER, J. R. SWEDLOW, L. Y. JAN *et al.*, 1991 Role of neurogenic genes in establishment of follicle cell fate and oocyte polarity during oogenesis in *Drosophila*. *Cell* **66**: 433-449.
- SADAKATA, T., C. KUO, H. ICHIKAWA, E. NISHIKAWA, S. Y. NIU *et al.*, 2000 Puralpha, a single-stranded DNA binding protein, suppresses the enhancer activity of cAMP response element (CRE). *Brain Res Mol Brain Res* **77**: 47-54.
- SAFAK, M., G. L. GALLIA, S. A. ANSARI and K. KHALILI, 1999 Physical and functional interaction between the Y-box binding protein YB-1 and human polyomavirus JC virus large T antigen. *J Virol* **73**: 10146-10157.
- SCHUPBACH, T., and E. WIESCHAUS, 1986 Germline autonomy of maternal-effect mutations altering the embryonic body pattern of *Drosophila*. *Dev Biol* **113**: 443-448.
- SCHUPBACH, T., and E. WIESCHAUS, 1991 Female sterile mutations on the second chromosome of *Drosophila melanogaster*. II. Mutations blocking oogenesis or altering egg morphology. *Genetics* **129**: 1119-1136.
- SHAH, C., and K. FORSTEMANN, 2008 Monitoring miRNA-mediated silencing in *Drosophila melanogaster* S2-cells. *Biochim Biophys Acta* **1779**: 766-772.
- SNOW, P. M., A. J. BIEBER and C. S. GOODMAN, 1989 Fasciclin III: a novel homophilic adhesion molecule in *Drosophila*. *Cell* **59**: 313-323.
- STEINBERG, M. S., 2007 Differential adhesion in morphogenesis: a modern view. *Curr Opin Genet Dev* **17**: 281-286.
- TANENTZAPF, G., C. SMITH, J. MCGLADE and U. TEPASS, 2000 Apical, lateral, and basal polarization cues contribute to the development of the follicular epithelium during *Drosophila* oogenesis. *J Cell Biol* **151**: 891-904.
- TEIVE, H. A., 2009 Spinocerebellar ataxias. *Arq Neuropsiquiatr* **67**: 1133-1142.
- TEKOTTE, H., D. BERDNIK, T. TOROK, M. BUSZCZAK, L. M. JONES *et al.*, 2002 Dcas is required for importin-alpha3 nuclear export and mechano-sensory organ cell fate specification in *Drosophila*. *Dev Biol* **244**: 396-406.
- THATIKUNTA, P., B. E. SAWAYA, L. DENISOVA, C. COLE, G. YUSIBOVA *et al.*, 1997 Identification of a cellular protein that binds to Tat-responsive element of TGF beta-1 promoter in glial cells. *J Cell Biochem* **67**: 466-477.
- TODD, P. K., and H. L. PAULSON, 2010 RNA-mediated neurodegeneration in repeat expansion disorders. *Ann Neurol* **67**: 291-300.
- TORRES, I. L., H. LOPEZ-SCHIER and D. ST JOHNSTON, 2003 A Notch/Delta-dependent relay mechanism establishes anterior-posterior polarity in *Drosophila*. *Dev Cell* **5**: 547-558.

- TRETIKOVA, A., G. L. GALLIA, N. SHCHERBIK, B. JAMESON, E. M. JOHNSON *et al.*, 1998 Association of Puralpha with RNAs homologous to 7 SL determines its binding ability to the myelin basic protein promoter DNA sequence. *J Biol Chem* **273**: 22241-22247.
- TRETIKOVA, A., A. STEPLEWSKI, E. M. JOHNSON, K. KHALILI and S. AMINI, 1999 Regulation of myelin basic protein gene transcription by Sp1 and Puralpha: evidence for association of Sp1 and Puralpha in brain. *J Cell Physiol* **181**: 160-168.
- VALVERDE, R., L. EDWARDS and L. REGAN, 2008 Structure and function of KH domains. *FEBS J* **275**: 2712-2726.
- VERROTTI, A. C., and R. P. WHARTON, 2000 Nanos interacts with cup in the female germline of Drosophila. *Development* **127**: 5225-5232.
- WANG, D. O., K. C. MARTIN and R. S. ZUKIN, 2010 Spatially restricting gene expression by local translation at synapses. *Trends Neurosci* **33**: 173-182.
- WANG, H., A. IACOANGELI, D. LIN, K. WILLIAMS, R. B. DENMAN *et al.*, 2005 Dendritic BC1 RNA in translational control mechanisms. *J Cell Biol* **171**: 811-821.
- WANG, H., M. WANG, K. REISS, N. DARBINIAN-SARKISSIAN, E. M. JOHNSON *et al.*, 2007 Evidence for the involvement of Puralpha in response to DNA replication stress. *Cancer Biol Ther* **6**: 596-602.
- WANG, L. G., E. M. JOHNSON, Y. KINOSHITA, J. S. BABB, M. T. BUCKLEY *et al.*, 2008 Androgen receptor overexpression in prostate cancer linked to Pur alpha loss from a novel repressor complex. *Cancer Res* **68**: 2678-2688.
- WARING, G. L., 2000 Morphogenesis of the eggshell in Drosophila. *Int Rev Cytol* **198**: 67-108.
- WHARTON, K. A., B. YEDVOBNICK, V. G. FINNERTY and S. ARTAVANIS-TSAKONAS, 1985 opa: a novel family of transcribed repeats shared by the Notch locus and other developmentally regulated loci in *D. melanogaster*. *Cell* **40**: 55-62.
- WHITE, M. K., E. M. JOHNSON and K. KHALILI, 2009 Multiple roles for Puralpha in cellular and viral regulation. *Cell Cycle* **8**: 1-7.
- WILHELM, J. E., M. BUSZCZAK and S. SAYLES, 2005 Efficient protein trafficking requires trailer hitch, a component of a ribonucleoprotein complex localized to the ER in Drosophila. *Dev Cell* **9**: 675-685.
- WILHELM, J. E., M. HILTON, Q. AMOS and W. J. HENZEL, 2003 Cup is an eIF4E binding protein required for both the translational repression of oskar and the recruitment of Barentsz. *J Cell Biol* **163**: 1197-1204.
- WILSCH-BRAUNINGER, M., H. SCHWARZ and C. NUSSLEIN-VOLHARD, 1997 A sponge-like structure involved in the association and transport of maternal products during Drosophila oogenesis. *J Cell Biol* **139**: 817-829.

- WU, X., P. S. TANWAR and L. A. RAFTERY, 2008 Drosophila follicle cells: morphogenesis in an eggshell. *Semin Cell Dev Biol* **19**: 271-282.
- XI, R., J. R. MCGREGOR and D. A. HARRISON, 2003 A gradient of JAK pathway activity patterns the anterior-posterior axis of the follicular epithelium. *Dev Cell* **4**: 167-177.
- YANISCH-PERRON, C., J. VIEIRA and J. MESSING, 1985 Improved M13 phage cloning vectors and host strains: nucleotide sequences of the M13mp18 and pUC19 vectors. *Gene* **33**: 103-119.
- ZAPPAVIGNA, V., F. PICCIONI, J. C. VILLAESCUSA and A. C. VERROTTI, 2004 Cup is a nucleocytoplasmic shuttling protein that interacts with the eukaryotic translation initiation factor 4E to modulate Drosophila ovary development. *Proc Natl Acad Sci U S A* **101**: 14800-14805.